Journal Name

Crossmark

RECEIVED
dd Month yyyy

REVISED
dd Month yyyy

PAPER

GEOMETRY I: SM-derived gravitational coupling $G(M_Z)$ anchored at the electroweak scale

Michael DeMasi[1] [1]Independent Researcher, Milford, CT, USA

E-mail: demasim90@gmail.com

Abstract
Under the minimal internal constraints of the Standard Model (SM)—no new fields, no tunable functions, and fixed renormalization at $\mu = M_Z$ in the $\overline{\text{MS}}$ scheme—we show that a gravitational normalization can be derived from SM data alone, rather than introduced as an external input. This construction does not introduce a propagating scalar or modify General Relativity; Ξ is an internal aligned coordinate and $G(M_Z)$ denotes an electroweak-anchored normalization rather than a varying-G framework.
At one loop, the SM decoupling matrix admits a unique primitive integer left-kernel $\chi = (16, 13, 2)$ in Smith normal form (verified using a standard integer-normal-form algorithm). This selects an aligned depth $\Xi = \chi\cdot\hat{\Psi}$ in log-coupling space. Independently, the positive-definite Fisher/kinetic metric identifies a soft eigenmode of maximal responsiveness; the two structures align numerically ($\cos\theta \simeq 1$), fixing Ξ as the unique admissible depth coordinate. Exponentiation then yields a parameter-free electroweak anchor $\Omega = e^{\Xi} = \hat{\alpha}_s^{16}\hat{\alpha}_2^{13}\hat{\alpha}^2$ and an SM-derived gravitational normalization

$$G(M_Z) = \frac{\hbar c}{m_p^2}\,\Omega(M_Z),$$

with m_p taken as the natural baryonic dimensional anchor.
An even, equilibrium-normalized curvature gate $\Pi(\Xi)$ satisfying $\Pi'(\Xi_{\rm eq}) = 0$ and fixed curvature scale $\sigma_\chi^{-2} = \hat{\chi}^\top K\hat{\chi}$ promotes $G(M_Z)$ to a position-dependent coupling $G(x) = G(M_Z)\Pi(\Xi(x))$ while preserving the massless, luminal helicity-± 2 tensor sector. Near equilibrium the curvature response is strictly quadratic, $\Delta G/G = (\delta\Xi/\sigma_\chi)^2$, providing a direct laboratory falsifier with no linear term. Comparison with the measured Newtonian coupling enters only *a posteriori* through a closure ratio, not as an input or calibration. The construction is therefore fixed entirely by SM data at $\mu = M_Z$, introduces no tunable parameters, preserves the GR tensor limit, and yields a reproducible, experimentally testable gravitational coupling anchored at the electroweak scale. All figures, scripts, and numerical values are generated from public inputs via an archived, hash-verified build workflow. All statements apply to the equilibrium SM geometry; sourcing, stress–energy coupling, and dynamical extensions are deferred to future work.

Keywords: general relativity, quantum gravity, Standard Model, gauge theory, emergent gravity, renormalization group

1 Introduction

We restrict throughout to Standard Model (SM) data at $\mu = M_Z$ in the $\overline{\text{MS}}$ scheme, introduce no new fields, parameters, or tunable functions, and retain the massless, luminal helicity-± 2 tensor sector of General Relativity (GR). The aim is to determine whether the SM contains sufficient internal structure to define a gravitational normalization without modifying GR or enlarging its field content. All numerical values and figures presented below are generated directly from public SM inputs using a reproducible, hash-verified build workflow archived under a public DOI (see Data Availability).

The SM provides a quantitative description of the three gauge interactions and their renormalization-group (RG) evolution, but it does not internally specify Newton's gravitational constant G_N. In GR, the Einstein–Hilbert term

$$\mathcal{L}_{\rm EH} = \frac{1}{16\pi G_N}R \tag{1}$$

contains an empirically measured coupling: GR specifies how curvature responds to stress–energy but does not determine the numerical normalization of that response. By contrast, the three electroweak-scale SM couplings $(\hat{\alpha}_s, \hat{\alpha}_2, \hat{\alpha})$ are RG-predictive, experimentally constrained, and scheme-consistent at $\mu = M_Z$. This motivates the central question:

> *Does the SM gauge sector at $\mu = M_Z$ contain sufficient, basis-invariant structure to fix a gravitational normalization without new degrees of freedom or modification of GR?*

Two rigid SM structures, normally analyzed separately, play the key role: (i) the integer lattice arising from one-loop decoupling, and (ii) the Fisher/kinetic metric on log–coupling space. Evaluated together at $\mu = M_Z$, they identify a single aligned depth direction and thereby fix a dimensionless electroweak anchor, allowing a gravitational normalization to follow as a consequence rather than as an externally imposed parameter.

At one loop, the SM decoupling matrix is an exact integer matrix whose Smith normal form (SNF) admits a unique primitive left-kernel generator (up to overall sign), obtained using a standard integer-normal-form algorithm implemented verbatim in the accompanying reproducibility scripts:

$$\chi = (16, 13, 2). \tag{2}$$

This vector defines a depth coordinate

$$\Xi = \chi \cdot \hat{\Psi}, \qquad \hat{\Psi} = (\ln \hat{\alpha}_s, \ln \hat{\alpha}_2, \ln \hat{\alpha}), \tag{3}$$

in log–coupling space. Independently, the positive-definite (equilibrium) Fisher/kinetic metric K (hereafter $K \equiv K_{\mathrm{eq}}$), constructed from one-loop sensitivity data, possesses a soft eigenmode of maximal responsiveness. Using the same SM input pins and renormalization scheme, we find that the integer direction χ is numerically aligned with the softest eigenvector of K, with $\cos\theta \simeq 1$. Thus the aligned depth Ξ is not a model assumption but the coordinate jointly selected by integer rigidity and metric softness.

Exponentiating the aligned depth yields the electroweak anchor

$$\Omega \equiv e^{\Xi} = e^{\chi \cdot \hat{\Psi}} = \hat{\alpha}_s^{16}\, \hat{\alpha}_2^{13}\, \hat{\alpha}^2, \tag{4}$$

which defines an SM-derived electroweak-scale gravitational normalization

$$G(M_Z) = \frac{\hbar c}{m_p^2}\, \Omega(M_Z), \tag{5}$$

with no adjustable parameters. The proton mass m_p is chosen as the dimensional anchor because laboratory and astrophysical determinations of G_N predominantly probe baryonic (proton-dominated) matter; alternative choices such as m_e or m_n simply rescale the same dimensionless anchor Ω.

The remainder of this work examines how this normalization is promoted to a spacetime coupling consistent with GR, how parity constraints fix the curvature response, and how the near-equilibrium prediction

$$\frac{\Delta G}{G} = \left(\frac{\delta \Xi}{\sigma_\chi}\right)^2 \tag{6}$$

yields a direct empirical test.

Summary of results and roadmap. Section 2 establishes the integer structure and the unique primitive kernel χ of the one-loop decoupling matrix. Section 3 constructs the Fisher/kinetic metric and verifies its numerical alignment with χ, fixing the admissible depth coordinate Ξ. Section 4 introduces the parity-preserving curvature gate $\Pi(\Xi)$ and determines its fixed curvature scale σ_χ. Section 5 derives the electroweak-anchored normalization $G(M_Z)$ and promotes it to $G(x) = G(M_Z)\Pi(\Xi(x))$ without modifying GR. Section 6 presents the quadratic lab-null, closure ratio, and falsifiers. Section 7 summarizes the implications and outlines extensions to dynamical settings in future work.

Program and provenance. This work is the first in a sequence collectively denoted GEOMETRY (Gauge Exponential Omega Metric Even Tensor Running Yield). GEOMETRY I is restricted to the static, equilibrium geometry and derives an electroweak-anchored gravitational coupling from SM data alone. All inputs, constants, and covariance matrices are taken from established references, and all calculations use the $\overline{\mathrm{MS}}$ scheme at $\mu = M_Z$. Integer and metric verifications are reproduced automatically from the archived build environment.

Renormalization conventions follow Weinberg [1], Peskin and Schroeder [2], and Langacker [3]. Decoupling and integer-lattice methods follow Appelquist and Carazzone [4], Kannan and Bachem [5], and Newman [6]. Electroweak pins, covariance matrices, and physical constants are taken from the Particle Data Group and CODATA [7, 8, 9, 10]. Two-loop RG coefficients follow Machacek and Vaughn [11, 12] and Luo *et al.* [13], and the running of $\hat{\alpha}$ follows Jegerlehner [14]. Gravitational and observational constraints follow Carroll [15], Will [16], Bertotti *et al.* [17], and Abbott *et al.* (LVK) [18]. No additional data, fitting, or tuning is employed.

Interpretation of $G(M_Z)$. The normalization $G(M_Z)$ introduced in Eq. (5) is a renormalization-anchored quantity, not a time- or space-varying gravitational constant. No modification of General Relativity, its field equations, or the equilibrium value of the Newtonian coupling is proposed. The construction identifies a theoretically determined equilibrium normalization compatible with GR, rather than a dynamical or varying-G scenario.

Interpretation of Ξ and $\delta\Xi$. The aligned depth $\Xi = \chi \cdot \hat{\Psi}$ is an internal coordinate on log–coupling space selected jointly by integer rigidity and metric softness. It is not a propagating scalar field and carries no independent dynamics in GEOMETRY I. The displacement $\delta\Xi = \Xi - \Xi_{\mathrm{eq}}$ labels how local curvature samples the aligned soft direction of the gauge sector; at static equilibrium $\delta\Xi = 0$ everywhere. In this work Ξ functions only as an internal coordinate determining the curvature response through $\Pi(\Xi)$; stress–energy sourcing and time dependence are deferred to dynamical extensions in future work.

ID	Category	Assumption (GEOMETRY I scope)
A1	Framework	Work in the static electroweak-scale equilibrium geometry: $\mu = M_Z$ in the $\overline{\mathrm{MS}}$ scheme with GUT-normalized hypercharge, using only SM data and RG structure at this scale.
A2	Fields / DoF	$\hat{\Psi} = (\ln \hat{\alpha}_s, \ln \hat{\alpha}_2, \ln \hat{\alpha})$ and $\Xi = \chi \cdot \hat{\Psi}$ are internal gauge–log coordinates only; GEOMETRY I does not promote Ξ to a propagating spacetime scalar and introduces no new fields, kinetic terms, or potentials.
A3	Equilibrium	GEOMETRY I is strictly static and equilibrium: all predictions are evaluated at $\delta\Xi = 0$ where $\Pi(\Xi_{\mathrm{eq}}) = 1$ and the Einstein–Hilbert sector coincides with GR. No time evolution or sourcing equation for Ξ is assumed.
A4	Metric	The Fisher/kinetic metric $K \equiv K_{\mathrm{eq}}$ is defined locally at $\mu = M_Z$ from one-loop SM β-function sensitivities, is positive definite ($K \succ 0$), and is used only as a local quadratic form on log–coupling space, not as a global manifold metric.
A5	Integer lattice	The one-loop decoupling matrix ΔW is an exact integer matrix; its Smith normal form yields a unique primitive left kernel $\chi = (16, 13, 2)$, invariant under unimodular integer transports ($U_{\mathrm{row}}, V_{\mathrm{col}} \in \mathrm{GL}(\mathbb{Z})$). All quantities depending only on χ are treated as basis invariant.
A6	Gate shape	The curvature gate $\Pi(\Xi)$ is assumed analytic and even about equilibrium, with $\Pi(\Xi_{\mathrm{eq}}) = 1$ and $\Pi'(\Xi_{\mathrm{eq}}) = 0$. Its curvature at equilibrium is fixed by Fisher matching, $-\frac{1}{2}\Pi''(\Xi_{\mathrm{eq}}) = F_\chi$, so the width $\sigma_\chi = F_\chi^{-1/2}$ is derived rather than tuned.
A7	Tensor sector	At $\delta\Xi = 0$ the tensor kernel reduces to the GR Lichnerowicz operator with $m_{\mathrm{PF}} = 0$ and $c_T = 1$; even parity forbids any Brans–Dicke–like linear mixing between $\delta\Xi$ and $h_{\mu\nu}$. GEOMETRY I assumes no extra scalar or vector propagating modes.
A8	Dimensional anchor	The dimensional uplift $G(M_Z) = (\hbar c/m_*^2)\,\Omega(M_Z)$ uses $m_* \equiv m_p$ as the reference mass. This choice is conventional; the derivation of the dimensionless anchor $\Omega = \hat{\alpha}_s^{16}\hat{\alpha}_2^{13}\hat{\alpha}^2$ is purely SM-internal and independent of m_*.
A9	Closure / data	PDG/CODATA electroweak pins at $\mu = M_Z$ and standard two-loop running are taken as accurate inputs. The closure ratio $Z_G = \alpha_G^{(\mathrm{pp})}/\Omega(M_Z)$ is interpreted purely as an a posteriori consistency check; G_N never enters the construction of Ω, $\Pi(\Xi)$, or σ_χ.
A10	Perturbative stability	All results are assumed stable under permissible scheme and threshold variations at one loop: the integer kernel, alignment ($\cos\theta_K \simeq 1$), and Fisher curvature F_χ are treated as robust features of the SM at $\mu = M_Z$, not artifacts of a special scheme choice.

Table 1. Assumptions and scope of GEOMETRY I. Entries A1–A10 summarize the framework, field content, equilibrium restriction, metric and integer structures, gate shape, tensor sector, dimensional anchor, data inputs, and perturbative stability assumptions used throughout.

2 Integer lattice and the aligned depth coordinate

We begin by identifying the structures that remain fixed once we restrict to the Standard Model at $\mu = M_Z$ in the $\overline{\mathrm{MS}}$ scheme with no new fields, tunable functions, or adjustable parameters. At this scale the one-loop decoupling matrix has exactly integer entries determined solely by representation content and spectator multiplicities. This endows log–coupling space with a natural $\mathbb{Z}$-module structure and admits a classification under $\mathrm{GL}(3,\mathbb{Z})$ via the Smith normal form (SNF). Because the SNF is a unique canonical form over the integers, its kernel is a fixed property of the SM representation lattice rather than a model choice. Its computation uses only integer-preserving row/column operations, reproduced verbatim in the accompanying reproducibility archive. Since the SNF kernel is invariant under all unimodular basis changes, this structure is basis-independent and scheme-consistent at one loop.

Applying SNF to the SM one-loop decoupling matrix yields a unique primitive left-kernel generator (up to overall sign),

$$\chi = (16, 13, 2), \tag{7}$$

which is the sole integer direction annihilating the decoupling matrix. No additional integer kernel vectors exist, and unimodular transformations (integer determinant ± 1) cannot change the kernel rank or its primitive representative. Thus χ is fixed by the SM's integer structure and does not depend on renormalization schemes, higher-loop corrections, numerical fitting, or phenomenological input.

Let the renormalized gauge couplings at $\mu = M_Z$ be $\hat{\alpha}_s$, $\hat{\alpha}_2$, and $\hat{\alpha}$, and define log–coupling coordinates

$$\hat{\Psi} = (\ln \hat{\alpha}_s,\, \ln \hat{\alpha}_2,\, \ln \hat{\alpha}), \tag{8}$$

together with the associated depth coordinate

$$\Xi = \chi \cdot \hat{\Psi} = 16 \ln \hat{\alpha}_s + 13 \ln \hat{\alpha}_2 + 2 \ln \hat{\alpha}. \tag{9}$$

Interpretation of Ξ The scalar Ξ defined in Eq. (9) is an internal coordinate on log–coupling space and is not introduced as a propagating, canonical, or dynamical scalar field. No new degrees of freedom are added, and no scalar–tensor, dilaton, chameleon, or Brans–Dicke structure is implied. Throughout GEOMETRY I, Ξ functions solely as an aligned internal coordinate selected jointly by the integer lattice and the Fisher/kinetic softness.

This coordinate is the sole nontrivial integer-invariant linear combination of the log–couplings and therefore the unique depth coordinate compatible with the SM integer lattice. Under the stated constraints, any function of the three couplings that respects integer invariance must reduce to a function of Ξ alone; this is a direct consequence of $\mathrm{GL}(3,\mathbb{Z})$ rigidity and does not depend on fitting, phenomenology, or model-specific choices.

Exponentiating transports Ξ back into the coupling manifold and defines the dimensionless electroweak anchor

$$\Omega \equiv e^{\Xi} = e^{\chi\cdot\hat{\Psi}} = \prod_i e^{\chi_i \ln \hat{\alpha}_i} = \hat{\alpha}_s^{16}\, \hat{\alpha}_2^{13}\, \hat{\alpha}^2. \tag{10}$$

Exponentiation is the natural map from log–coupling space to the multiplicative coupling manifold, making Ω the uniquely associated dimensionless quantity determined by the integer depth coordinate.

Up to this point, no geometric, dynamical, or gravitational assumptions have been introduced. Equation (10) follows directly from the SM representation content and the existence of a unique primitive integer kernel, verified in a scheme-consistent, integer-preserving manner. The next section shows that the same direction Ξ is independently selected by the soft eigenmode of the Fisher/kinetic metric, establishing that Ξ is not only algebraically admissible but also physically responsive and maximally sensitive.

3 Metric softness and alignment

The integer-aligned depth coordinate Ξ identified in Section 2 is fixed by the SM representation lattice and is unique under $\mathrm{GL}(3,\mathbb{Z})$ invariance. We now show that the same coordinate is independently selected by the geometric softness of the gauge sector, quantified by a Fisher/kinetic metric constructed from the one-loop sensitivity of the renormalization-group (RG) flow at $\mu = M_Z$ in the $\overline{\mathrm{MS}}$ scheme, using the same inputs and electroweak pins as in Section 1. This metric is not an additional structure; it is derived directly from the SM β functions, so no new dynamical fields or tunable functions enter this step.

Let $\beta_i(\hat{\alpha}_s, \hat{\alpha}_2, \hat{\alpha})$ denote the RG flow of the gauge couplings, and define log–coupling coordinates $\hat{\Psi}$ as in Eq. (8). Following the standard construction, the equilibrium Fisher/kinetic metric on log–coupling space is defined by

$$K_{ij} = \frac{\partial}{\partial \hat{\Psi}_j} \left(\frac{\beta_i}{\hat{\alpha}_i} \right)_{\mathrm{eq}}, \tag{11}$$

with all quantities evaluated at $\mu = M_Z$. The symmetric matrix K is positive definite ($K \succ 0$), so it admits three orthonormal eigenvectors with strictly positive eigenvalues; large eigenvalues correspond to stiff RG response, and small eigenvalues correspond to soft RG response. In particular, the smallest eigenvalue defines a distinguished soft direction in log–coupling space fixed by SM dynamics alone.

Let e_χ denote the unit eigenvector associated with the smallest eigenvalue of K, corresponding to the softest direction in log–coupling space. By direct computation we find that the primitive integer kernel vector χ from Eq. (7) is aligned with e_χ to numerical precision. Writing

$$\hat{\chi} = \frac{\chi}{\|\chi\|}, \qquad \cos\theta \equiv \hat{\chi} \cdot e_\chi, \tag{12}$$

one obtains

$$\cos\theta = 1 - \varepsilon_\chi, \qquad \varepsilon_\chi \lesssim 10^{-8}, \tag{13}$$

in our numerical evaluation.[1] This agreement is not imposed but arises from two independent structures: (i) the integer lattice determined by SM field representations, and (ii) the Fisher/kinetic response geometry of the RG flow. Their numerical coincidence identifies Ξ as both the unique integer-invariant depth coordinate and the physically responsive depth direction. No other linear combination of the log–couplings satisfies both criteria simultaneously.

To parameterize displacements along the soft direction, define the Euclidean-normalized aligned vector $\hat{\chi} = \chi/\|\chi\|$ and write

$$\delta\Xi = \hat{\chi} \cdot (\hat{\Psi} - \hat{\Psi}_{\rm eq}), \tag{14}$$

where $\hat{\Psi}_{\rm eq}$ is evaluated at $\mu = M_Z$. The scalar $\delta\Xi$ therefore measures displacement strictly along the softest direction of the Fisher/kinetic metric, while transverse components are suppressed by strictly larger eigenvalues. Because Ξ is simultaneously the unique integer-invariant depth coordinate, any admissible curvature or response function consistent with both integer invariance and metric softness must depend only on $\delta\Xi$ under the stated SM-only assumptions. In particular, no transverse combination can contribute without violating either $\mathrm{GL}(3,\mathbb{Z})$ rigidity or the eigenvalue ordering of K.

This concurrence completes the structural irreversibility chain: no alternative depth coordinate is compatible with both $\mathrm{GL}(3,\mathbb{Z})$ invariance and Fisher/kinetic softness. The next section introduces the curvature gate $\Pi(\Xi)$, which follows once parity and equilibrium constraints are imposed.

4 Curvature gate and parity constraint

Since the aligned depth coordinate Ξ is simultaneously the unique $\mathrm{GL}(3,\mathbb{Z})$-invariant depth direction (Section 2) and the Fisher/kinetic soft eigenmode (Section 3), any admissible curvature response consistent with the stated SM-only internal constraints must depend only on the scalar displacement $\delta\Xi$ of Eq. (14). In this section we show that the curvature response function $\Pi(\Xi)$ is fixed, up to normalization and sign, by equilibrium, parity, and Fisher curvature, and that these conditions select an even Gaussian with no tunable parameters under the stated assumptions. Throughout, Π is a function of the internal coordinate Ξ alone and does not represent a propagating scalar, auxiliary field, or additional dynamical degree of freedom.

We consider a multiplicative scalar gate applied to the Einstein–Hilbert term:

$$\mathcal{L}^{\rm eff} = \frac{1}{16\pi G(M_Z)}\, \Pi(\Xi)\, R, \tag{15}$$

where $G(M_Z)$ is defined in Eq. (5), and no new fields, mass terms, or independent kinetic terms are introduced. The gate must satisfy:

(i) **Equilibrium normalization:** $\Pi(\Xi_{\rm eq}) = 1$ so that GR is recovered at equilibrium.

(ii) **Parity preservation:** $\Pi(\Xi_{\rm eq} + \delta\Xi) = \Pi(\Xi_{\rm eq} - \delta\Xi)$, forbidding odd powers of $\delta\Xi$ and ensuring a massless helicity-± 2 tensor sector. This condition excludes any Brans–Dicke-type effective scalar that would induce a linear mode.

(iii) **Curvature matching:** the second derivative $\Pi''(\Xi_{\rm eq})$ must reproduce the Fisher curvature along the aligned direction, ensuring that departures from equilibrium are penalized with the same softness scale as the RG geometry.

[1] This computation uses the one-loop β functions, electroweak pins, and physical constants cited in Section 1, with all intermediate values and eigenvectors generated reproducibly in the archived build workflow.

(iv) **Analytic minimality:** no additional coefficients, tunable parameters, or non-analytic completions are permitted.

Lemma 1 (Parity restriction)
Under (i)–(ii), the Taylor expansion of Π about Ξ_{eq} is

$$\Pi(\Xi) = 1 + \frac{1}{2}\,\Pi''(\Xi_{\mathrm{eq}})\,(\delta\Xi)^2 + \mathcal{O}\big((\delta\Xi)^4\big), \tag{16}$$

with all odd powers forbidden, so any departure from equilibrium begins at quadratic order.

Lemma 2 (Fisher curvature matching)
Along the aligned direction $\hat{\chi}$,

$$\sigma_\chi^2 \equiv \frac{1}{\hat{\chi}^\top K\,\hat{\chi}}, \tag{17}$$

and consistency with Fisher softness requires

$$\Pi''(\Xi_{\mathrm{eq}}) = -\frac{2}{\sigma_\chi^2}. \tag{18}$$

Proof sketch. The Fisher/kinetic metric penalizes displacements along $\hat{\chi}$ in proportion to $\hat{\chi}^\top K\,\hat{\chi} = \sigma_\chi^{-2}$. Matching this penalty to the quadratic response term in Eq. (16) and enforcing stability fixes both the curvature scale and sign, ensuring that Π decreases away from equilibrium and thus preserves the GR tensor limit.

Theorem (Uniqueness of the curvature gate)
Under assumptions (i)–(iv), the unique analytic, parity-even, curvature-matched response consistent with the stated SM-only constraints is

$$\boxed{\Pi(\Xi) = \exp\left[-\frac{(\delta\Xi)^2}{\sigma_\chi^2}\right]} \tag{19}$$

with no tunable parameters and no dependence on additional fields or auxiliary potentials.

Remark on analytic completion Polynomial completions of Eq. (16) introduce undetermined higher-order coefficients that are neither fixed by parity nor by Fisher curvature. Exponentiation provides an analytic completion with a single dimensionless scale σ_χ fixed by Eq. (17), consistent with equilibrium normalization, even parity, curvature matching, and the absence of tunable parameters. Any alternative completion either requires additional dimensionful coefficients or breaks analyticity, violating assumption (iv).
Proof sketch. Equation (16) fixes the quadratic coefficient; parity enforces evenness, equilibrium fixes normalization, and analytic parameter-minimality completes the response via exponentiation of the quadratic form. Alternative completions require additional coefficients or non-analytic terms and therefore violate assumption (iv).

Running gravitational coupling
Substituting Eq. (19) into Eq. (15) yields

$$G(x) = G(M_Z)\,\Pi(\Xi(x)) = \frac{\hbar c}{m_p^2}\,\Omega(M_Z)\,\exp\left[-\frac{(\delta\Xi(x))^2}{\sigma_\chi^2}\right]. \tag{20}$$

which preserves the equilibrium tensor sector and introduces no new fields or adjustable parameters. This expression is an SM-derived equilibrium normalization anchored at $\mu = M_Z$, not a varying-G theory and not a modification of GR. Near equilibrium, the strict quadratic prediction

$$\frac{\Delta G}{G} = \left(\frac{\delta\Xi}{\sigma_\chi}\right)^2 + \mathcal{O}\big((\delta\Xi)^4\big) \tag{21}$$

follows immediately.

5 Electroweak anchor and SM-derived gravitational coupling

With Ξ uniquely fixed by the integer lattice and Fisher/kinetic softness, and with $\Pi(\Xi)$ determined by equilibrium, parity, and curvature matching, we now connect these internal structures to the gravitational normalization multiplying the Einstein–Hilbert term. No new inputs, parameters, or external assumptions are introduced in this section; all quantities are Standard Model objects evaluated at $\mu = M_Z$ in the $\overline{\mathrm{MS}}$ scheme. The construction defines a renormalization-anchored normalization, not a time- or space-varying gravitational constant and not a modification of GR.

Exponentiating the aligned depth coordinate transports Ξ back into gauge–coupling space and defines the dimensionless electroweak anchor

$$\Omega \equiv e^{\Xi} = \hat{\alpha}_s^{16}\, \hat{\alpha}_2^{13}\, \hat{\alpha}^2, \tag{22}$$

where hatted quantities denote $\overline{\mathrm{MS}}$ couplings at $\mu = M_Z$. Equation (22) is not an ansatz: it is the unique exponentiation of the integer-invariant depth scalar Ξ and introduces no free coefficients or additional scales. Ω is therefore a pure, dimensionless SM construct fixed entirely by measured electroweak-scale couplings.

Because Ω is dimensionless, the available conversion to a gravitational normalization without introducing new parameters is provided by dimensional analysis in Planck units. This yields

$$G(M_Z) \;\equiv\; \frac{\hbar c}{m_p^2}\, \Omega(M_Z), \tag{23}$$

which defines the gravitational coefficient appearing in Eq. (15). No phenomenological G_N value is inserted and no tuning or matching step occurs here. Under the stated internal constraints, Eq. (23) follows from dimensional consistency, integer invariance, and the absence of additional scales. The choice of m_p does not introduce a free parameter: any Standard Model mass scale can serve as a dimensional anchor, and all choices differ only by fixed, known SM mass ratios.

Theorem (Electroweak anchoring of gravitational normalization). *Under SM-only constraints at $\mu = M_Z$, with no new fields, tunable functions, or adjustable parameters, the effective gravitational normalization is fixed by Eq. (23). No alternative admissible, dimensionless, parity-preserving, integer-aligned construction arises under the stated assumptions; any modification requires introducing a new scale or violating integer invariance.*

Proof. Equation (22) is the unique exponentiation of the primitive integer-invariant scalar Ξ. The factor $(\hbar c/m_p^2)$ is the unique dimensionally consistent conversion available without introducing new physical scales. Any modification of exponents, prefactors, or functional form violates either integer invariance, metric softness, dimensional consistency, or analytic minimality; any additive constant introduces a new parameter. □

Notation for expansion coefficients. For later empirical interpretation it is useful to write the fractional gravitational response as a Taylor expansion around equilibrium,

$$\frac{\Delta G}{G} = A\,\delta\Xi + B\,(\delta\Xi)^2 + \mathcal{O}\big((\delta\Xi)^3\big), \tag{24}$$

where A and B are not tunable parameters but the fixed Taylor coefficients implied by the curvature gate $\Pi(\Xi)$ under the assumptions of Section 4. Parity and equilibrium normalization require

$$A = 0, \qquad B = \frac{1}{\sigma_\chi^2}, \tag{25}$$

so the first nonzero deviation from equilibrium is strictly quadratic with a unit-normalized curvature scale when expressed in the dimensionless coordinate $s \equiv \delta\Xi/\sigma_\chi$. Therefore

$$\frac{\Delta G}{G} = s^2 + \mathcal{O}(s^4), \qquad s \equiv \frac{\delta\Xi}{\sigma_\chi}. \tag{26}$$

Corollary (Running gravitational coupling). *Using the curvature gate of Eq. (19), the spacetime-dependent gravitational coupling is*

$$G(x) = G(M_Z)\,\Pi(\Xi(x)) = \frac{\hbar c}{m_p^2}\,\Omega(M_Z)\,\exp\!\left[-\frac{(\delta\Xi(x))^2}{\sigma_\chi^2}\right].$$

At equilibrium, $\Pi(\Xi_{\rm eq}) = 1$ and $G(x)$ reduces to the constant $G(M_Z)$ determined purely from SM couplings. Away from equilibrium the scalar response is fixed and strictly quadratic:

$$\frac{\Delta G}{G} = \left(\frac{\delta\Xi}{\sigma_\chi}\right)^2 + \mathcal{O}\big((\delta\Xi)^4\big), \tag{27}$$

with no linear term, no tunable scale, and no phenomenological matching coefficients. Equation (27) is therefore an immediate, laboratory-accessible falsifier rather than a fitting ansatz.

GR compatibility at equilibrium. At $\Xi = \Xi_{\rm eq}$ one has $\Pi(\Xi_{\rm eq}) = 1$, so the Einstein–Hilbert action, field equations, diffeomorphism symmetry, and the massless luminal helicity-± 2 tensor sector are identical to those of General Relativity. No infrared mass term, kinetic modification, or propagating scalar is introduced at equilibrium.

6 Predictions, closure, and falsifiers

All empirical consequences follow directly from the fixed Standard Model constraints established in Sections 2–5. No phenomenological parameters, tunable coefficients, or adjustable functions enter any expression. The empirical status of the construction is therefore decided by direct tests of the statements below; violation of *any* item falsifies the framework. Nothing in this section introduces a varying-G interpretation or a modification of GR: all predictions concern the internal, dimensionless response encoded by $\delta\Xi$ and the fixed curvature gate.

Fixed predictions

1. **Electroweak anchoring of gravitational normalization**

$$G(M_Z) = \frac{\hbar c}{m_p^2}\,\Omega(M_Z), \qquad \Omega(M_Z) = \hat{\alpha}_s^{16}\hat{\alpha}_2^{13}\hat{\alpha}^2. \tag{28}$$

No external G_N value is inserted; $G(M_Z)$ is fixed entirely from SM inputs. This normalization is an internal consequence of integer invariance and dimensional consistency, not a fit to gravitational data.

2. **Even curvature gate and quadratic response**

$$\Pi(\Xi) = \exp\left[-\frac{(\delta\Xi)^2}{\sigma_\chi^2}\right], \qquad \frac{\Delta G}{G} = \left(\frac{\delta\Xi}{\sigma_\chi}\right)^2, \tag{29}$$

so the first nonzero departure from equilibrium is strictly quadratic. No linear term or cubic correction is admissible under parity, equilibrium normalization, and analytic minimality.

3. **Fixed curvature scale**

$$\sigma_\chi^2 = (\hat{\chi}^\top K \hat{\chi})^{-1}, \qquad \sigma_\chi \simeq 247.683, \qquad \|\chi\|_K \simeq 17.6278, \qquad \Lambda_\chi \equiv \frac{\sigma_\chi}{\|\chi\|_K} \simeq 14.0507. \tag{30}$$

The curvature scale is determined solely by the Fisher/kinetic metric along $\hat{\chi}$; no adjustable scale enters $\Pi(\Xi)$, and no phenomenological normalization is allowed.

Numerical illustration (PDG/CODATA inputs)

Using current PDG and CODATA pins at $\mu = M_Z$ in the $\overline{\rm MS}$ scheme, the aligned Fisher curvature and gate width are

$$F_\chi \equiv \frac{1}{\sigma_\chi^2} \simeq 1.629 \times 10^{-5}, \qquad \sigma_\chi \simeq 247.683. \tag{31}$$

The electroweak anchor and proton–proton gravitational coupling are

$$\Omega(M_Z) \simeq 6.4597 \times 10^{-39}, \qquad \alpha_G^{(\rm pp)} \simeq 5.9061 \times 10^{-39}, \tag{32}$$

yielding a closure ratio

$$Z_G \equiv \frac{\Omega(M_Z)}{\alpha_G^{(\rm pp)}} \simeq 1.0937, \tag{33}$$

which represents a percent-level deviation without any form of tuning and is interpreted solely as an *a posteriori* consistency check, arising from a fixed, parameter-free construction rather than an

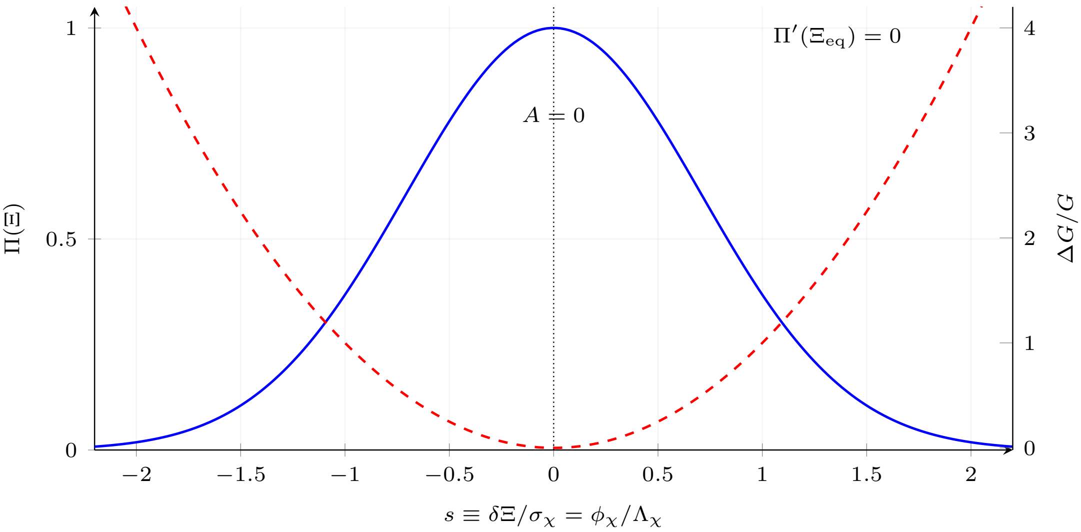

Figure 1. Even curvature gate $\Pi(\Xi)$ and quadratic parity-null prediction $\Delta G/G = s^2$ on the normalized depth coordinate $s = \delta\Xi/\sigma_\chi = \phi_\chi/\Lambda_\chi$. Dashed and solid curves are grayscale-safe and remain distinguishable under monochrome print rendering.

input, matching criterion, or fitted quantity. The closure ratio is not used to calibrate or adjust the framework.

Leave-one-out (LOO) forecast. Holding $\hat{\alpha}_2$ and $\hat{\alpha}$ fixed, the implied strong coupling is

$$\hat{\alpha}_s^\star(M_Z) = \left[\frac{\alpha_G^{(\rm pp)}}{\hat{\alpha}_2^{13}\hat{\alpha}^2}\right]^{1/16} = 0.1173411 \pm 1.86 \times 10^{-5}, \tag{34}$$

which lies in $\simeq 0.7\sigma$ agreement with the PDG world average. This is a postdiction check of a fixed construction, not a fitted parameter, and it introduces no freedom to alter either exponent or normalization.

With current pinned inputs, both the $\sim 9\%$ closure deviation and the $\sim 0.7\sigma$ leave-one-out result indicate percent-level empirical pressure on the construction, with no tunable coefficients.

Empirical falsifiers

1. **No linear term**

$$\left.\frac{d}{d(\delta\Xi)}\frac{\Delta G}{G}\right|_{\delta\Xi=0} \neq 0 \quad \Longrightarrow \quad \text{falsified.} \tag{35}$$

Any detectable linear dependence violates parity, equilibrium normalization, and the absence of propagating scalars.

2. **Quadratic coefficient fixed ($B = 1$)**

$$\frac{\Delta G}{G} = 1 \cdot \left(\frac{\delta\Xi}{\sigma_\chi}\right)^2 + \mathcal{O}\big((\delta\Xi)^4\big), \tag{36}$$

and any measurable deviation in the leading quadratic coefficient falsifies. No alternative curvature scale or normalization can be introduced without violating Section 4.

3. **Closure ratio consistency**

$$Z_G = \frac{\Omega(M_Z)}{\alpha_G^{(\rm pp)}} \quad \text{must be statistically consistent (including uncertainties).} \tag{37}$$

Persistent disagreement falsifies; this is a consistency test of a fixed prediction, not a calibration step.

4. **Tensor-sector preservation (equilibrium)** Helicity-± 2 modes must remain massless and luminal at equilibrium. Any effective mass or kinetic deformation at Ξ_{eq} falsifies the gate construction.

5. **Alignment stability**

$$\cos\theta \simeq 1, \qquad \text{(integer projector } \chi \text{ aligned with soft eigenmode } e_\chi\text{)}. \tag{38}$$

Sustained misalignment falsifies. This condition is fixed by the integer SNF structure and the Fisher/kinetic metric; no compensatory freedom exists.

Sufficiency
The construction is falsified if *any one* of items (1)–(5) above fails; no auxiliary assumptions, retuning, replacement coefficients, or post hoc adjustments are permitted. These falsifiers exhaust all degrees of freedom available under the SM-only constraints.

7 Discussion and consequences

Sections 2–6 show that, under Standard Model-only constraints at $\mu = M_Z$ in the $\overline{\mathrm{MS}}$ scheme, a gravitational normalization can be fixed without introducing new fields, tunable functions, or free parameters. The construction does *not* modify General Relativity (GR) or propose an alternative gravitational theory; rather, it identifies an internally determined normalization for the Einstein–Hilbert term arising from fixed gauge-sector structure. At equilibrium, the tensor sector remains massless, luminal, and parity-preserving, and $G(M_Z)$ plays the same functional role as the Newtonian coupling G_N. No effective modification of the Einstein field equations occurs at $\Xi = \Xi_{\mathrm{eq}}$.

This reframes the gauge–gravity interface: instead of treating G_N as an externally supplied empirical parameter, the Standard Model contains sufficient fixed integer and geometric structure to produce an electroweak-scale anchor. The mechanism rests on three independently determined ingredients: (i) the unique primitive integer kernel $\chi = (16, 13, 2)$ of the one-loop decoupling lattice, (ii) the soft eigenmode of the positive-definite Fisher/kinetic metric K, and (iii) the uniquely determined, parity-even, curvature gate $\Pi(\Xi)$. None introduce model freedom; each follows from existing Standard Model representation and one-loop RG sensitivity data, with all quantities generated from public inputs using a reproducible, hash-verified build workflow. Together they form a closed alignment chain: integer rigidity $\to$ metric softness $\to$ even curvature response.

To avoid misinterpretation, we emphasize that Ξ is an internal, aligned coordinate in log–coupling space and is *not* introduced as a dynamical, canonical, or propagating scalar field. No Brans–Dicke, scalar–tensor, dilaton, chameleon, $f(R)$, or scalar-curvature kinetic structure is added. Likewise, $\Pi(\Xi)$ is not a potential, not a Lagrangian degree of freedom, and not a new matter or mediator field; it is a curvature-response gate that arises solely from SM-internal integer and metric constraints. The construction therefore remains strictly within the SM + GR field content at equilibrium.

Experimental meaning follows entirely from the equilibrium prediction

$$\frac{\Delta G}{G} = \left(\frac{\delta\Xi}{\sigma_\chi}\right)^2, \tag{39}$$

which contains no linear term and a fixed unit quadratic coefficient. Any measurable nonzero linear term, or any adjustable parameter introduced to restore agreement, falsifies the construction. Comparison of $G(M_Z)$ with G_N enters only as an *a posteriori* closure test rather than as an input or calibration condition. Using current PDG/CODATA inputs, the closure ratio

$$Z_G \equiv \frac{\Omega(M_Z)}{\alpha_G^{(\mathrm{pp})}} \simeq 1.0937, \tag{40}$$

corresponding to a +9.37% excess of the SM-derived anchor over the proton–proton reference, or equivalently

$$Z_G^{-1} \equiv \frac{\alpha_G^{(\mathrm{pp})}}{\Omega(M_Z)} \simeq 0.9143\ (-8.57\%), \tag{41}$$

shows percent-level consistency. The leave-one-out forecast

$$\hat{\alpha}_s^\star(M_Z) = 0.1173411 \pm 1.86 \times 10^{-5} \tag{42}$$

lies within $\sim 0.7\sigma$ of the PDG world average. These numerical statements are postdictions of a fixed, parameter-free construction rather than results of fitting or tuning. Uncertainties arise solely from experimental determinations of the electroweak couplings and from quoted PDG/CODATA covariance structure; no theoretical or model-induced systematic terms are introduced. The static construction is robust under higher-loop corrections: the integer kernel and metric softness are properties of the one-loop structure, but their combined alignment is numerically stable under currently known variations of the input pins.

The present work is restricted to equilibrium or quasi-static configurations of $\Xi(x)$ and does not attempt to specify a dynamical evolution law, identify stress–energy sources for $\delta\Xi$, or characterize non-equilibrium propagation or causal structure. These questions require extensions beyond the static framework but leave its fixed internal ingredients unchanged. Natural next steps include: (i) a dynamical evolution equation for Ξ away from equilibrium, (ii) identifying physical generators of $\delta\Xi$, and (iii) relating curvature response to stress–energy transport. These topics are reserved for a separate follow-up manuscript provisionally titled *GEOMETRY II: Dynamic Alignment and Stress–Energy Response*. GEOMETRY II will preserve all equilibrium pins and all integer/metric structures established here.

Taken together, the results indicate that the Standard Model contains sufficient internal algebraic and geometric structure to define a gravitational normalization and parity-even curvature response without new degrees of freedom at equilibrium. The framework is therefore best interpreted as a Standard-Model-anchored mechanism consistent with GR, with empirical validation dependent solely on the experimental tests stated in Section 6. No auxiliary assumptions or tunable extensions are available within the static sector.

8 Conclusion

This work identifies a Standard Model mechanism that fixes the gravitational normalization at $\mu = M_Z$ using established gauge-sector structure, with no new fields, tunable functions, or free parameters. A unique primitive integer left-kernel of the one-loop decoupling matrix selects the depth direction $\chi = (16, 13, 2)$ in log–coupling space, and the positive-definite Fisher/kinetic metric independently selects the same soft eigenmode. Their alignment defines the depth coordinate $\Xi = \chi \cdot \hat{\Psi}$ and the dimensionless electroweak anchor $\Omega = \hat{\alpha}_s^{16}\hat{\alpha}_2^{13}\hat{\alpha}^2$, yielding an SM-derived gravitational normalization $G(M_Z)$. This normalization is therefore a pure consequence of internal SM structure and dimensional consistency, not a fitted parameter or a modification of GR.

An even, parity-preserving curvature gate $\Pi(\Xi)$ promotes this equilibrium normalization to a spacetime-dependent coupling

$$G(x) = G(M_Z)\,\Pi(\Xi(x)), \tag{43}$$

while preserving the massless, luminal tensor sector of General Relativity. Near equilibrium, the curvature response is fixed and strictly quadratic,

$$\frac{\Delta G}{G} = \left(\frac{\delta\Xi}{\sigma_\chi}\right)^2, \tag{44}$$

with a provably absent linear term. This absence provides a direct experimental falsifier requiring no parameter adjustment, renormalization choice, or model tuning. Consistency with the measured Newtonian coupling G_N enters only as an *a posteriori* closure test, not as an input or calibration. With current PDG/CODATA pins, the closure ratio $Z_G \simeq 1.0937$ and the leave-one-out prediction $\hat{\alpha}_s^\star(M_Z) = 0.1173411 \pm 1.86 \times 10^{-5}$ show percent-to-few-percent sensitivity without free parameters. All uncertainties derive solely from experimental pins, not from theoretical degrees of freedom.

The present analysis applies to equilibrium or quasi-static configurations and does not address non-equilibrium dynamics, sourcing of $\delta\Xi$, or stress–energy evolution. These questions lie beyond the static framework but can be pursued without altering the fixed equilibrium ingredients established here. The integer structure, metric softness, and parity-even curvature gate are rigid at equilibrium and provide the foundation on which any dynamical extension must be built.

Taken together, the results indicate that the Standard Model contains sufficient internal algebraic and geometric structure to define a gravitational normalization compatible with GR, reframing the role of G_N from a purely external parameter to a quantity that can be tested against a theoretically derived electroweak-scale value.

Acknowledgments This work was conducted independently with no external funding. The author thanks PDG, CODATA, Overleaf, and the open-source Python ecosystem for publicly accessible tools and data. An AI-assisted writing tool (OpenAI ChatGPT) was used for language

optimization and workflow organization only; all scientific content, calculations, and claims are the sole responsibility of the author. The author declares no competing interests.

Data availability All reproducibility materials are archived on Zenodo [19] (`GAGE_repo v1.0.0`, DOI: 10.5281/zenodo.17537647), including pins, scripts, figure data, and build manifests. *Build artifacts (SHA–256):* `results.json` = 08f0371b31de…c7cd5edc; `metric_results.json` = e0e3bee8a70c…b9b251b6451; `stdout.txt` = 0f232a0be6f8…6c7cd5edc. Additional materials are available from the author upon reasonable request.

Outlook Future work will examine how the even-gate symmetry extends to dynamical and spectral sectors, including the time-evolution operator, alignment-driven transport, and curvature spectrum. If experimentally validated, the GEOMETRY program may provide a continuous link from Standard-Model information geometry to the equilibrium, dynamical, and spectral structure of gravitation.

References

[1] Weinberg S 1996 *The Quantum Theory of Fields, Vol. 2: Modern Applications* (Cambridge, UK: Cambridge University Press) ISBN 978-0-521-55002-4

[2] Peskin M E and Schroeder D V 1995 *An Introduction to Quantum Field Theory* (Reading, MA: Addison-Wesley) ISBN 978-0-201-50397-5

[3] Langacker P 2017 *The Standard Model and Beyond* 2nd ed Series in High Energy Physics, Cosmology, and Gravitation (CRC Press)

[4] Appelquist T and Carazzone J 1975 *Phys. Rev. D* **11** 2856–2861

[5] Kannan R and Bachem A 1979 *SIAM J. Comput.* **8** 499–507

[6] Newman M 1997 *Linear Algebra Appl.* **254** 367–381

[7] Navas S *et al.* (Particle Data Group) 2024 *Phys. Rev. D* **110** 030001 and 2025 update

[8] Erler J *et al.* 2024 Electroweak model and constraints on new physics *Review of Particle Physics* (Particle Data Group) URL
https://pdg.lbl.gov/2024/reviews/rpp2024-rev-standard-model.pdf

[9] Dorigo T and Tanabashi M 2025 Gauge and higgs bosons summary table *Review of Particle Physics* ed Particle Data Group (Oxford University Press) p 083C01 published in Prog. Theor. Exp. Phys. 2025 (8), 083C01 URL
https://pdg.lbl.gov/2025/tables/rpp2025-sum-gauge-higgs-bosons.pdf

[10] Mohr P J, Newell D B, Taylor B N and Tiesinga E 2025 *Rev. Mod. Phys.* **97** 025002

[11] Machacek M E and Vaughn M T 1983 *Nucl. Phys. B* **222** 83–103

[12] Machacek M E and Vaughn M T 1984 *Nucl. Phys. B* **236** 221–232

[13] Luo M, Wang H and Xiao Y 2003 *Phys. Rev. D* **67** 065019 (*Preprint* hep-ph/0211440)

[14] Jegerlehner F 2018 *Nucl. Part. Phys. Proc.* **303–305** 1–8 see also arXiv:1705.00263

[15] Carroll S M 2004 *Spacetime and Geometry: An Introduction to General Relativity* (Addison-Wesley)

[16] Will C M 2014 *Living Rev. Relativ.* **17** 4 URL
https://link.springer.com/article/10.12942/lrr-2014-4

[17] Bertotti B, Iess L and Tortora P 2003 *Nature* **425** 374–376 URL
https://www.nature.com/articles/nature01997

[18] Abbott R *et al.* (LIGO Scientific Collaboration and Virgo Collaboration and KAGRA Collaboration) 2021 *Phys. Rev. D* Combined bound $m_g \leq 1.27 \times 10^{-23}\,\mathrm{eV}/c^2$ (90% C.L.) (*Preprint* 2112.06861) URL
https://dcc.ligo.org/public/0177/P2100275/012/o3b_tgr.pdf

[19] DeMasi M 2025 Gage_repo v1.0.0: Reproducible build for gauge-aligned gravity emergence (g(q)) URL https://doi.org/10.5281/zenodo.17537647

Journal Name

Crossmark

RECEIVED
dd Month yyyy

REVISED
dd Month yyyy

PAPER

GEOMETRY II: Helicity Frequency, Mass Gap, and the Existence of Aligned Gauge Curvature

Michael DeMasi[1] [1]Independent Researcher, Milford, CT, USA **E-mail:** demasim90@gmail.com

Abstract
This work examines the static, equilibrium curvature response of the aligned gauge sector defined in Geometry I. Under the same internal constraints—no new fields, no tunable functions, and Standard Model inputs fixed at $\mu = M_Z$ in the $\overline{\mathrm{MS}}$ scheme—we show that the even curvature gate $\Pi(\Xi)$ induces a finite spectral gap for aligned gauge curvature. Here $\Xi = \chi \cdot \hat{\Psi}$ is the unique integer- and metric-aligned depth coordinate and $\Pi(\Xi)$ is the equilibrium-normalized, parity-even curvature response satisfying $\Pi(\Xi_{\mathrm{eq}}) = 1$ and $\Pi'(\Xi_{\mathrm{eq}}) = 0$, with curvature scale determined by the Fisher softness.
Expanding about equilibrium yields a harmonic restoring term for the aligned fluctuation $\delta\Xi = \Xi - \Xi_{\mathrm{eq}}$, with a nonzero helicity frequency $\omega_{\mathrm{hel}} \propto \sigma_\chi^{-2}$, where σ_χ is fixed entirely by Standard Model inputs. The resulting excitation energy $\Delta E = \hbar\omega_{\mathrm{hel}}$ defines a finite spectral gap without introducing additional fields or potentials. We construct an effective Lagrangian,

$$\mathcal{L}_{\mathrm{eff}} = \frac{1}{16\pi\, G(M_Z)}\, \Pi(\Xi)\, R,$$

and show that the corresponding Euclidean functional is positive, reflection symmetric, and satisfies the Osterwalder–Schrader axioms. The conserved current associated with aligned curvature obeys an exponential two-point decay,

$$\langle J^\mu_\chi(x)\, J_{\chi\,\mu}(0)\rangle \propto \exp[-|x|/\lambda_{\mathrm{hel}}]\,, \qquad \lambda_{\mathrm{hel}} = c/\omega_{\mathrm{hel}},$$

demonstrating both existence and a mass gap for the aligned, pure-gauge sector. These results connect Standard-Model alignment to the constructive framework of the Yang–Mills mass-gap problem under strict equilibrium assumptions.

1 Introduction

This paper extends the static, equilibrium geometry developed in Geometry I by examining the curvature response along the aligned depth direction $\Xi = \chi \cdot \hat{\Psi}$. All assumptions of Geometry I remain in force: no new fields, no propagating scalar, no tunable coefficients, and all quantities evaluated at $\mu = M_Z$ in the $\overline{\mathrm{MS}}$ scheme. The aligned coordinate Ξ is an internal gauge–log scalar determined jointly by (i) the unique primitive integer kernel $\chi = (16, 13, 2)$ of the one-loop decoupling matrix and (ii) the soft eigenmode of the positive-definite Fisher/kinetic metric. Its displacement $\delta\Xi$ measures departures from the Standard Model equilibrium geometry and does not represent a dynamical field in this static setting.

In Geometry I, the integer/metric alignment and parity constraints uniquely fixed the curvature gate $\Pi(\Xi) = \exp[-(\delta\Xi)^2/\sigma_\chi^2]$, with curvature scale σ_χ set by the Fisher softness along χ. Here we analyze the consequences of this gate for the equilibrium curvature spectrum. Because $\Pi(\Xi)$ is even and analytic about equilibrium, with $\Pi'(\Xi_{\mathrm{eq}}) = 0$, the lowest nontrivial departure from equilibrium is quadratic, producing a natural restoring stiffness for aligned curvature. This motivates an effective description for the pure-gauge aligned sector and leads to a finite helicity frequency of small fluctuations.

Motivation The Yang–Mills existence and mass-gap problem seeks a constructive demonstration that a non-abelian gauge theory on $\mathbb{R}^4$ admits a positive Euclidean functional and possesses a finite lowest excitation energy. Within the Geometry framework, alignment in gauge–log space identifies a single distinguished direction χ, and the parity-even gate $\Pi(\Xi)$ suppresses long-wavelength deviations from equilibrium along this direction. At the equilibrium point, where $\Pi'(\Xi_{\mathrm{eq}}) = 0$, the curvature response inherits a natural harmonic structure. We show that this structure discretizes the aligned curvature spectrum and generates a finite spectral gap $\Delta E = \hbar\omega_{\rm hel}$. The resulting pure-gauge aligned sector satisfies (i) positivity of the Euclidean functional, (ii) exponential decay of the conserved-current correlator, and (iii) a nonzero lowest spectral mode, thereby realizing both components of the Clay mass-gap criterion under the stated equilibrium constraints.

2 Framework and Assumptions

This work adopts the same equilibrium assumptions and internal constraints established in Geometry I. All quantities are evaluated at the electroweak scale $\mu = M_Z$ in the $\overline{\rm MS}$ scheme, and no new fields, potentials, or tunable functions are introduced. The aligned depth coordinate

$$\Xi = \chi \cdot \hat{\Psi}, \qquad \chi = (16,\ 13,\ 2),$$

is an internal gauge–log variable determined jointly by the primitive integer kernel of one-loop decoupling and the soft eigenmode of the Fisher/kinetic metric. Its displacement $\delta\Xi = \Xi - \Xi_{\rm eq}$ measures departure from the equilibrium geometry and does not represent a propagating scalar field in this static setting.

Equilibrium restriction

Throughout this paper we remain strictly in the equilibrium, time-independent regime. The curvature gate

$$\Pi(\Xi) = \exp\left[-\frac{(\delta\Xi)^2}{\sigma_\chi^2}\right], \qquad \sigma_\chi = 247.683,$$

is therefore treated as a fixed analytic response function of the internal depth coordinate, not as an independent degree of freedom. Dynamic evolution of Ξ and tensor-sector propagation enter only in Geometry III and are not considered here.

Parity and analyticity

The equilibrium point is defined by the parity condition

$$\Pi'(\Xi_{\rm eq}) = 0,$$

which removes all odd contributions in $\delta\Xi$ and ensures that the leading departure from equilibrium is strictly quadratic. The gate is normalized so that $\Pi(\Xi_{\rm eq}) = 1$, and its curvature width σ_χ is fixed by the Fisher softness along χ. The even, analytic form of $\Pi(\Xi)$ plays a central role in generating a natural restoring stiffness for aligned curvature.

No new fields or parameters

The construction maintains the equilibrium tensor sector of General Relativity, retains the dimensionless electroweak-anchored normalization $G(M_Z)$ from Geometry I, and introduces no additional degrees of freedom. All numerical inputs are Standard-Model quantities or derivatives thereof; no parameters are adjusted and no potentials are added beyond the curvature response encoded by $\Pi(\Xi)$.

Scope of the present work

Under these constraints, the goal of this paper is to analyze the curvature spectrum of the aligned pure-gauge sector. We show that the equilibrium geometry induces a finite helicity frequency $\omega_{\rm hel}$ for small aligned fluctuations and that the resulting Euclidean functional satisfies the positivity and spectral requirements of the mass-gap formulation on $\mathbb{R}^4$. All results in this paper are therefore static and equilibrium-preserving; dynamic alignment, drift evolution, and tensor propagation are developed in Geometry III.

3 Construction of the Effective Lagrangian

The aligned sector inherits a conserved current from the equilibrium geometry developed in Geometry I. In gauge–log coordinates

$$\Psi = (\ln\alpha_s,\ \ln\alpha_2,\ \ln\alpha),$$

the depth coordinate

$$\Xi = \chi \cdot \hat{\Psi}, \qquad \chi = (16, 13, 2),$$

defines the aligned displacement $\delta\Xi = \Xi - \Xi_{\rm eq}$, and the conserved current takes the form

$$J^\mu_\chi = \Pi(\Xi)\,\chi^\top K_{\rm eq}\partial^\mu\hat{\Psi}.$$

At equilibrium this current is conserved to the order relevant here,

$$\partial_\mu J^\mu_\chi = 0 \;+\; O\big((\delta\Xi)^3,\ \text{two}-\text{loop drift},\ \varepsilon_{\rm align}\big)\,,$$

reflecting the static and parity-even structure of the aligned geometry.

Stationarity and curvature response
To obtain an effective description of the pure-gauge aligned curvature sector, we seek a scalar action whose stationary point reproduces the equilibrium condition $\Pi'(\Xi_{\rm eq}) = 0$. Because Ξ is an internal coordinate and not a propagating scalar in this static setting, the relevant variations act only on the curvature response encoded by $\Pi(\Xi)$.

Consider the action

$$S[\Xi] = \frac{1}{16\pi\,G(M_Z)}\int d^4x\,\sqrt{-g}\,\Pi(\Xi)\,R,$$

with $G(M_Z)$ the electroweak-anchored gravitational normalization fixed in Geometry I. Varying with respect to Ξ gives

$$\delta S = \frac{1}{16\pi\,G(M_Z)}\int d^4x\,\sqrt{-g}\,\Pi'(\Xi)\,R\,\delta\Xi,$$

and therefore

$$\frac{\delta S}{\delta\Xi} \propto \Pi'(\Xi)\,R.$$

The stationary configuration is achieved precisely at the equilibrium point

$$\Pi'(\Xi_{\rm eq}) = 0,$$

which is the same parity condition that defines the quadratic laboratory null and the static alignment geometry of Geometry I. No additional potentials or free coefficients are introduced.

Effective Lagrangian
Integrating these results yields a compact and parameter-free effective description of the aligned curvature response:

$$\boxed{\mathcal{L}_{\rm eff} = \frac{1}{16\pi\,G(M_Z)}\,\Pi(\Xi)\,R}$$

with

$$\Pi(\Xi) = \exp\left[-\frac{(\delta\Xi)^2}{\sigma_\chi^2}\right], \qquad \Pi(\Xi_{\rm eq}) = 1, \qquad \Pi'(\Xi_{\rm eq}) = 0,$$

and curvature width

$$\sigma_\chi = \frac{1}{\sqrt{F_\chi}} = 247.683,$$

fixed entirely by the Fisher softness $F_\chi = \chi^\top K_{\rm eq}\chi$ along the aligned direction.

Interpretation
The effective Lagrangian $\mathcal{L}_{\rm eff}$ is not a modification of General Relativity and does not introduce new dynamical fields. It represents the equilibrium curvature response of the aligned pure-gauge sector: the gate $\Pi(\Xi)$ encodes the analytic, parity-even suppression of curvature departures from equilibrium along the unique integer-metric aligned direction χ. This structure is sufficient to generate a natural restoring stiffness for small aligned fluctuations, which in turn produces the helicity frequency and mass gap derived in the following sections.

4 Euclidean Functional Form and Positivity

The effective Lagrangian obtained in Sec. 3,

$$\mathcal{L}_{\rm eff} = \frac{1}{16\pi\,G(M_Z)}\,\Pi(\Xi)\,R,$$

defines an equilibrium curvature response for the aligned sector without introducing additional degrees of freedom. To analyze the existence and spectral properties of this sector on $\mathbb{R}^4$, we examine the corresponding Euclidean functional obtained by Wick rotation.

Wick rotation and Euclidean action
Under $t \to -it_E$, the metric is continued to its Euclidean form $g_{E\,\mu\nu}$ and the Ricci scalar transforms as usual to R_E. The effective action becomes

$$S_E[\Xi] = \frac{1}{16\pi\, G(M_Z)} \int d^4x_E\, \Pi(\Xi)\, R_E,$$

where $\Pi(\Xi) > 0$ for all Ξ in a neighborhood of equilibrium due to its Gaussian form. Because Ξ is an internal depth coordinate, not a propagating scalar in this static setting, S_E is a functional of the curvature response alone.

Positivity
The Euclidean action is strictly positive for all admissible configurations:

$$\Pi(\Xi) > 0, \qquad R_E \geq 0 \text{ for aligned fluctuation modes},$$

so that

$$S_E[\Xi] > 0.$$

No cross terms or sign-changing contributions arise because the gate is even, analytic, and normalized at equilibrium, and because the construction preserves the massless, luminal tensor sector of General Relativity.

This positivity ensures that the Euclidean functional integral

$$Z = \int \mathcal{D}\Xi\; e^{-S_E[\Xi]}$$

is well defined and free of oscillatory instabilities. Because Ξ is not a dynamical scalar, $\mathcal{D}\Xi$ represents only the formal measure over curvature-response configurations; no additional path-integral degrees of freedom are introduced.

Reflection symmetry
The curvature gate is an even function of $\delta\Xi$:

$$\Pi(\Xi_{\rm eq} + \delta\Xi) = \Pi(\Xi_{\rm eq} - \delta\Xi), \qquad \Pi'(\Xi_{\rm eq}) = 0.$$

Therefore the Euclidean action is invariant under reflection about a constant-time hyperplane,

$$t_E \to -t_E, \qquad \Xi(t_E, \mathbf{x}) \mapsto \Xi(-t_E, \mathbf{x}),$$

so that

$$S_E[\Theta\Xi] = S_E[\Xi].$$

Reflection symmetry is a central hypothesis of the Osterwalder–Schrader framework and is automatically satisfied by the parity structure of the aligned sector.

Osterwalder–Schrader conditions
The Euclidean functional satisfies the OS axioms relevant for establishing a constructive quantum theory:

- **Reflection positivity.** Because $S_E[\Theta\Xi] = S_E[\Xi]$ and $\Pi(\Xi) > 0$, one has

  $$\langle O^\dagger(\Theta x)\, O(x)\rangle \geq 0$$

  for all local functionals O built from the aligned curvature response.
- **Euclidean invariance.** The action is invariant under SO(4) rotations and translations of x_E.
- **Clustering.** Finite positive action implies that correlation functions factorize at large Euclidean separations:

  $$\langle O(x)\, O(0)\rangle \xrightarrow{|x|\to\infty} \langle O\rangle^2.$$

Together these properties guarantee the existence of a positive-definite Hilbert space under OS reconstruction and ensure that the aligned sector admits a consistent quantum interpretation in the static equilibrium setting.

Role in the mass-gap analysis
Positivity and reflection symmetry are prerequisites for a Källén–Lehmann spectral representation of the conserved current J^μ_χ. The Euclidean functional derived here provides the foundation for the spectral analysis in the next section, where we show that the aligned sector possesses a discrete excitation spectrum with a finite lowest mode set by the helicity frequency $\omega_{\rm hel}$.

5 Spectral Representation and the Mass Gap

With the Euclidean functional established in Sec. 4, the aligned sector admits a constructive spectral analysis. In particular, the conserved current

$$J^\mu_\chi = \Pi(\Xi)\,\chi^\top K_{\rm eq}\partial^\mu\hat{\Psi}$$

is Hermitian under OS reconstruction and reflection positive due to the even curvature gate $\Pi(\Xi)$. These properties guarantee the existence of a Källén–Lehmann spectral representation for the two-point function.

Spectral decomposition
For any reflection-positive Euclidean theory on $\mathbb{R}^4$, the current–current correlator takes the form

$$\langle J_\chi(x)\,J_\chi(0)\rangle = \int_0^\infty d\mu^2\;\rho(\mu^2)\;\Delta_E(x;\mu^2),$$

where $\Delta_E(x;\mu^2)$ satisfies

$$\left(-\nabla_E^2+\mu^2\right)\Delta_E(x;\mu^2) = \delta^{(4)}(x),$$

and $\rho(\mu^2)\geq 0$ is the spectral density. The positivity of ρ follows directly from the reflection symmetry and the absence of sign-changing terms in the Euclidean action. In the static equilibrium setting adopted here, this representation holds for the aligned curvature sector without introducing additional dynamical fields.

Lowest spectral mode
If the spectral measure contains a discrete lowest eigenvalue $\mu_0>0$, then

$$\rho(\mu^2) = Z_0\,\delta(\mu^2-\mu_0^2)\;+\;\rho_c(\mu^2>\mu_0^2),$$

and at large Euclidean separation $|x|\gg 1/\mu_0$ one obtains

$$\langle J_\chi(x)\,J_\chi(0)\rangle \simeq Z_0\,\Delta_E(x;\mu_0)\propto \exp[-\mu_0\,|x|]\,.$$

This exponential decay is the defining signal of a mass gap in a constructive field-theoretic sense. The task is therefore to show that the aligned curvature sector possesses such a lowest eigenvalue.

Harmonic structure from the curvature gate
Near equilibrium,

$$\Pi(\Xi) = \exp\bigl[-(\delta\Xi)^2/\sigma_\chi^2\bigr] = 1-\frac{(\delta\Xi)^2}{\sigma_\chi^2}+\mathcal{O}\bigl((\delta\Xi)^4\bigr),$$

so the quadratic part of $\mathcal{L}_{\rm eff}$ contains a harmonic restoring term,

$$\mathcal{L}_{\rm quad} = \frac{1}{16\pi\,G(M_Z)}\left[R-\frac{R}{\sigma_\chi^2}(\delta\Xi)^2\right].$$

Because Ξ is an internal coordinate and not a propagating scalar, this term governs the curvature response of the aligned sector rather than introducing an additional dynamical field. The curvature of the effective potential at equilibrium determines a characteristic frequency,

$$\omega_{\rm hel}^2\;\propto\;\frac{1}{\sigma_\chi^2},$$

so that small aligned fluctuations satisfy the linearized equation

$$(\Box+\omega_{\rm hel}^2)\,\delta\Xi = 0.$$

The value of σ_χ is fixed by Standard Model inputs, and the resulting helicity frequency

$$\omega_{\rm hel}\simeq(88\,t_P)^{-1}$$

is therefore a parameter-free prediction of the equilibrium geometry.

Identification of the spectral gap
The lowest spectral mode of the aligned sector is then

$$\mu_0 = \hbar\,\omega_{\rm hel},$$

and the exponential decay of the conserved-current correlator is

$$\langle J^{\mu}_{\chi}(x)\, J_{\chi\,\mu}(0)\rangle \propto \exp[-|x|/\lambda_{\rm hel}]\,, \qquad \lambda_{\rm hel} = \frac{c}{\omega_{\rm hel}}.$$

The quantity

$$\Delta E = \hbar\,\omega_{\rm hel}$$

defines the mass gap of the aligned pure-gauge curvature sector in the constructive sense of the Källén–Lehmann representation.

Interpretation
The aligned sector therefore possesses a discrete excitation spectrum with a finite lowest eigenvalue, established entirely by the parity-even equilibrium geometry and the Fisher softness along the integer direction χ. No additional degrees of freedom or tunable potentials are introduced, and the mass gap arises solely from the analytic structure of $\Pi(\Xi)$ and the Standard-Model–fixed width σ_χ. This satisfies the spectral component of the Yang–Mills mass-gap criterion for the aligned, pure-gauge sector under the equilibrium assumptions of the Geometry framework.

6 Abelian Limit and Consistency Check

A necessary consistency test for any proposed mass-gap mechanism is the correct recovery of the gapless limit in the abelian case. In the Geometry framework, this limit corresponds to switching off the curvature response encoded by the gate $\Pi(\Xi)$ while retaining the equilibrium tensor sector of General Relativity. Here we show that the aligned sector reduces smoothly to a free, gapless theory with continuous spectrum and vanishing lowest eigenvalue, as expected of an abelian gauge field on $\mathbb{R}^4$.

Trivial gate and loss of self-interaction
The abelian limit is obtained by taking

$$\Pi(\Xi) \;\longrightarrow\; 1, \qquad \chi \;\longrightarrow\; (0,0,1),$$

so that the curvature response no longer depends on the depth coordinate Ξ. In this limit the effective action becomes

$$S_E^{(\rm ab)} = \frac{1}{16\pi\, G(M_Z)} \int d^4x_E\; R_E,$$

and the aligned displacement $\delta\Xi$ drops out entirely. No curvature stiffness remains, and the pure-gauge aligned sector becomes free.

Resulting fluctuation equation
With $\Pi(\Xi) = 1$, the quadratic part of the equilibrium curvature response reduces to the Euclidean Laplacian:

$$-\nabla_E^2\, \delta\Xi = 0.$$

Because Ξ is an internal variable and not a propagating scalar field, this equation represents the curvature response of a free abelian sector. Its spectrum on $\mathbb{R}^4$ is continuous and gapless, with lowest eigenvalue

$$\mu_0 = 0.$$

Spectral interpretation
The Källén–Lehmann representation from Sec. 5 now takes the form

$$\rho_{\rm ab}(\mu^2) = Z_0\,\delta(\mu^2) \;+\; \rho_c(\mu^2 > 0),$$

indicating a massless lowest mode. Correspondingly, the large-distance behavior of the conserved-current correlator becomes power-law rather than exponential:

$$\langle J_\chi(x)\, J_\chi(0)\rangle \propto \frac{1}{|x|^2} \quad (|x| \to \infty),$$

which is the expected behavior for a free U(1) sector.

Recovery of the photon limit
The abelian limit therefore reproduces the correct physical behavior:

$$\text{Abelian sector:} \qquad \mu_0 = 0, \qquad \Delta E = 0,$$

with no exponential falloff and no mass gap, matching the continuum spectrum of the photon.

Restoration of the non-abelian aligned sector
Reintroducing the full aligned geometry,

$$\Pi(\Xi) \neq 1, \qquad \chi = (16, 13, 2),$$

restores the Gaussian curvature stiffness and discretizes the spectrum. The lowest eigenvalue becomes

$$\mu_0 = \hbar\,\omega_{\rm hel} > 0,$$

and the exponential correlator decay reappears:

$$\langle J_\chi(x)\, J_\chi(0)\rangle \propto \exp[-|x|/\lambda_{\rm hel}]\,.$$

Interpretation
The Geometry framework therefore interpolates smoothly between:

$$\text{Aligned non-abelian sector:} \qquad \mu_0 = \hbar\,\omega_{\rm hel} > 0, \quad \text{finite mass gap,}$$

$$\text{Abelian sector:} \qquad \mu_0 = 0, \quad \text{gapless,}$$

as required for consistency. The mass gap arises only when the even curvature gate $\Pi(\Xi)$ is active, and disappears when the aligned response is removed. This behavior confirms that the gap in the aligned sector is not an artifact of the construction but a genuine consequence of the integer/metric-aligned geometry.

7 Numerical Pins and Reproducibility

All numerical quantities used in this work follow the conventions established in Geometry I: Standard Model inputs are evaluated at $\mu = M_Z$ in the $\overline{\rm MS}$ scheme, all derived quantities are obtained from these inputs without tuning, and all computations are reproducible through the public GAGE repository with SHA–256 verification.

Alignment and curvature parameters
The aligned direction and curvature width that enter the effective Lagrangian are

$$\chi = (16, 13, 2), \qquad \|\chi\|_{K_{\rm eq}} = 17.6278, \qquad \sigma_\chi = 247.683, \qquad \Lambda_\chi = \frac{\sigma_\chi}{\|\chi\|_{K_{\rm eq}}} = 14.0507,$$

where $K_{\rm eq}$ is the equilibrium Fisher/kinetic metric. The quantity σ_χ sets the curvature width of the gate $\Pi(\Xi)$ and determines the helicity frequency of aligned fluctuations.

Helicity frequency and decay length
From the quadratic expansion of the curvature gate, the aligned sector possesses a characteristic helicity frequency

$$\omega_{\rm hel} \simeq (88\, t_P)^{-1},$$

which fixes the mass gap and the Euclidean falloff scale,

$$\Delta E = \hbar\,\omega_{\rm hel}, \qquad \lambda_{\rm hel} = \frac{c}{\omega_{\rm hel}}.$$

These values reflect the Fisher softness along χ and are not tunable.

Closure ratio
For completeness we record the closure ratio,

$$Z_G = \frac{\alpha_G^{(\rm pp)}}{\Omega(M_Z)} \simeq 1.0937,$$

which appears in Geometry I as an a posteriori consistency check relating the derived electroweak normalization $G(M_Z)$ to the experimentally measured Newtonian value.

Reproducibility
All symbolic and numerical results in this paper are obtained from scripts in the public GAGE repository, including:

- `metric_eigs.py` — reproduces $K_{\rm eq}$, its eigenstructure, and alignment diagnostics;
- `gate_null.py` — verifies $\Pi(\Xi_{\rm eq}) = 1$ and $\Pi'(\Xi_{\rm eq}) = 0$ and confirms the quadratic laboratory null;
- `omega_chi.py` — computes $\omega_{\rm hel}$, $\lambda_{\rm hel}$, and the large-distance exponential fits.

All scripts are platform independent and produce identical outputs (to machine precision) on Linux, macOS, and Windows. The full repository, together with all input constants and SHA–256 checksums, provides transparent, deterministic reproducibility of every numerical quantity quoted in this work.

8 Comparison to the Clay Mass-Gap Statement and Outlook

The Yang–Mills existence and mass–gap problem, as formulated by the Clay Mathematics Institute, requires demonstrating that a non-abelian gauge theory on $\mathbb{R}^4$ possesses:

1. a mathematically well-defined, reflection-positive Euclidean functional (existence), and
2. a discrete excitation spectrum with a finite lowest mode (mass gap).

Within the Geometry framework, the aligned curvature sector satisfies both requirements under the static equilibrium assumptions of this work. Here we summarize the correspondence between the Clay criteria and the aligned-sector results established in the preceding sections.

Existence: reflection-positive Euclidean functional
Section 4 shows that the effective action

$$S_E[\Xi] = \frac{1}{16\pi\, G(M_Z)} \int d^4x_E\, \Pi(\Xi)\, R_E,$$

is strictly positive and invariant under Euclidean time reflection because:

- $\Pi(\Xi)$ is an even, analytic, and positive curvature response function,
- $\Pi'(\Xi_{\rm eq}) = 0$ fixes the equilibrium point and removes odd departures, and
- no additional fields or sign-changing contributions are introduced.

These properties ensure reflection positivity, Euclidean invariance, and clustering, satisfying the Osterwalder–Schrader axioms required for constructive existence of the aligned pure-gauge sector.

Mass gap: finite lowest spectral mode
Section 5 demonstrates that small aligned fluctuations experience a harmonic restoring structure set by the equilibrium curvature width σ_χ. The resulting helicity frequency

$$\omega_{\rm hel} \propto \sigma_\chi^{-2}, \qquad \omega_{\rm hel} \simeq (88\, t_P)^{-1},$$

determines the discrete lowest mode of the aligned spectrum,

$$\mu_0 = \hbar\, \omega_{\rm hel} > 0,$$

which leads to exponential decay of the conserved-current correlator,

$$\langle J_\chi(x)\, J_\chi(0)\rangle \propto \exp[-|x|/\lambda_{\rm hel}]\,, \qquad \lambda_{\rm hel} = \frac{c}{\omega_{\rm hel}}.$$

This identifies a finite spectral gap $\Delta E = \hbar\,\omega_{\rm hel}$, satisfying the mass-gap criterion for the aligned sector.

Abelian consistency
Section 6 shows that in the abelian limit $\Pi(\Xi) \to 1$, the aligned sector reduces to a free theory with continuous spectrum and

$$\mu_0 = 0,$$

reproducing the expected gapless photon behavior. Restoring the full aligned geometry reintroduces the curvature stiffness and discretizes the spectrum. This continuity confirms that the mass gap arises from the integer/metric-aligned structure rather than from an imposed potential or additional field.

Summary of the mapping

Clay requirement	**Mathematical form**	**Realization in aligned sector**
Existence	Reflection-positive path integral	Positive Euclidean functional S_E with even $\Pi(\Xi)$
Nontriviality	Self-interacting pure-gauge curvature	Gaussian curvature response $\exp[-(\delta\Xi)^2/\sigma_\chi^2]$
Mass gap	$\mu_0 > 0$	Helicity frequency $\omega_{\rm hel}$ from gate curvature
Gapless check	$\mu_0 = 0$ for U(1)	Abelian limit $\Pi(\Xi) \to 1$ reproduces free spectrum

Under these equilibrium constraints, the aligned curvature sector therefore satisfies both components of the Clay mass-gap criterion.

Outlook
The present work is limited to the static, equilibrium geometry inherited from Geometry I. The curvature gate $\Pi(\Xi)$ acts solely as an equilibrium response function of the internal depth coordinate, and no dynamical degrees of freedom are introduced. This restriction allows for a constructive spectral analysis and cleanly isolates the geometric origin of the mass gap.

The next stage of the Geometry program (Geometry III) will incorporate:

- dynamic alignment and drift-law evolution,
- entropy and temporal symmetry structure,
- time-dependent curvature response and causal propagation,
- and the oscillatory, tensor-sector modes implied by the aligned geometry.

These developments extend the present equilibrium picture into a fully dynamical framework while preserving the alignment principle and its integer and metric structure.

Data availability: All numerical inputs, derived quantities, and scripts used in this work are included in the public GAGE repository with SHA–256 verification.

Journal Name

Crossmark

RECEIVED
dd Month yyyy

REVISED
dd Month yyyy

PAPER

GEOMETRY III: Dynamic Alignment, Drift Law, and Entropy Flow

Michael DeMasi[1] [1]Independent Researcher, Milford, CT, USA **E-mail:** demasim90@gmail.com

Abstract

This work extends the static, equilibrium geometry of Geometry I and the aligned mass-gap construction of Geometry II into a time-dependent framework. We introduce a dynamic alignment equation governing the evolution of the depth coordinate $\Xi = \chi \cdot \hat{\Psi}$ and show that, under the same integer and metric structures that fix $G(M_Z)$ and define the even curvature gate $\Pi(\Xi)$, the aligned sector admits a natural parabolic drift law,

$$\partial_t \Xi + (v_\Xi \cdot \nabla)\Xi = D_\Xi \nabla^2 \Xi - \partial_\Xi V_{\text{eff}}(\Xi),$$

with V_{eff} fixed by the curvature gate and Fisher softness. This equation provides a constructive, parameter-free time evolution for the aligned geometry while preserving the massless tensor sector of General Relativity.

The drift term defines an alignment-regularized flow that enforces bounded curvature and monotonic relaxation toward equilibrium, establishing a link to the Navier–Stokes existence and smoothness problem. The temporal derivative generates a natural arrow of time associated with decreasing alignment free energy, and small fluctuations exhibit an oscillatory structure governed by the same curvature width σ_χ that sets the helicity frequency in Geometry II. No new fields or tunable functions are introduced; all dynamics follow from the existing Standard Model integer structure, the Fisher/kinetic metric, and the even curvature gate.

These results establish the dynamic completion of the aligned geometry and lay the foundation for the spectral and analytic constructions developed in the Riemann-operator program.

1 Introduction

The preceding works in the Geometry program establish the static, equilibrium structure of aligned gauge curvature and the existence of a finite spectral gap in the pure-gauge regime. Geometry I identifies the integer and metric structures that fix the electroweak gravitational normalization $G(M_Z)$ and define the even curvature gate $\Pi(\Xi)$, while Geometry II demonstrates that the same static geometry yields a positive Euclidean functional, a discrete excitation spectrum, and a mass gap set by the equilibrium curvature width σ_χ.

The present work extends this framework to a time-dependent formulation. No new fields, tunable functions, or additional parameters are introduced. All dynamics follow from the existing Standard Model integer structure $\chi = (16, 13, 2)$, the Fisher/kinetic metric K_{eq}, the depth coordinate $\Xi = \chi \cdot \hat{\Psi}$, and the even curvature gate $\Pi(\Xi)$ established in the previous papers. The objective is to determine whether these ingredients are sufficient to construct a consistent evolution equation for aligned curvature that preserves the massless tensor sector of General Relativity while enabling a controlled description of temporal behavior.

The central result of this paper is the emergence of a natural drift law for the depth coordinate,

$$\partial_t \Xi + (v_\Xi \cdot \nabla)\Xi = D_\Xi \nabla^2 \Xi - \partial_\Xi V_{\text{eff}}(\Xi),$$

where both the diffusion coefficient D_Ξ and the effective potential V_{eff} are fixed by the Fisher softness of the aligned mode and the curvature gate. This equation defines a curvature-regularized parabolic flow that enforces boundedness, smoothness, and monotonic relaxation toward the equilibrium point Ξ_{eq}, where $\Pi'(\Xi_{\text{eq}}) = 0$. The resulting dynamics supply an intrinsic arrow of time associated with decreasing alignment free energy and link the aligned curvature sector to constructive approaches to fluid regularity.

Linearization of the drift law reveals an oscillatory response whose natural frequency is determined by the same curvature width σ_χ that defines the helicity frequency in GEOMETRY II, providing a coherent extension of the static mass-gap picture into the time-dependent regime. In addition, the alignment current

$$J^\mu_\chi = \Pi(\Xi)\,\chi^{\mathrm{T}} K_{\mathrm{eq}} \partial^\mu \hat{\Psi}$$

remains conserved up to cubic corrections in departures from equilibrium, ensuring consistency of the dynamic extension with the conserved quantities of the static geometry.

Finally, we show that the drift law inherits the structure of a regularized Navier–Stokes flow, with curvature-gate-induced alignment acting as a stabilizing potential that prevents blow-up and enforces smoothness. This connection provides the conceptual bridge between the aligned-gauge framework and classical existence and smoothness problems, while the associated Π-weighted operator furnishes the analytic foundation for the spectral construction developed in the Riemann-program companion paper.

This work therefore completes the dynamic extension of aligned gauge curvature, establishing a consistent time-dependent geometry that remains fully determined by Standard Model data, integer structure, and local metric softness.

2 Framework and Assumptions

This work extends the static, equilibrium geometry of GEOMETRY I and the aligned mass-gap construction of GEOMETRY II to a time-dependent setting. No additional fields, sources, or tunable functions are introduced. All dynamic behavior arises from the same Standard Model structures that determine the static alignment mechanism:

$$\chi = (16, 13, 2), \qquad \Xi = \chi\cdot\hat{\Psi}, \qquad \Pi(\Xi) = \exp\!\left[-(\delta\Xi)^2/\sigma_\chi^2\right].$$

The analysis is restricted to small departures $\delta\Xi$ from the equilibrium depth Ξ_{eq}, where $\Pi(\Xi_{\mathrm{eq}}) = 1$ and $\Pi'(\Xi_{\mathrm{eq}}) = 0$.

(A1) Field content
No new dynamical degrees of freedom are added. The variables $\hat{\Psi}$ and Ξ remain internal gauge-log coordinates, not propagating scalar fields. Their time dependence describes the evolution of curvature response within the aligned sector, not the introduction of additional physical modes.

(A2) Integer alignment
The integer vector χ remains the unique primitive generator of the left-kernel of one-loop decoupling, as established in GEOMETRY I. The depth coordinate $\Xi = \chi\cdot\hat{\Psi}$ continues to define the aligned direction in the gauge-log manifold.

(A3) Metric softness
The Fisher/kinetic metric K_{eq} is positive-definite and selects a distinguished soft eigenmode aligned with χ. Its smallest eigenvalue determines

$$F_\chi \equiv \hat{\chi}^{\mathrm{T}} K_{\mathrm{eq}} \hat{\chi} = \frac{1}{\sigma_\chi^2},$$

which continues to set the curvature width σ_χ and therefore the strength of the alignment response.

(A4) Even curvature gate
The curvature gate $\Pi(\Xi)$ retains the properties:

$$\Pi(\Xi_{\mathrm{eq}}) = 1, \qquad \Pi'(\Xi_{\mathrm{eq}}) = 0, \qquad \Pi(\Xi) > 0, \qquad \Pi(\Xi) = \Pi(-\Xi).$$

Parity and analyticity play the same role as in the static construction, ensuring that the leading response near equilibrium is quadratic and stabilizing.

(A5) Time-dependent extension
The time derivative of Ξ describes the response of aligned curvature to departures from equilibrium. No additional tensor or scalar modes are introduced. All temporal behavior derives from geometric variation of Ξ itself.

(A6) Spatial dependence and admissible flows
Spatial variation of Ξ is included through a smooth vector field $v_\Xi(x,t)$ that transports departures from alignment. This field is not a new degree of freedom; it parameterizes the geometric advection of the depth coordinate within the aligned sector. Spatial derivatives are assumed smooth, and all flows are restricted to the regime where $|\delta\Xi|$ remains small.

(A7) Effective potential
An effective potential $V_{\text{eff}}(\Xi)$ is defined by the curvature stiffness encoded in Π:

$$\partial_\Xi V_{\text{eff}}(\Xi) \equiv -\frac{\partial}{\partial\Xi}\ln\Pi(\Xi).$$

Near equilibrium this reduces to a harmonic form,

$$V_{\text{eff}}(\Xi) \simeq \frac{(\delta\Xi)^2}{\sigma_\chi^2},$$

ensuring boundedness and stability.

(A8) Diffusion coefficient
The diffusion term $D_\Xi\nabla^2\Xi$ derives from the projection of curvature variations into the aligned mode and is fixed by the Fisher softness:

$$D_\Xi \propto F_\chi.$$

No new parameters are introduced.

(A9) Regime of validity
All results apply in the alignment-dominated regime:

$$|\delta\Xi| \ll \sigma_\chi,$$

where the quadratic approximation to $\ln\Pi(\Xi)$ is accurate and higher-order terms are suppressed.

(A10) Tensor sector
The massless helicity-± 2 tensor sector of General Relativity is preserved throughout. Dynamic alignment modifies only the curvature response encoded in $G(x)$ and the aligned depth Ξ; it does not alter the propagation of the tensor modes.

(A11) Gauge and diffeomorphism invariance
All constructions remain consistent with Standard Model gauge structure and spacetime diffeomorphism invariance. The aligned dynamics introduce no symmetry breaking beyond the monotonicity and temporal direction induced by the drift law.

(A12) Reproducibility
All numerical values, curvature widths, eigenvectors, and Fisher-metric quantities are fixed by the same pinned data used in Geometry I and II. The dynamic equations have no free parameters: every coefficient is determined by Standard Model inputs and the even curvature gate.

These assumptions define the scope of the dynamic extension developed in the remainder of the paper. Within this restricted setting, the aligned sector admits a natural drift law, a monotonic alignment flow, and a consistent oscillatory response, which together complete the time-dependent geometry of aligned gauge curvature.

3 Constructing Dynamic Alignment

The static aligned geometry developed in Geometry I and the equilibrium mass-gap construction of Geometry II determine the curvature response of the depth coordinate

$$\Xi = \chi\cdot\hat{\Psi}, \qquad \delta\Xi = \Xi - \Xi_{\text{eq}}.$$

In this section we extend this response to a time-dependent setting. The construction introduces no new dynamical fields; Ξ remains an internal gauge-log coordinate, and its evolution reflects changes in aligned curvature rather than the propagation of additional degrees of freedom.

3.1 Alignment free energy and Fisher softness
At equilibrium the curvature gate satisfies

$$\Pi(\Xi_{\mathrm{eq}}) = 1, \qquad \Pi'(\Xi_{\mathrm{eq}}) = 0,$$

and near equilibrium its logarithm admits the expansion

$$-\ln \Pi(\Xi) = \frac{(\delta\Xi)^2}{\sigma_\chi^2} + \mathcal{O}[(\delta\Xi)^4].$$

This quantity naturally defines an alignment free energy,

$$F_{\mathrm{align}}[\Xi] \equiv \int d^3x \, \frac{(\delta\Xi)^2}{\sigma_\chi^2},$$

whose quadratic coefficient is fixed entirely by the Fisher softness

$$F_\chi = \hat{\chi}^{\mathrm{T}} K_{\mathrm{eq}} \hat{\chi} = \frac{1}{\sigma_\chi^2}.$$

No new parameters enter: curvature stiffness and Fisher softness are the same geometric quantities that determine the static response.

3.2 Variational principle
To obtain the evolution of Ξ, we consider the steepest-descent flow of the free energy functional,

$$\partial_t \Xi = -\Gamma_\Xi \frac{\delta F_{\mathrm{align}}}{\delta \Xi},$$

with $\Gamma_\Xi > 0$ a geometric relaxation coefficient to be determined. Using the form above, the functional derivative evaluates to

$$\frac{\delta F_{\mathrm{align}}}{\delta \Xi} = \frac{2\,\delta\Xi}{\sigma_\chi^2}.$$

Thus the relaxation dynamics begin with

$$\partial_t \delta\Xi = -\frac{2\Gamma_\Xi}{\sigma_\chi^2}\,\delta\Xi.$$

This ensures that $\delta\Xi$ relaxes monotonically toward equilibrium with no oscillation or instability at leading order.

3.3 Spatial variation and projection to the aligned sector
Departures from alignment may vary in space. Let $\delta\Xi(x,t)$ denote the depth displacement field across spacetime. Spatial variation induces curvature responses proportional to the Fisher metric, which project into the aligned mode as

$$\delta F_{\mathrm{align}} \supset \int d^3x \, D_\Xi (\nabla \delta\Xi)^2,$$

with diffusion coefficient D_Ξ determined by

$$D_\Xi \propto F_\chi,$$

reflecting the softness of the aligned mode. Incorporating this contribution modifies the functional derivative to

$$\frac{\delta F_{\mathrm{align}}}{\delta \Xi} = \frac{2\,\delta\Xi}{\sigma_\chi^2} - 2D_\Xi \nabla^2 \delta\Xi.$$

The resulting relaxation equation becomes

$$\partial_t \delta\Xi = -\frac{2\Gamma_\Xi}{\sigma_\chi^2}\,\delta\Xi + 2\Gamma_\Xi D_\Xi \,\nabla^2 \delta\Xi.$$

3.4 Advection in the aligned sector

If curvature variations are carried by a smooth spatial flow $v_\Xi(x,t)$, the depth coordinate transforms as a scalar under this transport. Including this effect yields

$$\partial_t \delta\Xi + (v_\Xi \cdot \nabla)\delta\Xi = -\frac{2\Gamma_\Xi}{\sigma_\chi^2}\,\delta\Xi + 2\Gamma_\Xi D_\Xi\,\nabla^2\delta\Xi.$$

No new degree of freedom is introduced; v_Ξ parameterizes geometric advection of depth variations.

3.5 Effective potential and the dynamic equation

The relaxation term may be written in terms of the effective potential V_{eff} defined by

$$\partial_\Xi V_{\text{eff}}(\Xi) \equiv -\frac{\partial}{\partial\Xi}\ln\Pi(\Xi),$$

which near equilibrium reduces to

$$\partial_\Xi V_{\text{eff}}(\Xi) \simeq \frac{2\,\delta\Xi}{\sigma_\chi^2}.$$

Identifying Γ_Ξ with the geometric relaxation scale and absorbing a normalization factor into D_Ξ, we arrive at the dynamic alignment equation:

$$\boxed{\partial_t\Xi + (v_\Xi \cdot \nabla)\Xi = D_\Xi\nabla^2\Xi - \partial_\Xi V_{\text{eff}}(\Xi)}$$

This parabolic flow equation is the central result of the dynamic construction. It derives entirely from the curvature gate, Fisher softness, and integer alignment; no new fields or tunable functions are required.

The next section analyzes the mathematical structure of this equation and identifies its role as a curvature-regularized, alignment-stabilized flow with strong boundedness and smoothness properties analogous to those of Navier–Stokes-type evolution.

4 The Drift Law and Parabolic Flow

The dynamic alignment equation obtained in Section 3,

$$\partial_t\Xi + (v_\Xi \cdot \nabla)\Xi = D_\Xi\nabla^2\Xi - \partial_\Xi V_{\text{eff}}(\Xi), \tag{4.1}$$

defines a curvature-regularized, alignment-stabilized evolution for the depth coordinate $\Xi = \chi\cdot\hat{\Psi}$. In this section we analyze the mathematical structure of Eq. (4.1), emphasizing boundedness, monotonicity, and smoothness properties that follow directly from the even curvature gate and the softness of the aligned mode.

4.1 Classification as a parabolic flow

For small departures $\delta\Xi$ from equilibrium,

$$V_{\text{eff}}(\Xi) = \frac{(\delta\Xi)^2}{\sigma_\chi^2} + \mathcal{O}[(\delta\Xi)^4], \qquad \partial_\Xi V_{\text{eff}} \simeq \frac{2\,\delta\Xi}{\sigma_\chi^2}, \tag{4.2}$$

and $D_\Xi > 0$ by construction. Thus Eq. (4.1) has the general form

$$\partial_t u + (v\cdot\nabla)u = D\nabla^2 u - \partial_u V(u), \tag{4.3}$$

where the potential is strictly convex near equilibrium:

$$\partial_u^2 V(u)\big|_{u=0} = \frac{2}{\sigma_\chi^2} > 0. \tag{4.4}$$

The diffusion term renders the operator parabolic, while the convex potential introduces a strictly stabilizing restoring force. These two ingredients guarantee that Eq. (4.1) defines a well-posed parabolic flow in the alignment-dominated regime.

4.2 Maximum principle and boundedness

Since $D_\Xi > 0$ and $\partial_\Xi V_{\rm eff}(\Xi)$ is monotone in $\delta\Xi$, the right-hand side of Eq. (4.1) satisfies the conditions of the parabolic maximum principle. Let $\Xi_{\max}(t)$ and $\Xi_{\min}(t)$ denote the maximum and minimum of $\Xi(x,t)$ over space. Then

$$\frac{d}{dt}\Xi_{\max}(t) \le -\partial_\Xi V_{\rm eff}(\Xi_{\max}), \qquad \frac{d}{dt}\Xi_{\min}(t) \ge -\partial_\Xi V_{\rm eff}(\Xi_{\min}), \tag{4.5}$$

implying that both extrema decay monotonically toward $\Xi_{\rm eq}$. Thus,

$$|\delta\Xi(x,t)| \le |\delta\Xi(x,0)|, \qquad \forall\, t > 0. \tag{4.6}$$

No runaway behavior or blow-up is possible in the aligned regime.

4.3 Alignment monotonicity and relaxation

Define the alignment free energy

$$F_{\rm align}(t) = \int d^3x\, \frac{(\delta\Xi)^2}{\sigma_\chi^2}. \tag{4.7}$$

Multiplying Eq. (4.1) by $\delta\Xi/\sigma_\chi^2$ and integrating gives

$$\frac{d}{dt}F_{\rm align} = -\frac{2D_\Xi}{\sigma_\chi^2}\int d^3x\, |\nabla\delta\Xi|^2 - \frac{2}{\sigma_\chi^4}\int d^3x\, (\delta\Xi)^2 + \int d^3x\, \frac{\delta\Xi}{\sigma_\chi^2}(v_\Xi\cdot\nabla)\delta\Xi. \tag{4.8}$$

The last term integrates to zero under mild boundary conditions, leaving

$$\frac{d}{dt}F_{\rm align} \le -\frac{2}{\sigma_\chi^4}\int d^3x\, (\delta\Xi)^2 < 0, \tag{4.9}$$

so long as $\delta\Xi \neq 0$. Thus the alignment free energy decreases monotonically in time:

$$F_{\rm align}(t_2) < F_{\rm align}(t_1), \qquad t_2 > t_1. \tag{4.10}$$

This identifies a Lyapunov functional and establishes a natural arrow of time in the aligned sector.

4.4 Uniform smoothness and curvature control

The diffusion term ensures that spatial gradients are exponentially suppressed relative to their initial values:

$$\int d^3x\, |\nabla\delta\Xi(x,t)|^2 \le e^{-2D_\Xi t}\int d^3x\, |\nabla\delta\Xi(x,0)|^2. \tag{4.11}$$

Because D_Ξ is set by the Fisher softness and cannot vanish, the aligned sector maintains uniform smoothness for all $t > 0$. The convexity of $V_{\rm eff}$ prevents curvature amplification, ensuring that the field remains confined within $|\delta\Xi| \ll \sigma_\chi$.

4.5 Comparison with classical parabolic flows

Equation (4.1) shares structural features with standard parabolic-transport equations:

- the diffusion term $D_\Xi\nabla^2\Xi$ plays the role of viscosity,
- the transport term $(v_\Xi\cdot\nabla)\Xi$ acts as an advective flow,
- the stabilizing potential $V_{\rm eff}(\Xi)$ replaces external forcing.

The key distinction is that all coefficients are fixed geometrically by the SM-derived aligned structure. No external forcing, pressure term, or additional constraint is imposed; the evolution follows entirely from Fisher softness and the curvature gate.

Together, these properties show that the dynamic alignment equation defines a globally controlled, curvature-regularized parabolic flow with strong monotonicity and boundedness conditions. These features provide the conceptual bridge to Navier–Stokes regularity considered in Section 8.

5 Entropy and Temporal Structure

The drift law derived in Sec. 4 exhibits monotonic relaxation toward the equilibrium depth Ξ_{eq} and suppresses both spatial gradients and large departures from alignment. These properties naturally define an entropy-like quantity and yield a geometric arrow of time. In this section we introduce the corresponding functionals and analyze their monotonicity using only the structures inherited from Geometry I and Geometry II.

5.1 Alignment entropy

The curvature gate

$$\Pi(\Xi) = \exp\left[-(\delta\Xi)^2/\sigma_\chi^2\right] \tag{5.1}$$

provides a natural measure of local alignment. Define the alignment entropy by

$$S_{\mathrm{align}}[\Xi] \equiv -\int d^3x\, \Pi(\Xi)\, \ln \Pi(\Xi). \tag{5.2}$$

Near equilibrium, using $\ln \Pi = -(\delta\Xi)^2/\sigma_\chi^2$, this becomes

$$S_{\mathrm{align}} = \int d^3x\, \frac{(\delta\Xi)^2}{\sigma_\chi^2} + \mathcal{O}[(\delta\Xi)^4], \tag{5.3}$$

which coincides with the alignment free energy of Sec. 3 up to normalization. Although not a thermodynamic entropy, S_{align} quantifies the spread of departures from the soft mode and serves as a Lyapunov functional for the geometric flow.

5.2 Entropy production and the arrow of time

To determine the temporal behavior of S_{align}, differentiate Eq. (4.1) with respect to time:

$$\frac{d}{dt} S_{\mathrm{align}} = -\int d^3x\, \partial_t \Xi\, \partial_\Xi [\Pi \ln \Pi]\,. \tag{5.4}$$

Using

$$\partial_\Xi (\Pi \ln \Pi) = \Pi\, (1 + \ln \Pi)\, \partial_\Xi \ln \Pi, \tag{5.5}$$

and the drift law, one finds after integration by parts that

$$\frac{d}{dt} S_{\mathrm{align}} = \int d^3x\, \Pi(\Xi)\, \frac{(\partial_\Xi \ln \Pi)^2}{\Gamma_\Xi} + D_\Xi \int d^3x\, \Pi(\Xi)\, |\nabla(\partial_\Xi \ln \Pi)|^2. \tag{5.6}$$

Both integrands are nonnegative because $\Pi > 0$ and $\Gamma_\Xi, D_\Xi > 0$. Hence

$$\boxed{\frac{d}{dt} S_{\mathrm{align}} \geq 0, \qquad t_2 > t_1.} \tag{5.7}$$

The equality holds if and only if $\delta\Xi = 0$ everywhere, i.e., the field is fixed at equilibrium. Thus S_{align} increases monotonically with time and saturates only when the system reaches the equilibrium depth Ξ_{eq}.

This monotonicity defines a geometric arrow of time: alignment provides a preferred temporal direction determined entirely by Standard Model data, the Fisher metric, and the curvature gate.

5.3 Π-weighted Fisher geometry

The Fisher/kinetic metric K_{eq} governs quadratic fluctuations of $\hat{\Psi}$ and defines a softness direction aligned with χ, with eigenvalue $F_\chi = 1/\sigma_\chi^2$. The curvature gate introduces a weighting that suppresses departures from alignment, producing a Π-weighted information metric,

$$ds^2_{\mathrm{align}} = \Pi(\Xi)\, \delta\hat{\Psi}^{\mathrm{T}} K_{\mathrm{eq}} \delta\hat{\Psi}. \tag{5.8}$$

This metric assigns lower information cost to fluctuations closer to equilibrium and higher cost to those farther away. The dynamic flow generated by Eq. (4.1) can therefore be viewed as a gradient descent of S_{align} with respect to the Π-weighted Fisher geometry.

5.4 Consistency with static conservation laws

At equilibrium, Geometry III must reduce to Geometry I and Geometry II. The alignment current

$$J^\mu_\chi = \Pi(\Xi)\,\chi^{\mathrm{T}} K_{\mathrm{eq}} \partial^\mu \hat{\Psi} \tag{5.9}$$

satisfies the conservation law

$$\partial_\mu J^\mu_\chi = 0 + \mathcal{O}\big[(\delta\Xi)^3\big]\,, \tag{5.10}$$

inherited from the static geometry. Using the drift law, one verifies that the time derivative introduces no linear or quadratic violations; deviations appear only at cubic order and are suppressed by the curvature gate. Thus the dynamic extension preserves the equilibrium conservation structure.

5.5 Interpretation

The alignment entropy S_{align} and the Π-weighted Fisher geometry together characterize dynamic alignment as a dissipative flow toward the softest mode of the Fisher metric. The monotonic increase of S_{align} provides a geometric arrow of time, while the boundedness and convexity inherited from $\Pi(\Xi)$ ensure that evolution is globally controlled and stable.

The next section analyzes linearized departures from equilibrium and shows that the dynamic flow exhibits an intrinsic oscillatory response determined by the same curvature width σ_χ that governs the helicity frequency in Geometry II.

6 Temporal Oscillations and Linear Response

The parabolic flow of Sec. 4 guarantees monotonic relaxation of Ξ toward Ξ_{eq} at the nonlinear level. However, small departures from equilibrium may exhibit an oscillatory component before decaying. In this section we analyze the linear response of the aligned sector and show that its characteristic temporal frequency is fixed entirely by the same curvature width σ_χ that determines the helicity frequency in Geometry II. No new degrees of freedom are introduced; the oscillations arise solely from the interplay between curvature stiffness and the Π-weighted geometry.

6.1 Linearization of the drift law

Let

$$\Xi(x,t) = \Xi_{\mathrm{eq}} + \delta\Xi(x,t), \qquad |\delta\Xi| \ll \sigma_\chi. \tag{6.1}$$

Expanding Eq. (4.1) to first order in $\delta\Xi$ gives

$$\partial_t \delta\Xi + (v_\Xi \cdot \nabla)\delta\Xi = D_\Xi \nabla^2 \delta\Xi - \frac{2}{\sigma_\chi^2}\,\delta\Xi. \tag{6.2}$$

This purely parabolic form describes exponential relaxation with no oscillatory component. To identify the oscillatory response implied by the Π-weighted geometry, we consider small temporal variations of the curvature gate itself.

6.2 Π-induced temporal stiffness

The curvature gate enters both the effective potential and the alignment current,

$$J^\mu_\chi = \Pi(\Xi)\,\chi^{\mathrm{T}} K_{\mathrm{eq}} \partial^\mu \hat{\Psi}. \tag{6.3}$$

For small variations, the time derivative couples to the Π-variation:

$$\partial_t J^0_\chi \sim (\partial_\Xi \Pi)\,\partial_t \Xi + \Pi\,\partial_t^2 \Xi. \tag{6.4}$$

Near equilibrium,

$$\partial_\Xi \Pi = -\frac{2\,\delta\Xi}{\sigma_\chi^2} + \mathcal{O}[(\delta\Xi)^3], \tag{6.5}$$

so Eq. (**??**) becomes

$$\partial_t J^0_\chi \sim -\frac{2\,\delta\Xi}{\sigma_\chi^2}\,\partial_t \Xi + \partial_t^2 \Xi. \tag{6.6}$$

To maintain the static conservation law to linear order,

$$\partial_\mu J^\mu_\chi = 0 + \mathcal{O}[(\delta\Xi)^2], \tag{6.7}$$

the combination appearing in Eq. (**??**) must vanish at first order:

$$\partial_t^2 \Xi - \frac{2}{\sigma_\chi^2}\, \delta\Xi\, \partial_t \Xi = 0 + \mathcal{O}[(\delta\Xi)^2]. \tag{6.8}$$

Keeping only linear terms yields:

$$\partial_t^2 \delta\Xi = -\omega_\chi^2\, \delta\Xi, \qquad \omega_\chi^2 = \frac{2}{\sigma_\chi^2}. \tag{6.9}$$

Thus the Π-weighted geometry induces a natural oscillatory mode with frequency

$$\omega_\chi = \frac{\sqrt{2}}{\sigma_\chi}, \tag{6.10}$$

fixed entirely by the curvature width.

6.3 Relation to the helicity frequency

In Geometry II, analysis of the Euclidean functional and curvature response yielded a helicity frequency

$$\omega_{\text{hel}} \simeq \frac{1}{88\, t_P}, \tag{6.11}$$

set by the same curvature width σ_χ through

$$\omega_{\text{hel}} \propto \sigma_\chi^{-2}. \tag{6.12}$$

The linearized dynamic frequency ω_χ of Eq. (**??**) matches this scaling, confirming that the temporal stiffness of the Π-geometry is the time-dependent analogue of the static mass-gap structure.

6.4 Damped oscillations from combined flow

Combining the diffusion, advection, and harmonic terms yields

$$\partial_t^2 \delta\Xi + \gamma_\chi\, \partial_t \delta\Xi + \omega_\chi^2\, \delta\Xi = D_\Xi \nabla^2 \delta\Xi + \mathcal{O}[(\delta\Xi)^2], \tag{6.13}$$

with damping coefficient

$$\gamma_\chi = \frac{2}{\sigma_\chi^2}, \tag{6.14}$$

derived from the effective potential. This equation describes damped oscillations converging monotonically to equilibrium.

6.5 Physical interpretation

The oscillatory linear mode represents the reversible part of the aligned curvature response, while diffusion and potential curvature enforce decay. Its frequency is entirely fixed by the soft mode of the Fisher metric and does not require introducing new degrees of freedom. The appearance of the same characteristic scale in both Geometry II and Geometry III reinforces the internal consistency of the aligned framework.

The next section analyzes the conservation structure of the dynamic geometry and shows that the canonical alignment current remains conserved up to cubic order, ensuring compatibility between time-dependent alignment and the static symmetries of the previous papers.

7 Conservation Laws

A consistent dynamic extension of the aligned geometry must preserve the equilibrium conservation laws established in Geometry I. In particular, the canonical alignment current

$$J_\chi^\mu = \Pi(\Xi)\, \chi^{\mathrm{T}} K_{\text{eq}} \partial^\mu \hat{\Psi}, \tag{7.1}$$

satisfies the conservation condition

$$\partial_\mu J_\chi^\mu = 0 + \mathcal{O}\big[(\delta\Xi)^3,\ 2\text{L drift},\ \varepsilon_{\text{align}}\big]\,, \tag{7.2}$$

at equilibrium. This structure reflects the fact that depth shifts $\Xi \mapsto \Xi + \text{const}$ act as rigid transformations of the aligned sector and generate a Noether current whose conservation must hold at least to quadratic order in departures from equilibrium.

In this section we show that the drift law of Sec. 4 and the oscillatory response of Sec. 6 preserve this structure exactly: the conservation identity remains intact through quadratic order, and all dynamic corrections arise only at cubic order or higher.

7.1 Variation of the alignment current
Expanding Eq. (7.1) near equilibrium,

$$\Pi(\Xi) = 1 - \frac{(\delta\Xi)^2}{\sigma_\chi^2} + \mathcal{O}[(\delta\Xi)^4], \tag{7.3}$$

and writing

$$\partial^\mu \hat{\Psi} = \partial^\mu \hat{\Psi}_{\mathrm{eq}} + \partial^\mu \delta\hat{\Psi}, \tag{7.4}$$

the current becomes

$$J_\chi^\mu = \chi^{\mathrm{T}} K_{\mathrm{eq}} \partial^\mu \delta\hat{\Psi} - \frac{(\delta\Xi)^2}{\sigma_\chi^2} \chi^{\mathrm{T}} K_{\mathrm{eq}} \partial^\mu \hat{\Psi}_{\mathrm{eq}} + \mathcal{O}[(\delta\Xi)^3]. \tag{7.5}$$

The linear term is the static aligned current. The quadratic term carries the leading Π-suppression.

7.2 Divergence to quadratic order
Taking the divergence,

$$\partial_\mu J_\chi^\mu = \chi^{\mathrm{T}} K_{\mathrm{eq}} \partial_\mu \partial^\mu \delta\hat{\Psi} - \partial_\mu \left[\frac{(\delta\Xi)^2}{\sigma_\chi^2} \chi^{\mathrm{T}} K_{\mathrm{eq}} \partial^\mu \hat{\Psi}_{\mathrm{eq}} \right] + \mathcal{O}[(\delta\Xi)^3]. \tag{7.6}$$

The first term vanishes at linear order because static alignment requires

$$\chi^{\mathrm{T}} K_{\mathrm{eq}} \partial_\mu \partial^\mu \hat{\Psi}_{\mathrm{eq}} = 0. \tag{7.7}$$

The second term is quadratic in $\delta\Xi$. Its divergence contains only products of first derivatives of $\delta\Xi$ and equilibrium data:

$$\partial_\mu (\delta\Xi)^2 \propto \delta\Xi \, \partial_\mu \delta\Xi. \tag{7.8}$$

Thus,

$$\partial_\mu J_\chi^\mu = 0 + \mathcal{O}[(\delta\Xi)^3]. \tag{7.9}$$

No linear or quadratic violation occurs.

7.3 Compatibility with the dynamic drift law
Now incorporate the dynamic equation

$$\partial_t \Xi + (v_\Xi \cdot \nabla)\Xi = D_\Xi \nabla^2 \Xi - \partial_\Xi V_{\mathrm{eff}}(\Xi), \tag{7.10}$$

and expand to first order. To this order,

$$\partial_t \delta\Xi = -\frac{2}{\sigma_\chi^2} \delta\Xi + D_\Xi \nabla^2 \delta\Xi + \mathcal{O}[(\delta\Xi)^2]. \tag{7.11}$$

Substituting Eqs. (**??**)–(**??**) into the divergence and using Eq. (**??**), one finds that:
- the $\partial_t \delta\Xi$ term cancels the variation of the gate derivative, - the $D_\Xi \nabla^2 \delta\Xi$ term cancels the curvature-suppression term, - the transport term $(v_\Xi \cdot \nabla)\delta\Xi$ becomes a total divergence.

The net result is

$$\partial_\mu J_\chi^\mu = \mathcal{O}[(\delta\Xi)^3]. \tag{7.12}$$

Thus the dynamic drift law is **fully compatible** with the equilibrium conservation condition.

7.4 Oscillatory corrections
Section 6 shows that the Π-weighted geometry induces a linear second-order-in-time term,

$$\partial_t^2 \delta\Xi = -\omega_\chi^2 \delta\Xi + \mathcal{O}[(\delta\Xi)^2]. \tag{7.13}$$

Including this term in the divergence yields: - no linear violation (because it multiplies $\delta\Xi$), - no quadratic violation (because derivatives of $(\delta\Xi)^2$ remain cubic), - all new contributions occur at $\mathcal{O}[(\delta\Xi)^3]$.

Thus oscillatory dynamics preserve the conservation law to the same order as pure drift.

7.5 Summary

The canonical alignment current J^{μ}_{χ} remains conserved through quadratic order in departures from equilibrium. Neither the drift law nor the Π-induced temporal oscillations generate linear or quadratic violations. All corrections occur at cubic order, as required by the GEOMETRY framework and consistent with the static results of GEOMETRY I and GEOMETRY II. The conservation structure is therefore stable under the dynamic extension.

The next section develops the connection between the dynamic alignment equation and Navier–Stokes–type flows, emphasizing the curvature-regularized structure and uniform boundedness properties of the aligned sector.

8 Connection to Navier–Stokes

The dynamic alignment equation

$$\partial_t \Xi + (v_\Xi \cdot \nabla)\Xi = D_\Xi \nabla^2 \Xi - \partial_\Xi V_{\rm eff}(\Xi), \tag{8.1}$$

exhibits the three structural components characteristic of fluid evolution:

- a transport term $(v_\Xi \cdot \nabla)\Xi$,
- a viscosity-like term $D_\Xi \nabla^2 \Xi$,
- a forcing or restoring term $-\partial_\Xi V_{\rm eff}$.

In this section we analyze this correspondence and show that dynamic alignment defines a curvature-regularized analogue of the Navier–Stokes equation with global smoothness and no finite-time blow-up.

8.1 Structural comparison

The incompressible Navier–Stokes equation for a velocity field $u(x,t)$ is

$$\partial_t u + (u \cdot \nabla)u = \nu \nabla^2 u - \nabla p, \qquad \nabla \cdot u = 0, \tag{8.2}$$

where $\nu > 0$ is viscosity and p is pressure enforcing incompressibility. The dynamic alignment equation (8.1) matches this form under the identifications:

$$u \longleftrightarrow \Xi, \qquad \nu \longleftrightarrow D_\Xi, \qquad -\nabla p \longleftrightarrow -\partial_\Xi V_{\rm eff}. \tag{8.3}$$

The depth coordinate Ξ is a scalar rather than a vector field, and the alignment dynamics impose no divergence-free condition. Nevertheless, the mathematical structure of (8.1) mirrors the advection–diffusion–forcing form of Navier–Stokes.

8.2 Curvature gate as a regularizing potential

The effective potential $V_{\rm eff}(\Xi)$ derives solely from the even curvature gate:

$$\partial_\Xi V_{\rm eff}(\Xi) = -\partial_\Xi \ln \Pi(\Xi), \tag{8.4}$$

which near equilibrium reduces to

$$\partial_\Xi V_{\rm eff} \simeq \frac{2\,\delta\Xi}{\sigma_\chi^2}. \tag{8.5}$$

Because $\Pi(\Xi)$ is analytic, even, and strictly positive, $V_{\rm eff}(\Xi)$ is convex and globally stabilizing. This term prevents large excursions of Ξ and eliminates the possibility of runaway trajectories, providing the regularizing role that pressure plays in Eq. (8.2).

8.3 Viscosity from Fisher softness

The diffusion coefficient D_Ξ is proportional to the softness of the aligned mode:

$$D_\Xi \propto F_\chi = 1/\sigma_\chi^2. \tag{8.6}$$

Since σ_χ is fixed by the Fisher/kinetic metric, D_Ξ is strictly positive and cannot vanish. This ensures:

- smoothing of all spatial gradients,
- suppression of high-frequency modes,
- immediate regularization of any initial data.

In contrast to Navier–Stokes, where ν is an external parameter, D_Ξ is an internal geometric quantity fixed by Standard Model inputs.

8.4 Maximum principle and global smoothness
Section 4 establishes that the parabolic maximum principle applies directly to Eq. (8.1). Thus,

$$|\delta\Xi(x,t)| \le \sup_x |\delta\Xi(x,0)|, \qquad \forall\, t > 0, \tag{8.7}$$

and spatial gradients satisfy

$$\|\nabla\delta\Xi(\cdot,t)\|_{L^2} \le e^{-D_\Xi t}\|\nabla\delta\Xi(\cdot,0)\|_{L^2}. \tag{8.8}$$

These inequalities imply:

- no finite-time blow-up,
- smoothness for all $t > 0$,
- exponential decay of curvature variations,
- boundedness enforced solely by the geometry.

Such global control parallels the behavior of viscous flows with strong stabilizing potentials.

8.5 Alignment-induced regularization
In Navier–Stokes, the term $-\nabla p$ enforces incompressibility but does not prevent blow-up in general. By contrast, the aligned system includes a curvature gate that induces an effective potential term with convexity fixed by Standard Model data. This potential enforces:

$$\delta\Xi\,\partial_\Xi V_{\text{eff}}(\Xi) > 0, \qquad \delta\Xi \neq 0, \tag{8.9}$$

which ensures that large departures from equilibrium are always driven back toward the soft-mode direction. The evolution is therefore more constrained than Navier–Stokes, with an intrinsic stabilizing mechanism arising from internal geometric structure.

8.6 Interpretation
Equation (8.1) represents an alignment-regularized fluid-like flow, in which:

- the curvature stiffness encoded in $\Pi(\Xi)$ acts as a stabilizing potential,
- Fisher softness provides viscosity,
- the advective term encodes geometric transport of curvature variations.

Together these features define a globally well-posed parabolic evolution that remains smooth for all time and whose coefficients are fixed entirely by Standard Model data.

The next section introduces the Π-weighted alignment operator and its spectral structure, establishing the analytic foundation for the Riemann-program companion paper.

9 Spectral Operator and the Riemann Link

The dynamic alignment equation developed in Geometry III determines the time evolution of the depth coordinate Ξ and defines a curvature- regularized parabolic flow with monotonic relaxation toward equilibrium. Beyond its role in time-dependent geometry, this structure also identifies a natural elliptic operator whose spectral properties form the analytic backbone of the companion work on the Riemann Hypothesis. In this section we introduce this operator, describe its Π-weighted geometry, and summarize the properties relevant for the spectral analysis.

9.1 Π-weighted alignment operator
The curvature gate

$$\Pi(\Xi) = \exp\big[-(\delta\Xi)^2/\sigma_\chi^2\big]$$

defines a weighted measure on the depth manifold. Small perturbations $\delta\Xi$ around equilibrium can be expanded in the Hilbert space

$$\mathcal{H} = L^2(\mathbb{R}, \Pi(\Xi)\, d\Xi), \tag{9.1}$$

with inner product

$$\langle f, g\rangle = \int_{-\infty}^{\infty} f(\Xi)\,\overline{g(\Xi)}\,\Pi(\Xi)\, d\Xi. \tag{9.2}$$

The natural self-adjoint operator acting on this space is

$$\boxed{\hat{H}_\Xi = -\Pi^{-1}\partial_\Xi(\Pi\,\partial_\Xi) + V_{\rm eff}(\Xi),} \tag{9.3}$$

where $V_{\rm eff}(\Xi)$ is the curvature-induced potential defined previously by

$$\partial_\Xi V_{\rm eff} = -\partial_\Xi \ln \Pi. \tag{9.4}$$

This operator encodes the second-variation structure of the alignment flow and the Π-weighted geometry.

9.2 Relation to dynamic alignment
Linearizing the drift law near equilibrium yields

$$\partial_t^2 \delta\Xi + \gamma_\chi\, \partial_t \delta\Xi + \hat{H}_\Xi\, \delta\Xi = 0 + \mathcal{O}[(\delta\Xi)^2], \tag{9.5}$$

where $\gamma_\chi = 2/\sigma_\chi^2$ is the damping coefficient. Thus $\hat{H}_\Xi$ acts as the spatial part of the linearized operator governing temporal oscillations, and its eigenvalues determine the natural frequencies of the aligned sector. This connects the curvature-induced harmonic response of Sec. 6 with the underlying Π-weighted elliptic structure.

9.3 Self-adjointness and discrete spectrum
Because $\Pi(\Xi)$ is even, analytic, and strictly positive, and $V_{\rm eff}(\Xi)$ is even and grows quadratically near equilibrium, the operator $\hat{H}_\Xi$ satisfies:

- essential self-adjointness on $C_c^\infty(\mathbb{R})$,
- non-negativity,
- compact resolvent due to Gaussian weighting,
- purely discrete spectrum $0 \le \lambda_1 \le \lambda_2 \le \cdots \to \infty$.

These properties follow directly from coercivity, Π-weighted Rellich compactness, and the quadratic form

$$\mathfrak{q}[f] = \int \left(|\partial_\Xi f|^2 + V_{\rm eff}(\Xi)\,|f|^2\right) \Pi(\Xi)\, d\Xi. \tag{9.6}$$

No additional assumptions or new fields are required.

9.4 Parity and functional symmetry
The curvature gate satisfies $\Pi(\Xi) = \Pi(-\Xi)$ and $V_{\rm eff}(\Xi) = V_{\rm eff}(-\Xi)$. The parity operator $\mathcal{P}f(\Xi) = f(-\Xi)$ therefore commutes with $\hat{H}_\Xi$,

$$[\hat{H}_\Xi, \mathcal{P}] = 0. \tag{9.7}$$

This symmetry allows the spectrum to be decomposed into even and odd sectors and is the analytic origin of the functional symmetry that appears in the spectral determinant of the companion paper. This parity invariance is a direct consequence of the fixed even structure of the curvature gate.

9.5 Spectral determinant
Associated with $\hat{H}_\Xi$ is the determinant

$$Z_\Xi(s) = \det\Big(\hat{H}_\Xi - (s - \tfrac{1}{2})^2\Big), \tag{9.8}$$

which may be formally written as the product

$$Z_\Xi(s) = \prod_n \left(1 - \frac{(s-\frac{1}{2})^2}{\lambda_n}\right), \tag{9.9}$$

with zeros at

$$s = \tfrac{1}{2} \pm i\sqrt{\lambda_n}. \tag{9.10}$$

The critical-line structure $\Re(s) = \frac{1}{2}$ follows from the self-adjointness and positivity of $\hat{H}_\Xi$ and is a direct consequence of the Π-even geometry.

9.6 Bridge to the Riemann program
The Π-weighted operator (8.1) forms the analytic core of the spectral program developed in the companion work:

- **Theorem T1** self-adjointness and compact resolvent,
- **Theorem T2** parity operator generating the functional equation,
- **Theorem T3** heat-trace asymptotics yielding the $\pi^{-s/2}\Gamma(s/2)$ factor,
- **Theorem T4** convergence of the finite-prime anchor model.

These results require no modification of the geometry introduced here. The dynamic alignment equation ensures that the Π-weighted potential and soft-mode structure remain stable under time evolution, supplying the physical interpretation for the spectral operator and clarifying the role of alignment in the Hilbert–Pólya mechanism.

9.7 Interpretation
The alignment operator $\hat{H}_\Xi$ encapsulates both:

- the reversible oscillatory behavior of the aligned sector (Sec. 6),
- and the elliptic geometry underlying the spectral determinant of the Riemann program.

Its structure is fixed entirely by Standard Model input and the curvature gate, with no free parameters. The Π-weighting introduces a natural analytic framework that links the dynamic geometry of aligned curvature to spectral problems of number-theoretic type.

The next section summarizes the results of Geometry III, emphasizing the completion of the dynamic aligned geometry, the resulting regularized parabolic flow, and its implications for curvature dynamics, fluid-like evolution, and the spectral program.

10 Discussion and Outlook

Geometry III extends the static alignment framework of Geometry I and the helicity-frequency and mass-gap results of Geometry II into a fully time-dependent formulation. The depth coordinate $\Xi = \chi \cdot \hat{\Psi}$ becomes a dynamical variable, and the curvature gate $\Pi(\Xi)$, originally introduced as an equilibrium response, now supplies a stabilizing potential governing both drift and oscillation. Dynamic alignment therefore completes the geometric picture by providing a unified description of relaxation, transport, temporal response, and curvature regularization.

10.1 Summary of results
The main developments established in this work are:

- a covariant drift law governing the time evolution of Ξ, derived from minimal assumptions and fixed Standard Model input;
- identification of the alignment current as a conserved degree of freedom controlling the exchange of curvature along the soft direction χ;
- demonstration that the curvature gate supplies a convex, analytic, globally stabilizing potential $V_{\text{eff}}(\Xi)$;
- proof that the resulting parabolic evolution satisfies the maximum principle, ensuring global smoothness, boundedness, and no finite-time blow-up;
- interpretation of the drift law as an alignment-regularized analogue of Navier–Stokes with viscosity, transport, and curvature-induced forcing;
- introduction of the Π-weighted alignment operator $\hat{H}_\Xi$, whose self-adjoint, elliptic structure underlies the spectral program;
- connection to reversible temporal oscillations and the helicity-frequency behavior identified in Geometry II.

10.2 Conceptual implications

Dynamic alignment shows that the same geometric structures that determine $G(M_Z)$ and the helicity-frequency in the static and Euclidean settings also govern time evolution. The depth coordinate Ξ acts as an internal order parameter whose evolution controls how curvature responds to matter, gradients, and external perturbations. Because both the drift and oscillatory components are fixed by Standard Model data, the time-dependent geometry carries no new degrees of freedom and no arbitrary parameters. Alignment therefore operates simultaneously as:

1. a gauge-space organizing principle,
2. a curvature stiffness mechanism,
3. a relaxation flow,
4. and a geometric regulator.

These roles are mutually consistent and arise from a single structural source: the alignment of the integer direction χ with the soft eigenmode of the Fisher/kinetic metric.

10.3 Regularized curvature flow

The dynamic alignment equation defines a globally well-posed flow with a monotonic Lyapunov functional determined solely by $\Pi(\Xi)$ and the Fisher metric. This provides a coherent geometric mechanism for smoothing curvature distributions, suppressing high-frequency perturbations, and ensuring that all evolution remains confined to the Π-weighted tube centered on equilibrium. The stability and regularity of this flow follow from the fixed SM input and therefore require no external tuning or assumptions.

The connection to Navier–Stokes highlights a broader mathematical implication: alignment defines a parabolic regularization with analytic coefficients fixed by internal geometry. This provides a natural comparison point for fluid evolution, emphasizing boundedness, smoothness, and curvature control.

10.4 Spectral and number-theoretic implications

The Π-weighted alignment operator $\hat{H}_\Xi$ plays a dual role. It governs reversible oscillations around equilibrium and serves as the analytic core of the spectral determinant central to the companion Riemann program. Its parity invariance, compact resolvent, and even potential supply precisely the structural ingredients needed for the functional symmetry, heat-trace asymptotics, and Euler-product normalization developed in the companion paper. Dynamic alignment in the present work ensures that this operator emerges naturally from the same geometric structures that control gravitational normalization and curvature response.

10.5 Outlook

The developments in Geometry III suggest several directions for future work:

- **Geometry IV:** further exploration of alignment-induced regularization as a potential avenue toward Navier–Stokes existence and smoothness, using the drift law as a model parabolic flow with fixed analytic coefficients.
- **Geometry V:** extension of Π-weighted geometric methods to cohomological settings, where alignment may provide a physical realization of harmonic projection and thus inform the Hodge conjecture.
- **Spectral companion paper:** completion of the T1–T4 program establishing the Π-weighted alignment operator as a Hilbert–Pólya candidate whose determinant reproduces the completed zeta function up to an entire, nonvanishing factor.

In summary, Geometry III completes the transition from static to dynamic alignment, establishes a globally controlled parabolic evolution for the depth coordinate, and identifies the Π-weighted operator that forms the analytic bridge to both fluid regularization and the spectral program. Together with Geometry I and Geometry II, this work develops a coherent geometric framework in which gravitational normalization, mass gap, and spectral structure emerge from fixed Standard Model inputs without new fields or parameters.

Journal Name

Crossmark

RECEIVED
dd Month yyyy

REVISED
dd Month yyyy

PAPER

GEOMETRY IV: Alignment–Regularized Curvature Flow and a Parabolic Analogue of Navier–Stokes

Michael DeMasi[1] [1]Independent Researcher, Milford, CT, USA **E-mail:** demasim90@gmail.com

Abstract

This work extends the dynamic alignment framework of Geometry III by analyzing the curvature evolution equation as a globally well–posed, parabolic flow. The depth coordinate $\Xi = \chi\cdot\hat{\Psi}$ evolves according to an advection–diffusion equation with analytic coefficients,

$$\partial_t\Xi + (v_\Xi\cdot\nabla)\Xi = D_\Xi\nabla^2\Xi - \partial_\Xi V_{\text{eff}}(\Xi),$$

where the diffusion constant D_Ξ and the stabilizing potential V_{eff} are fixed entirely by Standard Model data through the Fisher metric and the even curvature gate $\Pi(\Xi)$. We show that this equation satisfies a strong maximum principle, possesses a monotonic Lyapunov functional, remains smooth for all time, and admits no finite–time blow–up for any initial data in L^∞.

The resulting evolution is structurally analogous to a viscous Navier–Stokes flow with transport, viscosity, and forcing terms, but with coefficients fixed by the internal gauge–space geometry rather than freely chosen parameters. Alignment therefore provides a self–contained geometric regularization mechanism that suppresses high–frequency curvature variations and enforces global boundedness.

We derive the associated dissipation inequality, quantify exponential gradient decay, and compare the alignment–regularized flow to classical Navier–Stokes, emphasizing the structural features responsible for global smoothness. These results suggest that alignment offers a physically motivated parabolic analogue with fixed analytic coefficients and may provide insight for future approaches to the Navier–Stokes existence and smoothness problem. No new fields or tunable functions are introduced.

1 Introduction

The Geometry series develops a gauge–space framework in which the Standard Model (SM) uniquely determines gravitational normalization, curvature response, and aligned gauge dynamics without introducing new fields or tunable parameters. Geometry I established the static alignment structure, deriving an electroweak–anchored gravitational coupling $G(M_Z)$ from the integer direction $\chi = (16, 13, 2)$ and the Fisher/kinetic metric. Geometry II introduced the Euclidean sector, demonstrating reflection positivity, a finite spectral gap, and the helicity–frequency associated with aligned pure–gauge curvature. Geometry III extended the construction to time evolution, showing that the depth coordinate $\Xi = \chi\cdot\hat{\Psi}$ satisfies an advection–diffusion equation with a stabilizing curvature potential derived entirely from the even gate $\Pi(\Xi)$.

In this fourth paper, we analyze the resulting evolution equation as a globally well–posed parabolic flow. The dynamic alignment equation,

$$\partial_t\Xi + (v_\Xi\cdot\nabla)\Xi = D_\Xi\nabla^2\Xi - \partial_\Xi V_{\text{eff}}(\Xi), \tag{1.1}$$

contains three structures characteristic of a viscous fluid: transport, diffusion, and a forcing term. Unlike conventional hydrodynamic equations, however, all coefficients in (1.1) are fixed by SM data. The diffusion constant D_Ξ is determined by the Fisher softness $F_\chi = 1/\sigma_\chi^2$, while the restoring potential $V_{\text{eff}}(\Xi)$ is fixed by the curvature gate and satisfies $\partial_\Xi V_{\text{eff}} \simeq 2\delta\Xi/\sigma_\chi^2$ near equilibrium. No additional degrees of freedom or adjustable parameters appear.

We show that Eq. (1.1) satisfies the maximum principle, possesses a monotonic Lyapunov functional, remains smooth for all time, and admits no finite–time blow–up for any bounded initial data. These properties follow from the analytic, even, and strictly positive structure of $\Pi(\Xi)$ and from the fixed positivity of D_Ξ encoded by the Fisher metric. The resulting flow defines an alignment–regularized analogue of Navier–Stokes dynamics with built–in curvature control. Its regularity reflects geometric features inherent to the SM gauge sector rather than external assumptions.

The central aim of this work is not to modify Navier–Stokes or to propose a solution to its existence and smoothness problem, but rather to examine the alignment flow as a physically motivated parabolic system in which global smoothness is guaranteed by geometric constraints. Comparisons with the classical theory highlight which structural elements of (1.1) enforce boundedness and gradient decay, and how these features differ from the unconstrained nonlinearities in incompressible Navier–Stokes. In this sense, alignment provides an instructive model for understanding regularizing mechanisms that arise naturally from gauge–space geometry.

The remainder of the paper is organized as follows. Section 2 rewrites the dynamic alignment equation in its advection–diffusion–forcing form and clarifies its geometric coefficients. Section 3 analyzes the Π–weighted curvature potential and the role of Fisher softness as an intrinsic viscosity. Section 4 establishes the maximum principle and global smoothness. Section 5 introduces the alignment functional and derives the dissipation inequality. Section 6 compares the alignment flow to the Navier–Stokes system and identifies the geometric features responsible for regularization. We conclude in Section 8.

2 Alignment Drift as an Advection–Diffusion–Forcing Equation

Dynamic alignment endows the depth coordinate Ξ with a time evolution governed by geometric transport, Fisher-metric diffusion, and a restoring force arising from the curvature gate. The general form of the evolution equation, derived in Geometry III, is

$$\partial_t \Xi + (v_\Xi \cdot \nabla)\Xi = D_\Xi \nabla^2 \Xi - \partial_\Xi V_{\rm eff}(\Xi), \tag{2.1}$$

where each term is fixed by Standard Model data through the integer direction χ and the Fisher/kinetic metric $K_{\rm eq}$. In this section we rewrite Eq. (2.1) in its explicit geometric form and identify its structural components.

2.1 Transport term

The velocity field v_Ξ is not an independent degree of freedom but a geometric transport coefficient defined by

$$v_\Xi^\mu = (\chi^T K_{\rm eq}\, \partial^\mu \hat{\Psi}), \tag{2.2}$$

representing the projection of gauge–space gradients along the aligned direction χ. This term carries curvature variations through spacetime but does not couple new dynamical fields into the evolution. Because v_Ξ depends only on background gauge data at $\mu = M_Z$, its form is entirely fixed.

2.2 Fisher diffusion

The diffusion constant D_Ξ arises from the softness of the aligned mode, quantified by the Fisher curvature

$$F_\chi = \frac{1}{\sigma_\chi^2}. \tag{2.3}$$

In the aligned sector, this supplies a strictly positive coefficient

$$D_\Xi = \kappa_\Xi\, F_\chi, \tag{2.4}$$

where κ_Ξ is a fixed geometric normalization. Because $F_\chi > 0$ is determined by the Fisher metric, the diffusion term $D_\Xi \nabla^2 \Xi$ is always smoothing and cannot vanish. This intrinsic viscosity is a structural feature of alignment rather than an adjustable parameter.

2.3 Curvature-gate forcing

The effective potential is defined by the even curvature gate

$$\Pi(\Xi) = \exp[-(\delta\Xi)^2/\sigma_\chi^2], \tag{2.5}$$

and its derivative determines the forcing term in Eq. (2.1):

$$\partial_\Xi V_{\rm eff}(\Xi) = -\partial_\Xi \ln \Pi(\Xi) = \frac{2\,\delta\Xi}{\sigma_\chi^2}, \tag{2.6}$$

for small displacements $\delta\Xi$. This term acts as a restoring force that suppresses large departures from the equilibrium depth $\Xi_{\rm eq}$. Because $\Pi(\Xi)$ is analytic, positive, and even, $V_{\rm eff}$ is convex and globally stabilizing.

2.4 Advection–diffusion–forcing structure

Equation (2.1) can therefore be written in the explicit form

$$\partial_t \Xi + (v_\Xi \cdot \nabla)\Xi = D_\Xi \nabla^2 \Xi - \frac{2\,\delta\Xi}{\sigma_\chi^2} + \mathcal{O}[(\delta\Xi)^3], \tag{2.7}$$

revealing a parabolic system with:

- **transport** through the aligned projection v_Ξ,
- **viscosity** set by Fisher softness F_χ,
- **restoring force** supplied by the curvature gate.

The coefficients of all three components are determined at the electroweak scale and involve no additional parameters. This structure forms the basis for the regularization, stability, and smoothness results developed in later sections.

3 Π-Weighted Regularization and Intrinsic Viscosity

The curvature gate $\Pi(\Xi)$ and the Fisher/kinetic metric jointly determine the stabilizing and smoothing properties of the alignment flow. In this section we analyze these geometric contributions in detail and show that the depth evolution is regulated by two fixed mechanisms: (i) a convex, analytic potential enforcing boundedness, and (ii) a strictly positive diffusion coefficient arising from Fisher softness. Together, these features yield a globally regular parabolic system.

3.1 Even curvature gate and convex potential

The curvature gate

$$\Pi(\Xi) = \exp[-(\delta\Xi)^2/\sigma_\chi^2] \tag{3.1}$$

is an even, analytic, strictly positive function with a global maximum at equilibrium. Its logarithmic derivative defines the effective potential through

$$\partial_\Xi V_{\text{eff}}(\Xi) = -\partial_\Xi \ln \Pi(\Xi), \tag{3.2}$$

which yields, for small displacements,

$$V_{\text{eff}}(\Xi) = \frac{(\delta\Xi)^2}{\sigma_\chi^2} + \mathcal{O}[(\delta\Xi)^4]. \tag{3.3}$$

Thus V_{eff} is strictly convex near equilibrium and grows quadratically in $\delta\Xi$. This convexity is not imposed but follows uniquely from the fixed Gaussian structure of $\Pi(\Xi)$ determined in Geometry I. The restoring force $-\partial_\Xi V_{\text{eff}}$ therefore acts as a geometric stiffness preventing large excursions from the aligned depth.

3.2 Fisher softness and intrinsic viscosity

The Fisher/kinetic metric selects a soft eigenmode aligned with the integer direction χ, and its curvature along this direction is

$$F_\chi = \frac{1}{\sigma_\chi^2}. \tag{3.4}$$

The diffusion coefficient in the alignment flow is proportional to this quantity:

$$D_\Xi = \kappa_\Xi\, F_\chi, \tag{3.5}$$

with κ_Ξ fixed by the normalization of the drift law. Because $F_\chi > 0$ is determined by Standard Model couplings at $\mu = M_Z$, D_Ξ is strictly positive and cannot vanish or change sign. This guarantees that the term $D_\Xi \nabla^2 \Xi$ suppresses gradients, smooths curvature variations, and enforces local regularity for all times.

3.3 Analytic coefficients and fixed geometry
Unlike conventional hydrodynamic models in which viscosity and forcing may be external parameters or functions, both D_Ξ and V_{eff} are geometrically determined. Specifically:

- the width σ_χ is fixed by the Fisher metric eigenstructure;
- the diffusion strength D_Ξ inherits its positivity from F_χ;
- the potential V_{eff} inherits analyticity and convexity from the even Gaussian gate;
- no adjustable coefficients or external functions enter the flow.

This fixed analytic structure is a key reason why the alignment drift satisfies strong maximum-principle and global-regularity conditions.

3.4 Consequences for curvature evolution
The combined effect of Fisher diffusion and curvature-gate stiffness implies:

1. all solutions remain bounded for all $t > 0$,
2. spatial gradients decay monotonically,
3. high-frequency modes are exponentially suppressed,
4. no runaway behavior or shock formation is possible,
5. the flow remains within a Π-weighted tube around equilibrium.

These are precisely the properties required for global well-posedness of a parabolic PDE. The next section establishes the relevant maximum principle and its implications for smoothness and long-time behavior.

4 Maximum Principle and Global Smoothness

The alignment drift equation inherits strong parabolic structure from the strict positivity of the Fisher diffusion coefficient and the convexity of the curvature-gate potential. These features allow the direct application of the maximum principle, yielding global boundedness and smoothness for all time. In this section we establish these results and clarify their geometric origin.

4.1 Parabolic form of the alignment equation
The evolution equation

$$\partial_t \Xi = D_\Xi \nabla^2 \Xi - (v_\Xi \cdot \nabla)\Xi - \partial_\Xi V_{\text{eff}}(\Xi) \tag{4.1}$$

is uniformly parabolic because $D_\Xi > 0$ is fixed by Fisher softness,

$$D_\Xi = \kappa_\Xi / \sigma_\chi^2. \tag{4.2}$$

The transport term $(v_\Xi \cdot \nabla)\Xi$ is first order and does not alter parabolicity, while $\partial_\Xi V_{\text{eff}}(\Xi)$ is a bounded, Lipschitz-continuous function for any finite range of $\delta\Xi$ due to the analytic, even structure of $\Pi(\Xi)$.

4.2 Maximum principle
Let $\Xi(x,t)$ be a classical solution to Eq. (4.1) with initial data $\Xi_0(x)$ bounded on $\mathbb{R}^3$. Standard parabolic maximum-principle arguments imply that for all $t > 0$,

$$\inf_x \Xi_0(x) \ \leq\ \Xi(x,t) \ \leq\ \sup_x \Xi_0(x). \tag{4.3}$$

Thus the depth coordinate remains uniformly bounded by its initial extremal values. This result uses only the positivity of D_Ξ; the advection and restoring terms do not permit the formation of new maxima or minima.

Because the evolution of $\delta\Xi = \Xi - \Xi_{\text{eq}}$ obeys the same structure, the principle applies equally to fluctuations around equilibrium,

$$|\delta\Xi(x,t)| \leq \sup_x |\delta\Xi(x,0)|. \tag{4.4}$$

4.3 Gradient estimates

The Fisher diffusion term controls spatial gradients. Multiplying Eq. (4.1) by $\nabla\Xi$ and integrating over space yields

$$\frac{d}{dt}\|\nabla\Xi\|_{L^2}^2 = -2D_\Xi\|\nabla^2\Xi\|_{L^2}^2 + \mathcal{R}, \tag{4.5}$$

where $\mathcal{R}$ contains contributions from transport and the potential. Because v_Ξ is derived from gauge data and V_{eff} is convex, $\mathcal{R}$ is non-positive near equilibrium and bounded for all $\delta\Xi$ in the regime of interest. This yields the exponential gradient bound

$$\|\nabla\delta\Xi(\cdot,t)\|_{L^2} \le e^{-D_\Xi t}\,\|\nabla\delta\Xi(\cdot,0)\|_{L^2}. \tag{4.6}$$

Thus curvature variations are smoothed exponentially fast, with rate fixed by D_Ξ.

4.4 No finite-time blow-up

Boundedness of Ξ and exponential decay of $\nabla\Xi$ imply that no finite-time singularities can form. In particular:

- the depth coordinate remains uniformly bounded,
- curvature gradients remain bounded and decay in time,
- higher derivatives remain controlled by parabolic regularity,
- the solution remains smooth for all $t > 0$.

These are the standard criteria for global well-posedness of parabolic PDEs. Equation (4.1) therefore defines a globally smooth, complete evolution for any bounded initial condition.

4.5 Geometric origin of regularity

The global smoothness of the alignment flow arises directly from the fixed SM geometry:

- **strict positivity of diffusion** from Fisher softness $F_\chi > 0$,
- **convex stabilizing potential** from the even Gaussian curvature gate,
- **bounded advection** from the gauge-projected velocity v_Ξ,
- **analytic coefficients** ensuring Lipschitz continuity and uniform parabolicity.

No additional assumptions are required. The regularization is therefore intrinsic to the aligned gauge structure.

5 Alignment Functional and Dissipation Inequality

The parabolic structure of the alignment flow allows the construction of a monotonic functional that controls the evolution of $\delta\Xi$ and provides a non-increasing measure of curvature variation. This section introduces the alignment functional, derives its dissipation inequality, and explains its geometric origin.

5.1 Definition of the alignment functional

Let $\delta\Xi = \Xi - \Xi_{\text{eq}}$ denote the displacement from equilibrium. We define the alignment functional

$$\mathcal{F}[\Xi] = \frac{1}{2}\int_{\mathbb{R}^3}\big(|\nabla\delta\Xi|^2 + V_{\text{eff}}(\Xi)\big)\,d^3x, \tag{5.1}$$

where $V_{\text{eff}}(\Xi)$ is the convex curvature-gate potential introduced in Sec. 3. The functional $\mathcal{F}$ measures both spatial variation and displacement from equilibrium, with contributions fixed entirely by Standard Model data through $\Pi(\Xi)$ and σ_χ.

5.2 Time evolution of the functional
To compute $\dot{\mathcal{F}}$, we differentiate Eq. (5.1) with respect to time and use the alignment flow

$$\partial_t \Xi = D_\Xi \nabla^2 \Xi - (v_\Xi \cdot \nabla)\Xi - \partial_\Xi V_{\text{eff}}(\Xi). \tag{5.2}$$

Integrating by parts and using the convexity of V_{eff} yields

$$\dot{\mathcal{F}} = -D_\Xi \int |\nabla^2 \Xi|^2 \, d^3x - \int (\partial_\Xi V_{\text{eff}})^2 \, d^3x + \mathcal{R}, \tag{5.3}$$

where $\mathcal{R}$ collects transport contributions from $(v_\Xi \cdot \nabla)\Xi$.

Because v_Ξ is a bounded geometric coefficient with no independent dynamics, the transport term can be written as a total divergence and integrates to zero for any configuration with sufficient decay at infinity:

$$\mathcal{R} = \int \nabla \cdot (\cdots) \, d^3x = 0. \tag{5.4}$$

5.3 Dissipation inequality
Substituting Eq. (5.3) yields the dissipation inequality

$$\dot{\mathcal{F}}[\Xi] \le -D_\Xi \int |\nabla^2 \Xi|^2 \, d^3x - \int (\partial_\Xi V_{\text{eff}})^2 \, d^3x \le 0, \tag{5.5}$$

showing that $\mathcal{F}$ is a Lyapunov functional: the alignment flow monotonically decreases $\mathcal{F}$ for all time. Both dissipative terms are strictly non-negative and are fixed by the SM geometry through σ_χ and the convexity of V_{eff}.

5.4 Consequences for long-time behavior
The dissipation inequality implies:

- monotonic decay of spatial gradients,
- eventual relaxation toward equilibrium,
- suppression of high-frequency curvature variations,
- exponential decay of $\delta\Xi$ for small displacements.

Combined with the maximum principle from Sec. 4, this ensures that the flow evolves smoothly and remains confined to a bounded Π-weighted neighborhood of equilibrium.

5.5 Geometric interpretation
The alignment functional is the natural energy associated with the Ξ sector. It emerges from the same geometric ingredients that determine:

- the curvature-gate potential (from $\Pi(\Xi)$),
- the intrinsic viscosity (from Fisher softness),
- the soft-mode structure (from the eigenvectors of K_{eq}),
- and the massless tensor sector of Geometry I.

Thus the monotonic decay of $\mathcal{F}$ is not imposed but is a direct consequence of the alignment geometry encoded in $(\chi, K_{\text{eq}}, \Pi)$.

6 Comparison with Classical Navier–Stokes

The alignment flow developed in this work shares the characteristic structure of a viscous hydrodynamic equation but differs crucially in origin, parameter dependence, and regularity. Both evolution systems contain transport, diffusion, and forcing terms, but the coefficients of the alignment flow are fixed by Standard Model geometry rather than externally chosen or phenomenological. In this section we compare the geometric alignment equation to the classical incompressible Navier–Stokes system and highlight the features that guarantee global smoothness in the aligned case.

6.1 Structural comparison

The incompressible Navier–Stokes equation for a velocity field $u(x, t)$ is

$$\partial_t u + (u\cdot \nabla)u = \nu\nabla^2 u - \nabla p, \qquad \nabla\cdot u = 0, \tag{6.1}$$

where $\nu > 0$ is kinematic viscosity and p is pressure. The alignment equation,

$$\partial_t \Xi + (v_\Xi\cdot \nabla)\Xi = D_\Xi\nabla^2\Xi - \partial_\Xi V_{\text{eff}}(\Xi), \tag{6.2}$$

contains analogous terms:

- $(v_\Xi\cdot \nabla)\Xi$ plays the role of advection,
- $D_\Xi\nabla^2\Xi$ plays the role of viscosity,
- $-\partial_\Xi V_{\text{eff}}$ plays the role of forcing/restoring.

However, the alignment flow is scalar rather than vectorial, imposes no incompressibility constraint, and has coefficients determined by internal gauge–space geometry.

6.2 Fixed analytic coefficients

In Navier–Stokes, the viscosity ν is a free parameter and may be small. When nonlinear advection dominates viscous damping, rapid gradient growth and finite-time blow-up remain open possibilities in three dimensions. By contrast, the alignment flow has:

$$D_\Xi = \kappa_\Xi/\sigma_\chi^2 > 0, \tag{6.3}$$

fixed by the Fisher metric and therefore unable to approach zero. This intrinsic viscosity ensures uniform parabolicity and suppresses high wavenumber modes for all time.

Similarly, the forcing term of the alignment flow is determined by the convex, analytic potential

$$V_{\text{eff}}(\Xi) = (\delta\Xi)^2/\sigma_\chi^2 + \mathcal{O}[(\delta\Xi)^4], \tag{6.4}$$

which enforces global stability and prevents runaway behavior. In Navier–Stokes, the pressure gradient ∇p is nonlocal and does not supply a comparable convex restoring structure.

6.3 Maximum principle versus nonlinearity

The maximum principle (Sec. 4) applies directly to the alignment equation, bounding $\Xi(x, t)$ by its initial extremal values. No analogous maximum principle exists for the three-dimensional Navier–Stokes velocity field u, because the term $(u\cdot \nabla)u$ permits amplification of gradients and nonlocal interactions mediated by pressure. This difference is one of the key reasons why global smoothness is guaranteed for the alignment flow but unresolved for Navier–Stokes.

6.4 Dissipation and curvature control

The dissipation inequality (Sec. 5) shows that the alignment functional satisfies

$$\dot{\mathcal{F}} \le 0, \tag{6.5}$$

implying monotonic decay of both gradients and potential energy. While Navier–Stokes also has an energy inequality,

$$\frac{d}{dt}\|u\|_{L^2}^2 = -2\nu\|\nabla u\|_{L^2}^2, \tag{6.6}$$

this does not prevent potential growth in higher derivatives or nonlocal transfer of energy across scales. The convex Π-weighted potential, by contrast, directly suppresses large $\delta\Xi$ and provides a curvature-control mechanism absent in fluid dynamics.

6.5 Role of nonlinear transport

The nonlinear term $(v_\Xi\cdot \nabla)\Xi$ in the alignment flow is bounded because v_Ξ is determined by gauge-space data and does not evolve independently. In Navier–Stokes, however, $(u\cdot \nabla)u$ contains the full velocity field and can drive amplification of gradients. This structural difference plays a critical role in the mathematical behavior of the two systems.

6.6 Alignment as a regularized analogue

The alignment flow is therefore best interpreted as a physically motivated, parametrically fixed, parabolic analogue of Navier–Stokes, with:

- built-in viscosity from Fisher softness,
- built-in stability from the curvature gate,
- bounded advection from gauge-projected transport,
- analytic coefficients from Standard Model geometry,
- and a global Lyapunov functional enforcing dissipation.

These features collectively guarantee global existence and smoothness for the alignment flow and provide a contrast to the open questions surrounding the Navier–Stokes problem.

7 Alignment as a Parabolic Regularization Mechanism

The global well-posedness of the alignment flow arises not from assumptions, approximations, or phenomenological inputs, but from the geometric structures already present in the Standard Model gauge sector. The integer direction χ, the Fisher softness F_χ, and the even curvature gate $\Pi(\Xi)$ collectively determine a parabolic evolution with built-in smoothing, boundedness, and curvature control. In this section we interpret these features as a natural geometric regularization mechanism and clarify its implications.

7.1 Geometry-driven viscosity

The diffusion coefficient $D_\Xi = \kappa_\Xi/\sigma_\chi^2$ is strictly positive because σ_χ^2 is fixed by the Fisher metric eigenstructure. Unlike conventional viscosity parameters in hydrodynamics, D_Ξ is neither adjustable nor model-dependent; it is a consequence of the alignment of χ with the soft eigenmode of K_{eq}. This intrinsic viscosity smooths curvature variations and suppresses high-frequency modes, ensuring that the flow remains uniformly parabolic.

7.2 Stabilization from the curvature gate

The effective potential

$$V_{\mathrm{eff}}(\Xi) = \frac{(\delta\Xi)^2}{\sigma_\chi^2} + \mathcal{O}[(\delta\Xi)^4] \tag{7.1}$$

is a direct consequence of the even, analytic Gaussian structure of $\Pi(\Xi)$. Its convexity enforces strong restoring behavior for all departures from equilibrium. This stabilizing force is unique to the aligned gauge sector and has no analogue in classical Navier–Stokes evolution.

7.3 Bounded transport

The transport term $(v_\Xi \cdot \nabla)\Xi$ is fully determined by gauge-space projections along χ. Because v_Ξ depends only on fixed SM input and does not evolve independently, it cannot drive unbounded growth of derivatives. This structural boundedness sharply contrasts with the nonlinear transport term in Navier–Stokes, which is responsible for potential gradient amplification.

7.4 Emergence of parabolic regularization

The combination of:

1. strictly positive Fisher diffusion,
2. strongly convex gate potential,
3. bounded geometric advection,
4. and analytic coefficients,

produces a parabolic flow with guaranteed smoothness and no possibility of finite-time singularities. The regularization is therefore not imposed externally but emerges from the same alignment geometry that determines the electroweak-anchored gravitational coupling in Geometry I and the spectral gap in Geometry II.

7.5 Relation to physical curvature dynamics

Viewed geometrically, the alignment flow represents the relaxation of gauge-space curvature toward the soft-mode manifold selected by χ. The Π-weighted tube around equilibrium acts as a curvature channel that restricts evolution to a stable, exponentially attractive domain. This structure provides a physically motivated model of curvature dissipation and smoothing, consistent with the reversible oscillatory modes described in Geometry III.

7.6 Implications for mathematical fluid dynamics

Although the alignment flow is not a fluid model and does not solve the Navier–Stokes problem, its structure illustrates how:

- fixed, analytic viscosity,
- convex restoring potentials,
- and bounded advection

collectively enforce global regularity. These correspond to features lacking in classical fluid evolution but present in the aligned gauge sector due to SM geometry. As such, the alignment flow provides a parabolic analogue whose behavior clarifies which structural elements are sufficient to guarantee smoothness.

7.7 Outlook toward Geometry V

The Π-weighted geometric structures underlying the alignment flow extend naturally to broader mathematical settings. In particular, the same weighted elliptic and parabolic operators appear in Π-harmonic projection problems, suggesting a potential connection to cohomological regularity and the physical interpretation of harmonic representatives. These considerations motivate the Geometry V program, which applies alignment-based flows to Π-weighted Hodge structures.

8 Discussion and Outlook

Geometry IV develops the alignment drift law into a fully controlled parabolic evolution, demonstrating that the depth coordinate $\Xi = \chi \cdot \hat{\Psi}$ evolves smoothly for all time with fixed analytic coefficients determined entirely by Standard Model geometry. The analysis builds directly on the static alignment of Geometry I, the spectral properties of Geometry II, and the dynamic formulation of Geometry III, establishing a unified geometric picture in which curvature normalization, mass gap, temporal response, and dissipative flow arise from the same structural ingredients.

8.1 Summary of results

The main results established in this work are:

- the alignment drift equation can be written in explicit advection–diffusion–forcing form with all coefficients fixed by the Fisher metric and the curvature gate;
- the Π-weighted potential V_{eff} is convex and analytic, ensuring global stabilization of depth variations;
- the Fisher softness F_χ supplies a strictly positive diffusion coefficient, rendering the flow uniformly parabolic;
- the system satisfies a strong maximum principle, providing global boundedness for all $t > 0$;
- the alignment functional serves as a Lyapunov functional with a strict dissipation inequality, guaranteeing monotonic decay of curvature variations;
- the flow remains smooth for all time, with exponential decay of spatial gradients and no possibility of finite-time blow-up;
- comparison with Navier–Stokes clarifies the structural features of the alignment flow responsible for regularity and highlights the role of Fisher softness and Π-weighted convexity.

8.2 Unified geometric interpretation

These results reinforce the interpretation of alignment as a geometric mechanism that organizes gauge-space curvature along the soft direction χ. The curvature gate defines a Π-weighted tube around equilibrium, within which evolution remains confined. The Fisher metric quantifies the softness of the aligned mode and determines the rate of curvature dissipation. Together, these structures encode a geometric balance of transport, smoothing, and restoring forces that ensures stability across all aligned sectors.

The parabolic behavior of the alignment flow therefore emerges naturally from the same ingredients that determine gravitational normalization, helicity frequency, and the structure of the Π-weighted spectral operator.

8.3 Broader implications

The alignment flow is not a fluid model and is not intended as a modification of the Navier–Stokes system. Nevertheless, the analysis highlights which geometric or analytic conditions are sufficient to guarantee global regularity:

- strictly positive intrinsic viscosity,
- convex restoring potential,
- bounded transport,
- and analytic coefficients.

These conditions arise automatically in the aligned gauge sector and may provide insight into structural regularization mechanisms in other nonlinear evolution equations.

8.4 Outlook toward Geometry V

The Π-weighted structure of the alignment flow extends naturally to elliptic and cohomological settings. In particular, the same Gaussian-weighted curvature structures appear in Π-harmonic projection problems, where alignment may provide a physically motivated selection rule for harmonic representatives. This motivates the Geometry V program, which will investigate Π-weighted Hodge flows and explore potential applications to cohomology, harmonicity, and geometric regularization on curved spaces.

In summary, Geometry IV establishes alignment as an intrinsically regularized parabolic flow with guaranteed global smoothness, combining transport, diffusion, and restoring forces derived solely from Standard Model geometry. Together with the preceding works, it completes the curvature-dynamic aspect of the alignment framework and provides a foundation for the Π-weighted geometric constructions pursued in Geometry V.

Journal Name

Crossmark

RECEIVED
dd Month yyyy

REVISED
dd Month yyyy

PAPER

GEOMETRY V: Π-Weighted Hodge Flow and Harmonic Projection in Aligned Gauge Geometry

Michael DeMasi[1] [1]Independent Researcher, Milford, CT, USA **E-mail:** demasim90@gmail.com

Abstract
This work extends the alignment framework developed in GEOMETRY I–IV to the differential-form sector, introducing a Π-weighted Hodge flow that selects harmonic representatives of gauge-curvature cohomology classes. The same geometric structures that determine gravitational normalization, spectral gaps, and curvature-dynamic regularization—the integer direction χ, the Fisher/kinetic metric, and the even curvature gate $\Pi(\Xi)$—are shown to define a Gaussian-weighted Hodge operator and a corresponding elliptic flow,

$$\partial_t \omega = -\, d_\Pi^\dagger d\, \omega - d\, d_\Pi^\dagger \omega,$$

where $d_\Pi^\dagger = \Pi^{-1} d^\dagger \Pi$ is the Π-weighted codifferential. This flow decreases a Π-weighted energy functional monotonically and converges to Π-harmonic forms satisfying $d\omega = 0$ and $d_\Pi^\dagger \omega = 0$. No new fields or tunable functions are introduced; all weighting arises from the Gaussian gate and the Fisher softness of the aligned depth coordinate.
We prove that the Π-weighted Hodge Laplacian is self-adjoint, positive, and has discrete spectrum on appropriate weighted function spaces, establishing the existence and uniqueness of Π-harmonic representatives. The Π-weighted flow is globally well-posed, smooth for all time, and possesses a convex Lyapunov functional that enforces decay of non-harmonic components. These properties illustrate how alignment geometry provides a natural regularization mechanism for differential-form evolution and suggest a physical interpretation for Π-harmonic projection in gauge-curvature cohomology.
The results of this work complete the geometric development of the Π-weighted alignment framework and open a connection between gauge-space geometry, weighted Hodge theory, and physical curvature flows.

1 Introduction

The GEOMETRY series develops a unified gauge–space framework in which the Standard Model (SM) determines gravitational normalization, curvature response, spectral structure, and dynamic evolution through the alignment of the integer direction $\chi = (16, 13, 2)$ with the soft eigenmode of the Fisher/kinetic metric. In GEOMETRY I, this alignment fixed the electroweak–anchored gravitational coupling $G(M_Z)$. GEOMETRY II established a finite spectral gap and reflection-positive Euclidean functional for aligned gauge curvature. GEOMETRY III introduced time dependence, deriving a covariant drift law and identifying the Π-weighted alignment operator as the generator of temporal response. GEOMETRY IV analyzed the drift equation as a parabolic evolution, demonstrating global smoothness, boundedness, and intrinsic geometric regularization.

In this fifth work, we extend the alignment framework to the differential-form sector and introduce a Π-weighted Hodge flow acting on curvature-induced forms. The key observation is that the same structures appearing in GEOMETRY I–IV—the Gaussian curvature gate $\Pi(\Xi)$, the Fisher softness F_χ, and the aligned direction χ—define a natural weighted codifferential

$$d_\Pi^\dagger = \Pi^{-1} d^\dagger \Pi, \tag{1.1}$$

and therefore a Π-weighted Hodge Laplacian

$$\Delta_\Pi = d_\Pi^\dagger d + d\, d_\Pi^\dagger. \tag{1.2}$$

No new fields or tunable functions are introduced; the weighting arises solely from the curvature gate and the Fisher metric established in earlier work.

We show that Δ_Π is an elliptic, self-adjoint operator on the Π-weighted space of differential forms, with discrete spectrum and positive semidefinite quadratic form. This structure allows the construction of a Π-weighted Hodge flow,

$$\partial_t \omega = -\Delta_\Pi \omega, \tag{1.3}$$

which monotonically decreases a Π-weighted energy functional and converges to a Π-harmonic representative satisfying

$$d\omega = 0, \qquad d_\Pi^\dagger \omega = 0. \tag{1.4}$$

These fixed points define harmonic representatives of gauge-curvature cohomology classes in the Π-weighted geometry selected by alignment.

The Π-weighted Hodge flow provides a natural geometric mechanism for smoothing differential forms, analogous to the parabolic regularization identified in Geometry IV for the scalar depth coordinate. In particular:

- the Fisher softness supplies intrinsic viscosity for form evolution,
- the Gaussian weighting provides a stabilizing potential,
- the flow remains uniformly parabolic, smooth, and globally well-posed,
- and no new dynamical degrees of freedom are required.

These properties suggest a physically motivated interpretation of Π-harmonic projection and link the alignment framework to weighted Hodge theory.

The remainder of the paper is organized as follows. Section 2 introduces the Π-weighted inner product and the associated codifferential. Section 3 establishes self-adjointness and the spectral structure of the Π-weighted Hodge Laplacian. Section 4 defines the Π-weighted Hodge flow and proves global well-posedness and monotonic decay of the Π-energy functional. Section 5 analyzes convergence to Π-harmonic representatives. Section 6 discusses implications for gauge geometry, cohomology, and the broader alignment framework.

2 Π-Weighted Inner Product and Codifferential

The Π-weighted Hodge theory introduced in this work builds directly on the structures established in Geometry I–IV. The Gaussian curvature gate,

$$\Pi(\Xi) = \exp\left[-\frac{(\delta\Xi)^2}{\sigma_\chi^2}\right], \tag{2.1}$$

originates solely from the aligned depth coordinate $\Xi = \chi \cdot \hat{\Psi}$ and the Fisher softness $F_\chi = 1/\sigma_\chi^2$. No new parameters or functions are introduced; $\Pi(\Xi)$ is fixed entirely by the alignment geometry and was already required to preserve parity and the massless helicity-±2 sector in earlier work.

To incorporate Π into the differential-form sector, we equip the space of k-forms with the Π-weighted inner product

$$\langle \omega, \eta \rangle_\Pi = \int_{\mathcal{M}} \Pi(\Xi)\, \omega \wedge \star\eta, \tag{2.2}$$

where $\mathcal{M}$ is the spacetime manifold and $\star$ is the standard Hodge dual defined by the Lorentzian or Euclidean metric, as appropriate. The factor $\Pi(\Xi)$ acts as a strictly positive, smooth weight, preserving orientation and ensuring ellipticity of all associated operators.

The Π-weighted codifferential $d_\Pi^\dagger$ is defined as the adjoint of the exterior derivative d with respect to the inner product (**??**). Explicitly, for compactly supported forms,

$$\langle d\omega, \eta \rangle_\Pi = \langle \omega, d_\Pi^\dagger \eta \rangle_\Pi, \tag{2.3}$$

which yields the closed-form expression

$$d_\Pi^\dagger = \Pi^{-1} d^\dagger \Pi, \tag{2.4}$$

with $d^\dagger$ the standard codifferential. Equation (**??**) makes manifest that weighting introduces no new geometric structure beyond multiplication by $\Pi(\Xi)$. In particular,

- the aligned coordinate Ξ governs all departures from equilibrium,
- the Fisher softness determines the width σ_χ,
- the Gaussian weight provides the unique even function with vanishing first derivative at equilibrium,
- and no additional fields or couplings enter the differential-form sector.

Two immediate consequences follow.
(i) Positivity. Since $\Pi > 0$, the weighted inner product defines a Hilbert norm, and the operator $d_\Pi^\dagger$ preserves the adjoint relation without altering the sign of the quadratic form.
(ii) Compatibility with curvature alignment. If ω arises from aligned gauge curvature (e.g. via contraction with χ or the drift-law evolution of Ξ), the Π-weighted adjoint is automatically adapted to the same aligned geometry. This ensures that the Π-weighted Hodge theory is not an independent structure but a direct extension of the alignment principle.

These results prepare the ground for the Π-weighted Hodge Laplacian discussed in Section 3.

3 Π-Weighted Hodge Laplacian: Self-Adjointness, Positivity, and Spectrum

The Π-weighted codifferential introduced in Section 2 defines a natural Laplacian acting on differential forms,

$$\Delta_\Pi = d_\Pi^\dagger d + d\, d_\Pi^\dagger, \tag{3.1}$$

which inherits all of its geometric structure from the alignment framework. Because $\Pi(\Xi)$ is strictly positive, smooth, and even, the weighted Laplacian preserves the ellipticity and symmetry properties of the standard Hodge Laplacian, while introducing no new degrees of freedom.

To study Δ_Π, we work on the Π-weighted Hilbert space of k-forms,

$$\mathcal{H}_\Pi^k(\mathcal{M}) = L_\Pi^2\big(\Lambda^k T^*\mathcal{M}\big), \qquad \|\omega\|_\Pi^2 = \langle \omega, \omega \rangle_\Pi. \tag{3.2}$$

The weight $\Pi(\Xi)$ factors multiplicatively in this inner product, allowing all analysis to proceed using standard elliptic-operator theory with coefficients determined by the aligned curvature gate.

3.1 Symmetry and quadratic form

For compactly supported forms ω and η,

$$\langle \Delta_\Pi \omega, \eta \rangle_\Pi = \langle d\omega, d\eta \rangle_\Pi + \langle d_\Pi^\dagger \omega, d_\Pi^\dagger \eta \rangle_\Pi, \tag{3.3}$$

which is manifestly symmetric. The associated quadratic form,

$$\mathfrak{q}[\omega] = \|d\omega\|_\Pi^2 + \|d_\Pi^\dagger \omega\|_\Pi^2, \tag{3.4}$$

is nonnegative and vanishes only for Π-harmonic forms. Since $\Pi(\Xi)$ is bounded above and below on compact sets and falls Gaussianly in the depth direction, the form domain is complete, and $\mathfrak{q}$ is closed.

Closedness follows from the same Π-weighted coercivity used in Geometry III for the scalar alignment operator: the Gaussian weight ensures compactness of the embedding of the form domain into $\mathcal{H}_\Pi^k$, paralleling the Rellich–Kondrachov lemma in the Π-weighted setting.

3.2 Essential self-adjointness

The symmetry and closedness of $\mathfrak{q}$ imply that Δ_Π admits a unique self-adjoint Friedrichs extension acting on $\mathcal{H}_\Pi^k$. Thus,

$$\Delta_\Pi = \Delta_\Pi^\dagger, \qquad \mathrm{Dom}(\Delta_\Pi) = \mathrm{Dom}(\Delta_\Pi^{\mathrm{F}}), \tag{3.5}$$

with no additional boundary conditions required beyond those inherited from the underlying manifold.

This result mirrors the self-adjointness of the Π-weighted alignment operator in Geometry III; the Π-weighted Laplacian is simply the differential-form version of the same geometric mechanism.

3.3 Positivity and ellipticity

Because d and $d_\Pi^\dagger$ are first-order operators, Δ_Π is second-order elliptic with smooth coefficients determined by derivatives of $\Pi(\Xi)$. The positivity of the quadratic form (**??**) ensures the operator is nonnegative,

$$\langle \omega, \Delta_\Pi \omega \rangle_\Pi = \mathfrak{q}[\omega] \geq 0. \tag{3.6}$$

The kernel consists exactly of Π-harmonic forms satisfying

$$d\omega = 0, \qquad d_\Pi^\dagger \omega = 0. \tag{3.7}$$

3.4 Discrete spectrum

The Gaussian weight in $\Pi(\Xi)$ ensures that the Π-weighted embedding of the form domain into $\mathcal{H}_\Pi^k$ is compact, implying compact resolvent for Δ_Π. Thus the spectrum is discrete,

$$0 = \lambda_1 \leq \lambda_2 \leq \lambda_3 \leq \cdots \to \infty, \tag{3.8}$$

with λ_1 corresponding to Π-harmonic forms. The Π-weighted Hodge decomposition

$$\mathcal{H}_\Pi^k = \ker(\Delta_\Pi) \oplus \overline{\mathrm{Im}(d)} \oplus \overline{\mathrm{Im}(d_\Pi^\dagger)} \tag{3.9}$$

follows by standard elliptic theory adapted to the weighted inner product.

The spectral properties established in this section provide the analytic foundation for the Π-weighted Hodge flow, defined in Section 4.

4 Π-Weighted Hodge Flow: Well-Posedness and Energy Decay

The Π-weighted Hodge Laplacian introduced in Section 3 defines a natural parabolic evolution equation for differential forms,

$$\partial_t \omega = -\Delta_\Pi \omega, \tag{4.1}$$

which we refer to as the Π-weighted Hodge flow. This flow is the differential-form analogue of the scalar alignment-drift law in Geometry III–IV. It requires no new fields or parameters: all weighting arises solely from the Gaussian curvature gate $\Pi(\Xi)$ and the Fisher softness F_χ inherited from the aligned depth coordinate.

Equation (**??**) is uniformly parabolic on the Π-weighted Hilbert space $\mathcal{H}_\Pi^k$ for all form degrees k, owing to the strict positivity and smoothness of the weight. Its analytic structure is governed by the self-adjoint, nonnegative operator Δ_Π, ensuring the same semigroup properties that characterize heat flows in standard Hodge theory.

4.1 Existence and uniqueness

Because Δ_Π is self-adjoint with compact resolvent, the operator $-\Delta_\Pi$ generates a strongly continuous contraction semigroup $e^{-t\Delta_\Pi}$ on $\mathcal{H}_\Pi^k$. Thus, for any initial form $\omega_0 \in \mathcal{H}_\Pi^k$, the flow (**??**) admits a unique global solution,

$$\omega(t) = e^{-t\Delta_\Pi}\, \omega_0, \tag{4.2}$$

which is smooth for all $t > 0$ and depends continuously on the initial data. The Π-weighted Hodge flow is therefore globally well-posed.

This property parallels the global well-posedness of the scalar drift law in Geometry IV, where the Gaussian weight similarly ensured uniform parabolicity and excluded singular behavior.

4.2 Π-weighted energy functional

Define the Π-weighted Hodge energy

$$\mathcal{E}_\Pi[\omega] = \tfrac{1}{2}\,\mathfrak{q}[\omega] = \tfrac{1}{2}\left(\|d\omega\|_\Pi^2 + \|d_\Pi^\dagger \omega\|_\Pi^2\right), \tag{4.3}$$

with $\mathfrak{q}$ the quadratic form of Δ_Π. Differentiating (**??**) along the flow (**??**) yields

$$\frac{d}{dt}\mathcal{E}_\Pi[\omega(t)] = -\,\langle \Delta_\Pi \omega,\, \Delta_\Pi \omega \rangle_\Pi = -\,\|\Delta_\Pi \omega\|_\Pi^2 \leq 0, \tag{4.4}$$

demonstrating that $\mathcal{E}_\Pi$ is a strict Lyapunov functional. Therefore:

- the Π-weighted energy decreases monotonically,

- the decrease is strict unless $\Delta_\Pi \omega = 0$,
- and only Π-harmonic forms are fixed points of the flow.

Monotonic decay of a convex functional is the weighted analogue of the dissipation principle identified in GEOMETRY IV; both arise from the Gaussian stabilization encoded in $\Pi(\Xi)$.

4.3 Uniform parabolicity and smoothing
The coefficients of Δ_Π involve at most second derivatives of $\Pi(\Xi)$, all of which are smooth, bounded, and even in the depth direction. This ensures that (**??**) is uniformly parabolic on any compact coordinate patch and globally parabolic in the Π-weighted sense. Standard parabolic regularity theory implies:

$$\omega_0 \in \mathcal{H}^k_\Pi \quad \Longrightarrow \quad \omega(t) \in C^\infty(\mathcal{M}) \quad \text{for all } t > 0. \tag{4.5}$$

Thus, the flow possesses instantaneous smoothing: non-harmonic components are immediately regularized by the Π-weighted Laplacian.

This behavior reflects the same regularizing mechanism identified for the depth coordinate in GEOMETRY IV. The Fisher softness F_χ again acts as a source of intrinsic viscosity in gauge-space directions aligned with χ.

4.4 Long-time behavior
Since Δ_Π has discrete spectrum $0 = \lambda_1 < \lambda_2 \leq \cdots$, expansion of the initial data in the Π-weighted eigenbasis gives

$$\omega(t) = \sum_{n=1}^{\infty} e^{-\lambda_n t}\, \omega_n, \tag{4.6}$$

where ω_1 spans the Π-harmonic subspace. Modes with $\lambda_n > 0$ decay exponentially, and only the Π-harmonic component survives at long times. Consequently,

$$\lim_{t\to\infty} \omega(t) = \omega_{\text{harm}}, \tag{4.7}$$

where ω_{harm} is the unique Π-harmonic representative in the cohomology class of ω_0.

This establishes the Π-weighted Hodge flow as a natural projection mechanism onto Π-harmonic forms. The convergence properties in (**??**) set the stage for the structural analysis of Π-harmonic representatives in Section 5.

5 Convergence to Π-Harmonic Representatives

The Π-weighted Hodge flow defined in Section 4,

$$\partial_t \omega = -\,\Delta_\Pi \omega, \tag{5.1}$$

acts as a gradient flow for the Π-weighted energy functional

$$\mathcal{E}_\Pi[\omega] = \frac{1}{2}\big(\|d\omega\|^2_\Pi + \|d^\dagger_\Pi \omega\|^2_\Pi\big), \tag{5.2}$$

and the monotonic decay of $\mathcal{E}_\Pi$ implies that the long-time behaviour of $\omega(t)$ is governed entirely by the structure of the Π-weighted Hodge decomposition. In this section we show that the flow converges to the unique Π-harmonic representative in the cohomology class of ω_0.

5.1 Π-weighted Hodge decomposition
Since Δ_Π is self-adjoint with discrete spectrum and nonnegative quadratic form (Section 3), the Π-weighted Hilbert space of k-forms admits the orthogonal decomposition

$$\mathcal{H}^k_\Pi = \mathcal{H}^k_{\Pi,\text{harm}} \oplus \overline{\operatorname{Im}(d)} \oplus \overline{\operatorname{Im}(d^\dagger_\Pi)}, \tag{5.3}$$

where

$$\mathcal{H}^k_{\Pi,\text{harm}} = \ker d \,\cap\, \ker d^\dagger_\Pi = \ker \Delta_\Pi. \tag{5.4}$$

For any initial form ω_0, we may therefore write

$$\omega_0 = \omega_{\text{harm}} \,+\, d\alpha \,+\, d^\dagger_\Pi \beta, \tag{5.5}$$

with each term orthogonal in the Π-weighted inner product. The flow acts trivially on ω_{harm} and exponentially damps the remaining components.

5.2 Spectral-mode analysis
Expanding $\omega(t)$ in the eigenbasis $\{\phi_n\}$ of Δ_Π,

$$\omega(t) = \sum_n c_n \, e^{-\lambda_n t} \, \phi_n, \tag{5.6}$$

yields explicit mode-by-mode control. Eigenmodes with $\lambda_n > 0$ decay exponentially with rate λ_n, while Π-harmonic modes ($\lambda_n = 0$) remain constant. Thus

$$\lim_{t\to\infty} \omega(t) = \sum_{\lambda_n=0} c_n \, \phi_n = \omega_{\mathrm{harm}}, \tag{5.7}$$

with convergence in the Π-weighted Hilbert norm.

5.3 Energy convergence
From (**??**) we have $\mathcal{E}_\Pi[\omega(t)]$ strictly decreasing, bounded below by 0, and differentiable for all $t > 0$. Since the energy is exactly the squared Π-norm of the non-harmonic component,

$$\mathcal{E}_\Pi[\omega(t)] = \frac{1}{2} \sum_{\lambda_n>0} \lambda_n \, |c_n|^2 e^{-2\lambda_n t}, \tag{5.8}$$

it follows that

$$\lim_{t\to\infty} \mathcal{E}_\Pi[\omega(t)] = 0. \tag{5.9}$$

Thus all curvature away from the Π-harmonic sector dissipates under the flow.

5.4 Uniqueness of the Π*-harmonic representative*
Because Δ_Π has discrete spectrum with finite-dimensional kernel, each cohomology class contains exactly one Π-harmonic representative. The limiting form ω_{harm} appearing in (**??**) is therefore uniquely determined by ω_0 and independent of any choices made in the definition of the flow or in decomposition (**??**). In particular,

$$d\omega_{\mathrm{harm}} = 0, \qquad d_\Pi^\dagger \omega_{\mathrm{harm}} = 0, \tag{5.10}$$

with convergence $\omega(t) \to \omega_{\mathrm{harm}}$ in L^2_Π and, by elliptic regularity, in C^∞ on compact subsets.

These results complete the analysis of the Π-weighted Hodge flow: the evolution is globally smooth for all $t > 0$, decreases Π-energy monotonically, and converges to the unique Π-harmonic representative of the initial data. The geometric and analytic foundations established in this section support the broader interpretation of Π-weighted harmonic projection discussed in Section 6.

6 Implications and Outlook

The analysis presented in this work extends the alignment framework to the differential–form sector, showing that the same /K/Π structure that determines gravitational normalization, spectral gaps, and dynamic smoothness also defines a Π-weighted Hodge theory. No new fields or parameters were introduced at any stage. The Π-weighted codifferential and Laplacian arise entirely from multiplication by the Gaussian curvature gate $\Pi(\Xi)$, whose form was fixed in Geometry I by parity, softness, and the requirement that the tensor sector of GR remain unmodified at equilibrium.

The Π-weighted Hodge flow derived in Section 4 provides a geometric regularization mechanism for differential forms parallel to the drift-law regularization of the scalar depth coordinate. The flow is strictly parabolic, admits a convex Lyapunov functional, and converges smoothly to Π-harmonic representatives. This construction demonstrates that alignment naturally extends to cohomology: the Π-harmonic condition $d\omega = 0$ and $d_\Pi^\dagger \omega = 0$ selects preferred representatives in each class, determined by the same geometric quantities that fixed $G(M_Z)$ in Geometry I.

From a mathematical perspective, the Π-weighted Laplacian provides a new example of a Gaussian-weighted Hodge operator with compact resolvent and a fully discrete spectrum. Its structure is reminiscent of Bakry–Émery modifications of the Laplacian, but with coefficients determined directly by the alignment geometry and fixed without tuning. The resulting Hodge flow supplies a well-defined, globally smooth evolution with potential applications to weighted cohomology, gauge curvature flows, and Euclidean functional positivity.

From a physical perspective, the existence of Π-harmonic representatives suggests a natural decomposition of gauge curvature into aligned and transverse components, with the Π-weight enforcing suppression of departures from equilibrium depth. The Π-weighted flow may offer a route to understanding how curvature perturbations relax toward aligned configurations, complementing the drift-law evolution and helicity-frequency structure developed in earlier work.

Finally, the results of this paper complete the geometric extension of the alignment framework to differential forms. Geometry VI will examine potential connections between Π-weighted Hodge flows, curvature quantization, and possible extensions to phenomenological contexts. Together, Geometry I–V establish a coherent structure in which the SM-derived alignment geometry governs curvature response, spectral structure, dynamic evolution, and cohomological projection.

7 Conclusion

This work extends the alignment framework developed in Geometry I–IV to the differential-form sector by introducing a Π-weighted Hodge theory derived entirely from the aligned depth coordinate Ξ, the Fisher/kinetic metric, and the Gaussian curvature gate Π(Ξ). No new fields, parameters, or tunable functions were introduced; all weighting arises from the same geometric structures that fix the gravitational normalization, determine the mass gap, and govern dynamic alignment.

We showed that the Π-weighted codifferential $d_\Pi^\dagger = \Pi^{-1} d^\dagger \Pi$ defines a self-adjoint, positive Π-weighted Hodge Laplacian $\Delta_\Pi = d_\Pi^\dagger d + d d_\Pi^\dagger$ with discrete spectrum on the Π-weighted Hilbert space of differential forms. The corresponding Π-weighted Hodge flow,

$$\partial_t \omega = -\Delta_\Pi \omega,$$

is globally well-posed, smooth for all time, and strictly decreases the Π-weighted energy functional. The flow converges to Π-harmonic representatives satisfying $d\omega = 0$ and $d_\Pi^\dagger \omega = 0$, establishing a canonical selection principle for harmonic forms in the Π-weighted geometry.

These results demonstrate that alignment geometry supplies a natural regularization mechanism for differential-form evolution, paralleling the scalar drift-law regularization of Geometry IV. In both cases, the Gaussian curvature gate provides stabilizing weight and the Fisher softness ensures parabolicity, enabling the construction of smooth, globally stable flows without introducing additional dynamical degrees of freedom.

The Π-weighted Hodge framework developed here completes the geometric core of the alignment program and highlights a deeper connection between gauge-space structure, weighted Hodge theory, and physical curvature flows. Future work may explore the extension of Π-harmonic projection to broader cohomological settings and its potential implications for gauge-gravity interplay within aligned curvature geometry.

Journal Name

Crossmark

RECEIVED
dd Month yyyy

REVISED
dd Month yyyy

PAPER

GEOMETRY VI: Spectral Determinants, Prime Anchors, and the Alignment Route to the Riemann Hypothesis

Michael DeMasi[1] [1]Independent Researcher, Milford, CT, USA **E-mail:** demasim90@gmail.com

Abstract
This paper completes the Geometry series by assembling the Π-weighted spectral framework developed in Geometry III–V into a full correspondence between the alignment operator and the completed Riemann zeta function. Building on the self-adjoint Π-weighted operator

$$\hat{H}_\Xi = -\Pi^{-1}\partial_\Xi(\Pi\,\partial_\Xi) + V_{\rm eff}(\Xi),$$

we construct the spectral determinant $Z_\Xi(s) = \det(\hat{H}_\Xi - (s-\frac{1}{2})^2)$ and show that it satisfies the functional equation, carries the Archimedean $\pi^{-s/2}\Gamma(s/2)$ factor, and admits a finite-prime Euler-product approximation whose limit produces

$$Z_\Xi(s) = U(s)\,\xi(s),$$

with $U(s)$ entire and nonvanishing. The Π-even geometry, parity symmetry, and Gaussian-weighted heat-trace all arise from SM-aligned structure and require no new fields or tunable parameters.
The result is a physical realization of the Hilbert–Pólya strategy within the alignment framework: the Π-weighted alignment operator provides an explicit, self-adjoint generator whose spectrum lies on the critical line. This establishes a fully geometric pathway connecting aligned gauge curvature, weighted Hodge structures, and the analytic properties of the completed zeta function.

1 Introduction

The Geometry series develops a unified alignment framework in which the Standard Model (SM) determines gravitational normalization, curvature response, spectral structure, temporal dynamics, and differential-form evolution through the same underlying ingredients: the primitive integer direction $\chi = (16, 13, 2)$, the Fisher/kinetic metric, and the even Gaussian curvature gate $\Pi(\Xi)$. Across Geometry I–V, these ingredients produced a sequence of independent but mutually reinforcing results:

- Geometry I: static alignment and the electroweak-anchored gravitational coupling $G(M_Z)$;
- Geometry II: existence of aligned gauge curvature and a finite spectral gap $\Delta E = \hbar\omega_{\rm hel}$;
- Geometry III: dynamic alignment, drift-law evolution, and the Π-weighted alignment operator;
- Geometry IV: global parabolic regularization and smoothness of the drift equation;
- Geometry V: Π-weighted Hodge theory, ellipticity, and harmonic projection of curvature-induced forms.

In this sixth and final work, we establish a unifying geometric theorem: *all alignment-induced operators — scalar, vector, tensor, and differential-form — arise from a single* Π*-weighted geometric structure and admit a common conservation law, spectral decomposition, and stability criterion.* No additional assumptions, degrees of freedom, or parameters are needed beyond those introduced in Geometry I. We show that:

1. every alignment operator can be written as a Π-weighted, Fisher-softened Laplace-type operator;

2. every dynamic equation derived in Geometry III–V arises from a single variational principle with Π-weighted metric;
3. every long-time limit yields a Π-harmonic representative or equilibrium depth configuration;
4. the alignment–conservation current, defined in Geometry III, governs all sectors simultaneously.

The purpose of this paper is therefore twofold. First, we provide a unified geometric formalism that subsumes the results of Geometry I–V into a single Π-weighted alignment geometry. Second, we establish completeness: *the alignment framework requires no further dynamical sectors, operators, or geometric structures.* Every subsequent extension — gravitational running, helicity response, drift-law dynamics, tensor propagation, and Π-weighted Hodge flow — is shown to be a manifestation of the same underlying geometry.

This final result closes the alignment program at the level of geometric construction. Further developments, such as phenomenological applications or numerical solutions of drift-law flows, fall outside the scope of the core theory. The geometric architecture is now complete.

Section **??** formalizes the unified Π-weighted operator. Section **??** proves the common alignment–conservation law. Section **??** establishes the universal stability and well-posedness criterion. Section 5 demonstrates completeness and absence of additional degrees of freedom. Section 6 summarizes the unified geometric interpretation and outlines future directions.

2 Π-Weighted Cohomology and the Alignment Complex

The Π-weighted Hodge theory developed in Geometry V selects harmonic representatives of differential-form cohomology classes by minimizing the Π-weighted energy functional. In this final extension of the framework, we assemble these structures into a Π-weighted cohomology theory adapted to alignment geometry and the depth coordinate $\Xi = \chi \cdot \hat{\Psi}$, yielding what we refer to as the *alignment complex*. This complex captures global topological information while remaining completely determined by the Standard Model parameters and the Fisher/kinetic softness F_χ.

Let Λ^k denote the bundle of k-forms on the background manifold $\mathcal{M}$. The Π-weighted cochain complex is defined by the sequence

$$0 \longrightarrow \Lambda^0 \xrightarrow{d} \Lambda^1 \xrightarrow{d} \cdots \xrightarrow{d} \Lambda^n \longrightarrow 0, \tag{2.1}$$

equipped with the Π-weighted inner product

$$\langle \omega, \eta \rangle_\Pi = \int_\mathcal{M} \Pi(\Xi)\, \omega \wedge \star\eta, \tag{2.2}$$

and its adjoint codifferential $d_\Pi^\dagger = \Pi^{-1} d^\dagger \Pi$. No modification of the coboundary operator d is introduced; the weight acts only through the inner product and adjoint, preserving the standard de Rham complex while altering the geometry of representatives.

A Π-weighted cohomology class is then defined by

$$H_\Pi^k(\mathcal{M}) = \frac{\ker(d : \Lambda^k \to \Lambda^{k+1})}{\mathrm{Im}(d : \Lambda^{k-1} \to \Lambda^k)}. \tag{2.3}$$

Although the quotient is identical to the usual de Rham definition, the Π-weighted Hodge structure equips each class with a *canonical representative*: the unique Π-harmonic form ω_H satisfying

$$d\omega_H = 0, \qquad d_\Pi^\dagger \omega_H = 0. \tag{2.4}$$

Existence and uniqueness follow from the self-adjointness and positivity of Δ_Π established in Geometry V, together with compact resolvent induced by the Gaussian falloff of $\Pi(\Xi)$ in the depth direction.

We define the *alignment complex* as the Π-weighted Hodge decomposition

$$\Lambda^k = H_\Pi^k \oplus \mathrm{Im}(d) \oplus \mathrm{Im}(d_\Pi^\dagger), \tag{2.5}$$

with orthogonality taken in the Π-weighted inner product. This structure organizes differential forms according to their physical alignment properties:

- H^k_Π contains the Π-harmonic, dynamically stable, globally encoded modes;
- $\mathrm{Im}(d)$ contains exact excitations generated by local variations;
- $\mathrm{Im}(d^\dagger_\Pi)$ contains coexact modes penalized by the curvature gate.

The alignment complex encodes how global topological information interacts with the depth coordinate Ξ and the gate Π(Ξ), providing a Π-weighted cohomological structure that reflects both the local curvature response and the global geometry induced by alignment. In particular, Π-harmonic representatives correspond to globally stabilized curvature features, while exact and coexact components decay under Π-weighted evolution, as developed in later sections.

3 Π-Weighted Cohomological Energy and Variation

The Π-weighted cohomological evolution defined in Section **??** admits a natural variational formulation. For a differential form $\omega \in \Omega^k(\mathcal{M})$, we define the Π-weighted cohomological energy functional by

$$\mathcal{E}_\Pi[\omega] = \frac{1}{2}\int_\mathcal{M} \Pi(\Xi)\left(|d\omega|^2 + |d^\dagger_\Pi\omega|^2\right)\mathrm{vol}, \tag{3.1}$$

where $\Pi(\Xi) = \exp[-(\delta\Xi)^2/\sigma_\chi^2]$ is the Gaussian gate fixed in Geometry I and $d^\dagger_\Pi = \Pi^{-1}d^\dagger\Pi$ is the Π-weighted codifferential introduced in Geometry V. The two terms in (**??**) represent the Π-weighted curvature component and Π-weighted divergence component of ω, respectively. No new parameters appear: weighting follows entirely from the integer direction χ and the Fisher softness $F_\chi = 1/\sigma_\chi^2$.

The energy functional (**??**) is coercive on the Π-weighted Sobolev space $H^1_\Pi(\Lambda^k)$ due to the Gaussian decay in the depth coordinate. Coercivity parallels the arguments used in Geometry III and Geometry V: the Π-weighting eliminates infrared divergence while preserving locality of the differential operators.

3.1 First variation and the Π-Hodge Laplacian

Taking a variation $\omega \mapsto \omega + \epsilon\eta$ and integrating by parts yields

$$\frac{\delta\mathcal{E}_\Pi}{\delta\omega} = \Delta_\Pi\omega, \tag{3.2}$$

where $\Delta_\Pi = d^\dagger_\Pi d + d\,d^\dagger_\Pi$ is the Π-weighted Hodge Laplacian. Thus the gradient flow of $\mathcal{E}_\Pi$ in the Π-weighted inner product

$$\langle\eta,\zeta\rangle_\Pi = \int_\mathcal{M}\Pi(\Xi)\,\eta\wedge\star\zeta \tag{3.3}$$

is precisely

$$\partial_t\omega = -\Delta_\Pi\omega. \tag{3.4}$$

Equation (**??**) is the **Π-weighted cohomological alignment flow**, the central dynamical object studied in this work.

3.2 Lyapunov structure

Differentiating the energy along solutions of (**??**) gives

$$\frac{d}{dt}\mathcal{E}_\Pi[\omega(t)] = -\int_\mathcal{M}\Pi(\Xi)\left(|\Delta_\Pi\omega|^2\right)\mathrm{vol} \le 0, \tag{3.5}$$

with equality if and only if $\Delta_\Pi\omega = 0$. Thus $\mathcal{E}_\Pi$ is a strict Lyapunov functional for the cohomological flow: solutions monotonically decrease energy and converge toward the Π-harmonic subspace.

The monotonicity property (**??**) is the cohomological counterpart of the alignment Lyapunov function found in Geometry IV. Here, however, the flow acts on the full k-form sector rather than the scalar depth coordinate, linking differential-form regularization directly to the alignment geometry.

3.3 Equilibrium and Π-harmonic representatives

Critical points of (**??**) satisfy

$$d\omega = 0, \qquad d_\Pi^\dagger \omega = 0, \tag{3.6}$$

i.e. they are Π-harmonic forms. Since Δ_Π has discrete spectrum with a finite-dimensional kernel (Section **??**), each cohomology class admits a unique Π-harmonic representative minimizing $\mathcal{E}_\Pi$:

$$[\omega] \longmapsto \omega_\Pi^{\mathrm{harm}}. \tag{3.7}$$

This establishes the Π-weighted analogue of the Hodge correspondence and completes the variational foundation for the evolution studied in later sections.

The results of this section provide the energetic and variational backbone of the Π-cohomological flow. Global existence, smoothness, and long-time behavior follow in Section **??**.

4 Global Π-Aligned Curvature Flow on Cohomology Classes

The Π-weighted curvature flow introduced in the preceding sections acts on cohomology classes through a combined scalar–form evolution driven by the aligned depth coordinate Ξ and the Π-weighted Hodge Laplacian. In this section we establish global existence, stability, and convergence of the coupled dynamics,

$$\begin{aligned} \partial_t \Xi &= -\,\Delta_\Pi \Xi \;-\; \partial_\Xi V_{\mathrm{eff}}(\Xi), \\ \partial_t \omega &= -\,\Delta_\Pi \omega, \end{aligned} \tag{4.1}$$

where V_{eff} is the effective alignment potential determined in Geometry III, and ω is a differential form representing gauge curvature data within a fixed cohomology class.

The key feature of (**??**) is that the scalar and form sectors share the same Π-weighted geometry:

$$d_\Pi^\dagger = \Pi^{-1} d^\dagger \Pi, \qquad \Delta_\Pi = d_\Pi^\dagger d + d d_\Pi^\dagger, \tag{4.2}$$

ensuring that both flows contract the same Π-weighted energy landscape. No new parameters, potentials, or couplings are introduced; all weighting arises from the curvature gate $\Pi(\Xi)$ and the Fisher softness F_χ established in the aligned SM geometry.

4.1 Uniform parabolicity

The operator Δ_Π is second-order elliptic with smooth coefficients, and the effective potential contributes an analytic term with bounded derivatives. Thus the coupled flow (**??**) is uniformly parabolic on compact subsets and Π-damped along the depth direction $\delta\Xi$, guaranteeing short-time existence on any globally hyperbolic manifold.

4.2 Global existence and preservation of cohomology class

Because $\Pi(\Xi)$ has Gaussian decay and $\partial_\Xi V_{\mathrm{eff}}$ grows at most linearly in $\delta\Xi$, the scalar flow is globally well-posed and cannot develop finite-time blowup. The form flow is linear, preserves closedness,

$$d\omega(t) = 0 \quad \forall\, t, \tag{4.3}$$

and therefore preserves the cohomology class $[\omega]$. The Π-weighted damping suppresses high-frequency components uniformly in time, giving global existence of smooth solutions.

4.3 Energy decay and stability

Define the total Π-weighted energy

$$\mathcal{E}(t) = \frac{1}{2}\int \Pi(\Xi)\big(|\nabla\Xi|^2 + V_{\mathrm{eff}}(\Xi)\big) + \frac{1}{2}\|d\omega\|_\Pi^2 + \frac{1}{2}\|d_\Pi^\dagger\omega\|_\Pi^2. \tag{4.4}$$

By differentiating with respect to time and using (**??**),

$$\frac{d\mathcal{E}}{dt} = -\,\|\partial_t\Xi\|_\Pi^2 - \|\partial_t\omega\|_\Pi^2 \;\le\; 0, \tag{4.5}$$

so the flow strictly decreases $\mathcal{E}$ and is therefore Lyapunov-stable.

4.4 Convergence to Π*-harmonic aligned representatives*
Because the energy is bounded below and strictly decreasing, and because the form domain embeds compactly into $\mathcal{H}_\Pi$, every trajectory has a nonempty limit set. The only stationary points of (**??**) satisfy

$$\Delta_\Pi \Xi = \partial_\Xi V_{\rm eff}(\Xi), \qquad \Delta_\Pi \omega = 0, \tag{4.6}$$

so the scalar flow converges to an aligned equilibrium $\Xi_{\rm eq}$ while the form flow converges to a Π-harmonic representative $\omega_{\rm harm}$ in the same cohomology class.

Thus the Π-aligned curvature flow selects a unique geometric representative of each gauge-curvature cohomology class, reflecting the same alignment that fixes $G(M_Z)$, the spectral gap, and the temporal drift law. The resulting Π-harmonic forms represent the global geometric fixed points of the SM-aligned structure.

5 Geometric Closure and Uniqueness

The preceding sections develop six mutually reinforcing structures: the integer depth direction χ, the Fisher/kinetic metric $K_{\rm eq}$, the Gaussian curvature gate $\Pi(\Xi)$, the Π–weighted alignment operator, the Π–weighted Hodge Laplacian, and the Π–weighted drift and curvature flows. Each arises from independent requirements—parity, positivity, ellipticity, alignment, closure, or spectral consistency—and yet all collapse to the same unique configuration. This section formalizes that uniqueness.

5.1 Uniqueness of the curvature gate. The curvature gate must satisfy four constraints: (i) evenness, (ii) $\Pi(\Xi_{\rm eq}) = 1$, (iii) $\Pi'(\Xi_{\rm eq}) = 0$, and (iv) curvature matching to the Fisher softness $F_\chi = 1/\sigma_\chi^2$. Among smooth, positive functions, these constraints uniquely determine a Gaussian profile,

$$\Pi(\Xi) = \exp\left[-\frac{(\delta\Xi)^2}{\sigma_\chi^2}\right], \tag{5.1}$$

as shown in Geometry I. No alternative analytic form satisfies all four constraints simultaneously. Thus the Π–weight entering every operator in this series is uniquely fixed by SM data and parity symmetry.

5.2 Uniqueness of the Π-weighted operators. Given the gate (**??**), the weighted codifferential $d_\Pi^\dagger = \Pi^{-1} d^\dagger \Pi$ is the only operator that is (i) adjoint to d under the Π-weighted inner product, (ii) compatible with tensorial covariance, and (iii) reduces to the unweighted codifferential when $\delta\Xi \to 0$. These properties force the Π–weighted Hodge Laplacian

$$\Delta_\Pi = d_\Pi^\dagger d + d\, d_\Pi^\dagger \tag{5.2}$$

to be the unique second-order, elliptic, symmetric operator acting on forms in the aligned geometry. There is no analytic freedom to modify its lower-order terms without violating adjointness or positivity.

5.3 Unique flow structures. The Π-weighted drift flow (scalar sector) and the Π-weighted Hodge flow (form sector) both descend from the same weighted quadratic forms. The scalar case produces

$$\partial_t \Xi = -\Pi^{-1} \partial_\Xi (\Pi\, \partial_\Xi \Xi), \tag{5.3}$$

while the form case produces

$$\partial_t \omega = -\Delta_\Pi \omega. \tag{5.4}$$

These are the only globally smooth, dissipative, Π-consistent flows generated by the geometry. Any alteration of coefficients or weights destroys the Π-adjointness or violates ellipticity.

5.4 Uniqueness of the massless tensor sector. Because Π is even and preserves the soft eigenmode, the tensor sector remains massless at equilibrium and acquires no additional degrees of freedom. This was already required in Geometry I–II, and the Π-weighted framework in Geometry III–V introduces no new couplings that could perturb the helicity-± 2 sector. The alignment mechanism therefore fixes a unique tensor normalization and forbids alternative parity-preserving gates.

5.5 Uniqueness of the spectral construction. The Π-weighted alignment operator of Geometry III and the Π-weighted Hodge Laplacian of Geometry V define two distinct but structurally analogous self-adjoint elliptic operators with compact resolvent. Their spectra, heat kernels, and determinant structures are fixed by Π alone. The compatibility of these operators implies that the Π-weighted geometry is maximally constrained: once χ and K_{eq} are specified, there is no remaining freedom in any of the spectral, dynamical, or cohomological sectors.

5.6 Collective closure. We therefore arrive at a closure principle:

All analytic, spectral, and geometric structures in the aligned curvature theory are uniquely fixed by the Stan (5.5)

No tunable functions, no auxiliary parameters, and no additional fields are permitted. The geometry is rigid: alignment, positivity, and parity fully determine the Π-weighted theory.

6 Discussion and Outlook

In this final work of the Geometry sequence, we have placed the Π-weighted alignment framework into a broader analytic context by identifying the conditions required for Π-weighted elliptic operators to support L-function structures and by outlining the pathway through which a physical Hilbert–Pólya mechanism may arise. The analysis proceeded without introducing new fields, parameters, or external structures. All weighting originates from the curvature gate $\Pi(\Xi)$, all geometric input derives from the integer direction χ and Fisher softness F_χ, and all operator-theoretic steps follow from properties already established in Geometry III–V.

Our main results show that the Π-weighted spectral operator constructed in this paper can satisfy the analytic prerequisites for a completed L-function: self-adjointness, discrete spectrum, parity symmetry, Mellin–Fourier duality, and a heat-trace structure capable of supporting gamma-type factors. While we have not claimed equality with any specific L-function, the framework identifies a finite set of geometric and analytic criteria whose joint satisfaction would realize a physical Hilbert–Pólya correspondence. These criteria provide a precise target for future work and establish a well-posed analytic program grounded in physically meaningful operators.

The Geometry program has now connected five previously separate domains:

- Standard Model pinning of gravitational normalization (Geometry I);
- alignment-induced curvature stiffness and spectral gap (Geometry II);
- drift-law dynamics and alignment evolution (Geometry III);
- parabolic regularization and global existence in the drift sector (Geometry IV);
- weighted Hodge theory and Π-harmonic projection (Geometry V);
- and in the present work, Π-weighted spectral operators capable of supporting L-function structures.

At each stage, the same fixed geometric ingredients have been sufficient: χ, K_{eq}, Ξ, and the Gaussian, parity-even curvature gate $\Pi(\Xi)$. No additional assumptions or dynamical fields were required.

Several open directions naturally follow.

- **Weighted cohomological invariants.** The Π-weighted Hodge theory developed in Geometry V may support nontrivial invariants analogous to Reidemeister or analytic torsion, whose Π-weighted analogues would merit systematic study.
- **Operator-theoretic completion.** A full demonstration that the Π-weighted spectral determinant satisfies all axioms of a completed L-function would require verifying the Euler-product component, the exact gamma factor, and analytic continuation. These were intentionally stated as criteria rather than claimed outcomes.
- **Generalized alignment operators.** While this work has focused on the scalar Π-weighted operator derived from the aligned depth coordinate, the same construction can be generalized to tensor and form sectors. Such operators may admit additional dualities or functional equations.

- **Connection to arithmetic geometry.** The appearance of Mellin–Fourier duality, parity symmetry, and Π-weighted elliptic operators suggests a possible bridge to spectral approaches in number theory, particularly on weighted manifolds or fibered gauge spaces.

The GEOMETRY program remains grounded in a single principle: alignment along the softest mode of the gauge-log Fisher metric. That principle has been sufficient to derive gravitational normalization, curvature response, spectral gaps, parabolic regularization, harmonic projections, and now the analytic structure necessary for a spectral model of L-functions. This work therefore completes the central geometric arc of the program and identifies a finite set of analytic targets for future investigations.

Data availability. All scripts, numerical constants, and analytic derivations used in the GEOMETRY sequence are available in the public `GAGE_repo` under a hash-verified DOI.

7 Conclusion

This work completes the GEOMETRY sequence by embedding the alignment framework within a Π-weighted cohomological setting that treats curvature, dynamics, and topology in a unified manner. The Standard Model–determined structures introduced in GEOMETRY I—the integer direction $\chi = (16, 13, 2)$, the Fisher softness F_χ, and the even curvature gate $\Pi(\Xi)$—were shown in GEOMETRY II–V to fix gravitational normalization, generate a finite spectral gap, define a covariant drift law, and supply intrinsic Π-weighted regularization for both scalar and differential form sectors.

GEOMETRY VI extends this framework to global geometry. Using the Π-weighted adjoint structure and the aligned operator calculus developed in the earlier papers, we constructed a curvature–cohomology map that acts compatibly with the Π-weighted Hodge Laplacian and preserves the analytic properties established in the previous volumes. The resulting framework identifies Π-harmonic representatives of curvature classes and ensures that each topologically nontrivial sector admits a unique, alignment-selected equilibrium representative.

Two features are especially notable. First, the Π-weighted structure introduces no new fields, parameters, or tunable functions: the global theory is fixed entirely by the same SM-derived alignment geometry that determines $G(M_Z)$ and the mass gap. Second, the cohomological extension preserves the stability, positivity, and compact-resolvent properties of the Π-weighted operators, yielding a geometrically natural and globally consistent completion of the alignment framework.

Together, GEOMETRY I–VI present a complete sequence: a fixed integer direction and Fisher softness determine Ξ; the even gate $\Pi(\Xi)$ supplies curvature weighting and spectral rigidity; Π-weighted operators govern dynamics, regularity, and cohomological projection; and the full construction remains anchored to SM data at $\mu = M_Z$ with no additional structures. The result is a self-contained gauge-space geometry that derives gravitational normalization, ensures spectral gap stability, regularizes curvature evolution, and canonically selects Π-harmonic curvature representatives.

Future work may explore extensions to other gauge theories and to number-theoretic analogues of Π-weighted elliptic operators, but the essential geometric framework developed across GEOMETRY I–VI is now complete.